



UNIVERSITAT DE
BARCELONA

New immunochemical approaches for Multiplexed diagnostics

Ana Sanchis Villariz

ADVERTIMENT. La consulta d'aquesta tesi queda condicionada a l'acceptació de les següents condicions d'ús: La difusió d'aquesta tesi per mitjà del servei TDX (www.tdx.cat) i a través del Dipòsit Digital de la UB (diposit.ub.edu) ha estat autoritzada pels titulars dels drets de propietat intel·lectual únicament per a usos privats emmarcats en activitats d'investigació i docència. No s'autoritza la seva reproducció amb finalitats de lucre ni la seva difusió i posada a disposició des d'un lloc aliè al servei TDX ni al Dipòsit Digital de la UB. No s'autoritza la presentació del seu contingut en una finestra o marc aliè a TDX o al Dipòsit Digital de la UB (framing). Aquesta reserva de drets afecta tant al resum de presentació de la tesi com als seus continguts. En la utilització o cita de parts de la tesi és obligat indicar el nom de la persona autora.

ADVERTENCIA. La consulta de esta tesis queda condicionada a la aceptación de las siguientes condiciones de uso: La difusión de esta tesis por medio del servicio TDR (www.tdx.cat) y a través del Repositorio Digital de la UB (diposit.ub.edu) ha sido autorizada por los titulares de los derechos de propiedad intelectual únicamente para usos privados enmarcados en actividades de investigación y docencia. No se autoriza su reproducción con finalidades de lucro ni su difusión y puesta a disposición desde un sitio ajeno al servicio TDR o al Repositorio Digital de la UB. No se autoriza la presentación de su contenido en una ventana o marco ajeno a TDR o al Repositorio Digital de la UB (framing). Esta reserva de derechos afecta tanto al resumen de presentación de la tesis como a sus contenidos. En la utilización o cita de partes de la tesis es obligado indicar el nombre de la persona autora.

WARNING. On having consulted this thesis you're accepting the following use conditions: Spreading this thesis by the TDX (www.tdx.cat) service and by the UB Digital Repository (diposit.ub.edu) has been authorized by the titular of the intellectual property rights only for private uses placed in investigation and teaching activities. Reproduction with lucrative aims is not authorized nor its spreading and availability from a site foreign to the TDX service or to the UB Digital Repository. Introducing its content in a window or frame foreign to the TDX service or to the UB Digital Repository is not authorized (framing). Those rights affect to the presentation summary of the thesis as well as to its contents. In the using or citation of parts of the thesis it's obliged to indicate the name of the author.



*Universitat de Barcelona, Facultat de
Farmàcia i Ciències de l'Alimentació*



*Consejo Superior de
Investigaciones Científicas*



*Institut de Química Avançada de
Catalunya*



*Nanobiotechnology for
Diagnostics group*



*Centro de Investigación Biomédica
en Red en Bioingeniería,
Biomateriales y Nanomedicina*

UNIVERSITAT DE BARCELONA

FACULTAT DE FARMÀCIA I CIÈNCIES DE L'ALIMENTACIÓ

**NEW IMMUNOCHEMICAL APPROACHES FOR MULTIPLEXED
DIAGNOSTICS**

Ana Sanchis Villariz 2018

UNIVERSITAT DE BARCELONA
FACULTAT DE FARMÀCIA I CIÈNCIES DE L'ALIMENTACIÓ
PROGRAMA DE DOCTORAT DE BIOTECNOLOGIA

**NEW IMMUNOCHEMICAL APPROACHES FOR MULTIPLEXED
DIAGNOSTICS**

Memòria presentada per Ana Sanchis Villariz per optar al títol de doctor
per la Universitat de Barcelona.

Directors:

Prof. M.-Pilar Marco Colás

Professora d'Investigació

Dept. de Nanotecnologia

Química y Biomolecular

Nb4D group, IQAC-CSIC

Dr. J.-Pablo Salvador Vico

Investigador associat

Programa de Nanomedicina

Nb4D group, CIBER-BBN

Doctorand:

Tutor:

Ana Sanchis Villariz

Dr. Josefa Badia Palacin

Professora titular

Departament de Bioquímica i Fisiologia

Universitat de Barcelona

Ana Sanchis Villariz 2018

AGRADECIMIENTOS

Parecía que nunca iba a llegar este día, pero por fin puede decirse que la etapa “tesis” está cerrada (o semi-cerrada en el momento de escribir esto, al menos). Esta memoria pretende ser un recogido de todo aquello vivido durante 4 años, aunque no nos engañemos, para ser fiel a tantos momentos únicos se deberían escribir 3 o 4 libros mínimo. De todas formas, y dado el tono emotivo de la ocasión, me gustaría agradecer a todos aquellos que han contribuido, por poco que fuera, a enriquecer y hacer más llevadera esta experiencia; aunque transmitir bien el agradecimiento sentido a veces no es fácil, y hacerlo en tan solo unas frases me resulta una tarea hercúlea.

Para empezar, he de decir que hay una frase que ha sido como una pequeña broma personal, pero que define muy bien mi concepto de este momento de la vida: *la tesis de los mil co-directores*. Por eso, muchas muchas gracias a toda la gente del Nb4D por su ayuda. Cada uno de vosotros ha aportado una pequeña porción a este librito. Trabajar y sacar adelante este proyecto ha hecho que me sintiera como parte de una gran familia. No solo hemos compartido lugar de trabajo, sino que hemos compartido desayunos, comidas y cenas; hemos celebrado y brindado logros y llorado fracasos y pérdidas. Puedo decir sin duda que la gente de este laboratorio está hecha de otra pasta. Dicho esto, empecemos poco a poco:

- Agradecer a mis directores de tesis Pilar y Pablo, por la oportunidad de realizar la tesis. Casi fue una casualidad que mi currículum llegara a vuestras manos, pero he de decir que durante estos años he tenido la oportunidad de crecer a vuestro lado no solo como científica, sino como persona. Y aunque en algunos puntos parecía que no se viera la luz al final del túnel, hemos luchado para que todo saliera lo mejor posible.
- El grupo del Cabs siempre merece mención especial. Gracias Núria y Ana por introducirme en el mundo de los anticuerpos, pero también por todos los momentos de apoyo. Siempre seré ardua defensora de los Supermercados Pascual, y Ana, ¡has hecho que me haga muy fan de Galicia!
- Gracias Montse por enseñarme lo poquito (muy poquito) que sé de química y a Roger por dejar que me aprovechara de tus discusiones

científicas con Marta (o con Rita o con Ginevra, he aprovechado todas las oportunidades).

- Gracias Luisa por esas eternas bromas y debates (tanto científicos como personales). ¡Y qué decir del resto de de las “nuevas incorporaciones” ... David, Enriquet, Ginevra, Inés...habéis hecho que el último año de tesis sea lo más divertido posible, y sabéis que eso es decir mucho!
- Pablico, tenemos que seguir descubriendo bares de Cornellà, que aún nos quedan muchos, y con Klaudia nos tenemos que convertir en artistas. Y tantas otras personas... Laura, Joanet y Albert, lo que dicen de lo bueno si es breve, dos veces bueno es totalmente cierto. Coincidimos poco en el lab, pero aquí estamos para apoyarnos a tope en todo momento.

Y obviamente hay una mención especial a Marta y a Álex. Aunque en la etapa final ya no compartiéramos laboratorio, creo que puedo decir sin duda alguna, que si no he tirado la toalla durante la tesis ha sido gracias a vosotros. El buen ambiente que había en *ELISA* ha sido único. Todas las discusiones científicas, las birras de los viernes, o simplemente las confidencias compartidas y el apoyo en los momentos más duros han marcado los mejores momentos de estos años. Muchas gracias de verdad, espero que esto dure durante muchos más años.

Gracias a mi familia por soportarme durante esta etapa. Soy consciente de la cantidad de quejas, de inseguridades, de charlas y de ensayos de presentaciones que habéis tenido que sufrir. Siempre habéis intentado aconsejarme lo mejor posible, y aunque a veces no se note, siempre es de agradecer.

Y finalmente, y aunque sé que ninguna frase podrá transmitir todo lo necesario, gracias Diego. No solo por tu apoyo sino por tu paciencia al escucharme repetir y repetir mil veces las mismas ideas. Siempre me has animado en los malos momentos, y has sido el que más has celebrado mis pequeños logros. Simplemente gracias.

ÍNDEX

1	NEW TECHNOLOGIES FOR ENVIRONMENTAL DIAGNOSIS	1
1.1	Introduction	2
1.2	Multiplexed immunochemical techniques as diagnostics tools	4
1.2.1	Site-encoded multiplexed platforms.....	5
1.2.2	Label-encoded multiplexed platforms	6
1.3	Matrix of interest.....	8
1.4	Current trends: Alternatives and needs	9
2	CONTEXT SCENARIO, OBJECTIVES AND STRUCTURE	13
2.1	Context scenario.....	14
2.2	Objectives and scientific strategy	14
2.3	Thesis structure	15
3	PYRETHROID ANTIBODIES. PRODUCTION AND CHARACTERIZATION	17
3.1	Introduction.....	18
3.1.1	Pyrethroids role in environmental monitoring	19
3.1.2	Detection methods for pyrethroids in the literature	21
3.2	Chapter overview.....	22
3.2.1	Immunochemical assays	23
3.3	Results and discussion	25
3.3.1	Immunoreagents production and evaluation	25
3.3.1.1	Selection of the immunizing hapten.....	26
3.3.1.2	Hapten synthesis	27
3.3.1.3	Preparation of the immunogens	30
3.3.1.4	Production of antibodies	31

3.3.1.4.1	<i>Development of aminodextran bioconjugates as coating antigens</i>	33
3.3.1.5	Competitors conjugation.....	34
3.3.2	Evaluation of different physico-chemical parameters on the As360/C134-AD assay.....	37
3.3.3	Matrix studies: Artificial seawater	38
3.3.4	Evaluation of the As360/C134-AD ELISA	39
3.3.4.1	Selectivity studies	40
3.3.4.2	Accuracy assays of the final platform.....	41
3.4	Chapter contributions.....	42
3.5	Materials and methods.....	43
4	DEVELOPMENT OF A MULTIANALYTE ELISA PLATFORM FOR THE DETECTION OF ENVIRONMENTAL POLLUTANTS IN SEAWATER	49
4.1	Introduction.....	50
4.1.1	Pollutants in aquatic environments	50
4.2	Chapter objective.....	52
4.3	Target Selection: Environmental Candidates.....	53
4.3.1.1	Herbicides: Irgarol 1051®	53
4.3.1.2	Antibiotics: Sulfapyridine and Chloramphenicol	54
4.3.1.3	Hormones: 17-β Estradiol.....	55
4.3.1.4	Industrial contaminants: Polybrominated diphenyl ethers.....	56
4.3.1.5	Algal toxins: Domoic acid	57
4.4	Results and discussion	58
4.4.1	Immunoreagents: Origin and precedents	58
4.4.2	Establishment of single-analyte ELISAs for the selected environmental contaminants	59
4.4.2.1	Bioconjugate preparation.....	59
4.4.2.2	Single-analyte ELISAs.....	60

4.4.2.3	Improvement of the detectability required: Pre-concentration step.	62
4.4.2.4	Solvent effect in the different ELISA assays	64
4.4.2.4.1	<i>Effect of Methanol</i>	65
4.4.2.4.2	<i>Effect of DMSO</i>	69
4.4.3	Multianalyte ELISA	73
4.5	Chapter contributions.....	78
4.6	Materials and methods.....	78
5	MULTIPLEXED MICROARRAY DEVELOPMENT FOR THE DETECTION OF ENVIRONMENTAL CONTAMINANTS IN SEAWATER.....	83
5.1	Introduction.....	84
5.1.1	Microarrays platforms in environmental applications.....	84
5.2	Chapter objective.....	88
5.3	Results and discussion	90
5.3.1	Establishment of single-analyte assays for environmental pollutants in a multiplexed fluorescent microarray configuration.....	90
5.3.1.1	Protein microarray: Immobilization protocol.....	90
5.3.1.1	Single-analyte microarray assays for seawater analysis.....	92
5.3.2	Fluorescent multiplexed microarray	94
5.3.2.1	Accuracy of the multiplexed microarray	98
5.4	Chapter contributions.....	102
5.5	Materials and methods.....	103
6	CONCLUSIONS OF THIS THESIS	107
6.1	Conclusions.....	108
7	ANNEX I: LASER RELEASE OF BIOMOLECULES FROM GOLD NANOPARTICLES	111
7.1	Introduction.....	112

7.1.1	Biofunctionalization choices	113
7.1.2	Gold nanoparticles	115
7.1.3	Laser release mechanisms.....	116
7.1.3.1	Irradiation modes	117
7.2	Chapter objective.....	119
7.3	Results and discussion	121
7.3.1	Section a: spherical gold nanoparticles functionalization and characterization	122
7.3.1.1	Gold nanoparticles synthesis.....	122
7.3.1.2	Gold nanoparticles bioconjugation	124
7.3.2	Section b: Non-spherical Gold nanoparticles functionalization and characterization	127
7.3.2.1	Gold nanoparticles and nanorods bioconjugation	129
7.3.3	Laser conditions for fluorophore release.....	130
7.3.4	Future proposals	132
7.4	Conclusions.....	132
7.5	Materials and methods.....	133
8	OPTOFLUIDIC SYSTEM FOR THE DETECTION OF C-REACTIVE PROTEIN IN BIOLOGICAL SAMPLES	137
8.1	Introduction.....	138
8.1.1	PDMS material and its implementation in modular optofluidic systems	138
8.1.2	Proof of concept: Cardiovascular diseases.....	140
8.1.2.1	C-Reactive Protein	141
8.2	Chapter objective.....	142
8.3	Results and discussion	143
8.3.1	Modular optofluidics systems: production	144
8.3.2	Modular optofluidics systems: functionalization	145
8.3.3	Proof of concept of the MOPs system	146

8.3.3.1	Enzymatically functionalized MOPs: Validation	147
8.3.3.2	MOPs as tool for early cardiovascular diagnosis: Detection of CRP148	
8.3.3.3	Benchmark of MOPs against standardized protocols.....	149
8.4	Conclusions	150
8.5	Materials and methodes.....	151
9	BIBLIOGRAPHY	153
10	ACRONYMS AND ABBREVIATIONS	169
10.1	Acronyms and abbreviations	170

1 NEW TECHNOLOGIES FOR ENVIRONMENTAL DIAGNOSIS

1.1 Introduction

River, lakes, and marine regions are considered high biodiversity areas with a huge economical potential, which have a direct impact on the quality of life in Europe including health, social and business development issues (see Figure 1.1). For that reason, the effort to understand the origin, fate and levels of pollutants in aquatic environments has been a hot topic since several years[1]. The pollutants causing water contamination include pesticides, persistent organic pollutants, pharmaceuticals and personal care products (PPCP) and biological contaminants such as biotoxins produced during algal blooms[2]. The increasing studies confirming the presence of PPCPs in different environmental compartments have raised concerns about their potential adverse effects due to their inherent ability to induce physiological effects at low doses[3], and their extensive use in human and veterinary medicine.

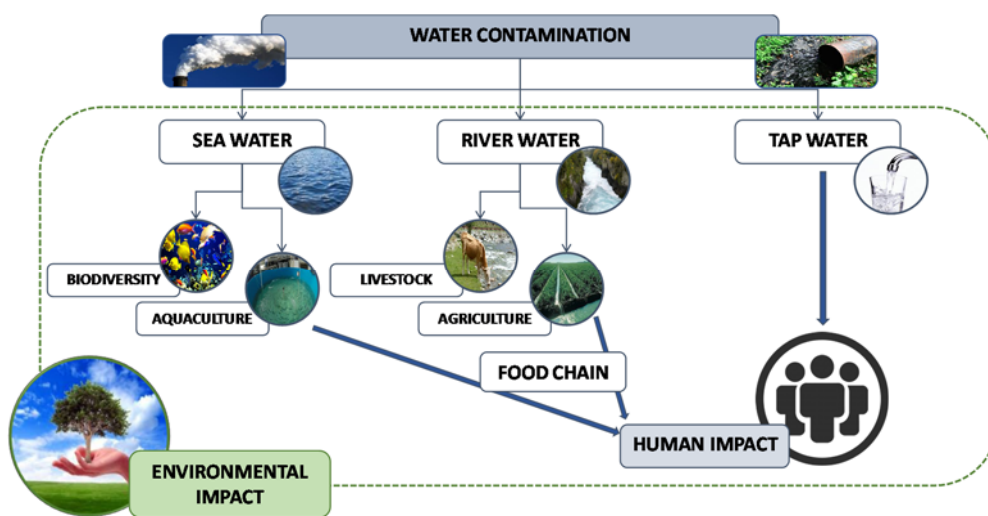


Figure 1.1. Scheme about different water sources and how its possible contamination could affect human population and the environment.

During the last decades a wide range of global and regional monitoring programs have been developed [4], aiming for early warning systems that can provide extreme sensitivity and selectivity information about contaminants. Together with the REACH (Registration, Evaluation, Authorization and Restriction of Chemicals) law (EC 1907/2006) and the Drinking Water Directive (DVD, the Council Directive 98/83/EC) new initiatives for the regulation of the presence of pollutants in aquatic environments have been published during the last years.

The creation of the Water Framework Directive (WFD, 2000/60/EC) in parallel with the Marine Strategy Directive (2008/56/EC) have the main goal to protect the inland surface waters, transitional waters, coastal waters and groundwater, and provide an overall framework for a cleaner and safer aquatic ecosystem. The final aim is to be able to achieve a good environmental status of the European Union's seawaters by 2020. On year 2000, an initial list of 33 priority substances was identified under the WFD aiming at establishing Environmental Quality Standards (EQS) to limit the concentrations of certain chemical substances for the next 20 years[5].

Regarding the technical approaches usually employed in environmental studies, chromatographic techniques are the reference analytical methods for environmental monitoring. They use of universal detectors such as UV or mass spectrometry able to detect multiple compounds simultaneously and providing high sensitive and accurate measurements in the range of ng L^{-1} . Several multiresidue methods for the analysis of a huge number of chemicals in environmental samples have been reported in the last years being most of these examples based on the use of high resolution chromatographical techniques such as gas chromatography (GC) [6], liquid chromatography [7], high-performance liquid chromatography (HPLC) [8] or ultra-performance liquid chromatography (UPLC) [9]. However, these methods often require a clean-up procedures or preconcentration step based on solid-phase extraction [10] with the aim to meet two objectives, first, reaching the low limit of detection required, and second, removing potential non-specific interferences from the matrix. This is added to the intrinsic sequential nature of the chromatographic methods, which made them not suitable for high sample throughput studies or for real-time monitoring of aquatic environments. Overall chromatographic methods are expensive, time-consuming and labor-intensive procedures, not suitable for on-site monitoring, as it would be required by the current environmental monitoring programs and marine legislation.

For that reason, in order to achieve the regulation and monitoring objectives presented, more efficient analytical techniques need to be developed[11]. This idea arises from the need to ensure that the levels of pollutants remains below the limits established and, for that reason, methods that can provide information on a continuous basis about the concentrations and fate of the numerous existing contaminants are required. Following this trail, immunoassays have

become great candidates to complement chromatographic techniques in environmental studies because of its attractive features, including its rapid detection, low cost, the possibility to directly analyze complex matrices without extensive sample treatment, the possibility for high-throughput screening, the wide variety of platforms that can be developed and finally, its multiplexation capabilities. Additionally, they can be used in a great range of configurations [11] from on-site technologies (i.e. lateral-flow assays) to high-throughput screening systems (i.e. ELISA, microarray) or automated laboratory benchtop analyzers based on classical immunoassay configurations or biosensors systems (see Figure 1). Moreover, due to the high specificity of the biomolecular interaction, collections of antibodies can be used in combination and use them for developing highly efficient and reliable multiplexed analytical technologies.

1.2 Multiplexed immunochemical techniques as diagnostics tools

A multiplexed system is distinguished by its ability to measure simultaneously several analytes from a single sample. Multiplexation has been accomplished through different approaches and using distinct technology platforms as it is described in the next sections. Modulating antibody selectivity, using labels showing distinct optical or electrochemical properties, or particular technological platforms are the most important elements investigated to accomplish multiplexation [12].

Advances in micro and nanobiotechnology have provided the possibility to develop multiplexing bioassays through two strategies: a) site-encoded identification (planar microarrays) [13, 14] or b) using multiple quantitation tags (non-planar microarrays) [15, 16] (see Figure 1.2). The first case, in which the identity of the target analyte is encoded by its location with a secondary reporter providing quantitative data (i.e., fluorescent dye), is the most widely used approach. However, a variety of distinct labels have also become available in the last years taking advances of the distinct properties of the material at the nanolevel.

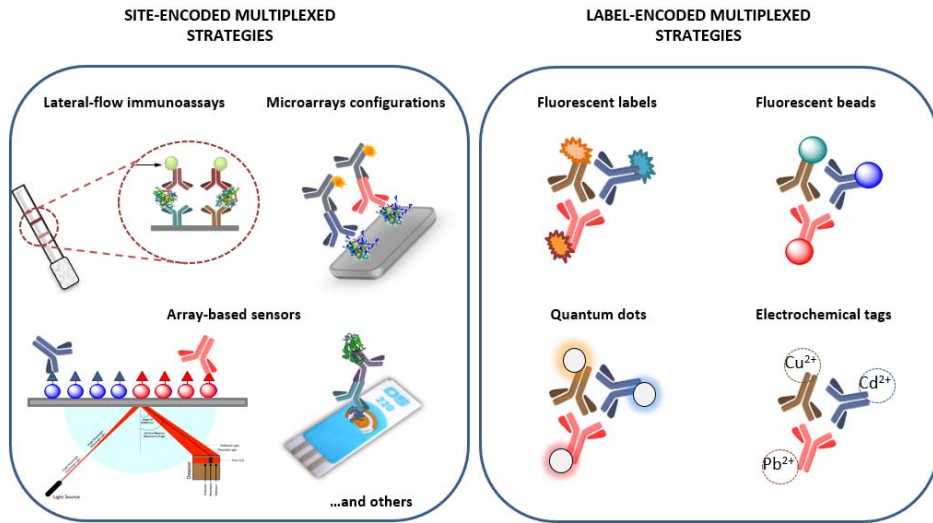


Figure 1.2. Schematic representation of different classes of site- and label-encoded multiplexed platforms.

1.2.1 SITE-ENCODED MULTIPLEXED PLATFORMS

Site codification of various analytes has been the most often applied method for multiplexed on-site platforms. Some examples of site-encoded multiplexed platforms are lateral flow assays (LFAs, fluorescent microarrays or array-based sensors coupled to a variety of detection systems involving or not the use of labels. In fact, high-throughput multiplexing systems based on high-density arrays are one of the most popular techniques in clinical diagnostics. Thanks to the new advances in fields such as genomics or proteomics, microarray technology including scanners and microspotters have become standard laboratory tools in analysis. Although both DNA and protein microarrays can be developed based on different readout, technologies relying on fluorescence or chemiluminescence detection are the ones most exploited in the literature [13, 14, 17]. One of the main advantages of microarrays is that are platforms which allow the characterization from hundreds to millions of proteins or DNA sequences at the same time. However, although comparable limit of detection (LOD) and accuracy have been reported in comparison with simpler techniques such as ELISA [18], there's still need for printing process optimization, particularly

in the case of the protein microarrays, and assay automation. On the other hand, signal can be either optical or electrical. Thus, although the most well-known microarrays are based on fluorescence labeling [19, 20], array-based electrochemical systems, which depend on individually addressable microelectrode arrays have also been reported [21]. In those cases, the direct immobilization on the electrode's surface of different biomolecules permit the detection of target analytes electrochemically via enzymatic reactions by, for instance, potentiometry or amperometry, or label free such in the case of impedance.

Array-based optical sensors such as the ones based on surface plasmon resonance (SPR) properties are commonly found in the literature. SPR biosensors detection relies in changes of refractive index derived from biomolecular recognition reactions [22]. In order to establish multiplexed platforms based on SPR, discrete regions of the chip have to be dedicated to the detection of each target analyte in order to allow the multidetection of several of them from a single sample. Although some attempts have been reported often the number of real samples analyzed is low or there is a lack of validation, however some examples focused on the detection of environmental pollutants [23], or algal toxins among others have been described [24].

Finally, in the literature examples of site-encoded systems based in lateral flow assays (LFA), by far the best established commercial products due to their simple, fast and low-cost protocols, can be also found. The mechanism of the platform is based on the diffusion of the sample by capillarity. Along the material in the flow zone, some reactions areas in which specific reagents are immobilized will be the responsible of the detection (on multidetection) of the target analytes. Different configurations of multiplexed gold-based lateral-flow strips for simultaneous detection of carbofuran and triazophos [25], or different chemicals in drinking water [26] have been developed, however, having the goal of improving the sensitivity of the assays, novel alternatives based in the use of fluorescent nanomaterials have been appearing [27].

1.2.2 LABEL-ENCODED MULTIPLEXED PLATFORMS

Multiple labels platforms often depend on the use of multiple labels or encoded carriers like particles. Different conceptual approaches can be considered: *i*) the

use of different labels with different optical or electrochemical properties [28], ii) the use of beads by either its size/shape or color [29], and iii) the use of beads biofunctionalized with by labels (i.e., enzymes, metals ions, redox tags or quantum dots) [30-32]. Suspension arrays of encoded microspheres are envisaged as a strategy to provide higher quality data than the most frequently used planar microarrays. Microspheres facilitate the separation and washing steps and may even allow eliminating these steps.

Fluorescent microspheres can be used as solid supports for immunoassay (see [33, 34] for extensive reviews). Nowadays there exists in the market a variety of beads with distinct fluorescent properties. The most well implemented suspension arrays are those based in the Luminex® xMAP® (Luminex's Multi-Analyte Profiling) technology. It uses mixtures of color-encoded beads functionalized with specific bioreceptors (i.e capture antibodies) to bind the analytes of interest combined with secondary reagents (i.e. detection antibodies) labelled with phycoerythrin or Alexa 532. Multiplexing is accomplished because the beads have two fluorochromes (i.e. Red (658-nm emission) and infrared (712-nm emission) at different concentrations, in such way that each bead from the 100 microspheres set has a distinct red-to-infrared ratio. The sample is mixed with these labelled reagents and after a short incubation time they are introduced on a bench-top flow cytometer, where the beads are read with a dual-laser, one to identify the target and the other to quantify. Each single-file microsphere suspension passes by two lasers. A 635-nm laser excites the red and infrared fluorochromes of the microspheres, which allows the classification of the bead and therefore the identity of the probe-target being analyzed. A 532-nm laser excites reporter fluorochromes of the secondary reagents for quantification. Such kind of assays are robust and provide high sample throughput capabilities, along with low operating costs, being great candidates for clinical diagnostics and central laboratories; however, are limited by the number of color-encoded beads possible, which usually is never greater than 500. Moreover, its long turnaround times, the size of the equipment, the need of qualified personnel and the cost of measurement instruments are features that have encouraged the search of simpler platforms that could offer similar levels of information but at lower cost and time analysis [15, 35]. This strategy using fluorescent microbeads associated with flow-citometry detection has been implemented for the detection of freshwater and brackish toxins [36] or polycyclic aromatic hydrocarbons [37] among others.

Quantum dots (QD) is another example of fluorescent particles that can be used for establishing multiplexed label-encoded platforms. They have been defined as colloidal fluorescent semiconductor nanocrystals ranging from 2 to 10 nm in diameter and although the elements of the quantum dots can be used as redox labels for multiplexing, usually the fluorescence capabilities of such composites are the feature selected for achieving the simultaneous detection of several targets. QDs have showed outstanding advantages in the longtime, multi-color fluorescence imaging and detection due to its features of being photostable and having a size- and composition-tunable emission spectra. They have been applied for the multidetection of microcystins and polycyclic aromatic hydrocarbons pollutants [38], or insecticides [39] in the field of environmental monitoring.

Finally, electrochemical redox-active substances are key elements on multiplexed immunoassays with electrochemical readout, allowing the use of different redox species for labeling immunoreagents against different target analytes [40]. To date, the most commonly used electrochemical redox species are dyes such as thionine, toluidine blue, methylene blue and heavy metal ions such as Cu^{2+} , Cd^{2+} or Pb^{2+} [41]. This approximation has been implemented in environmental studies [42]. Recently, it has also been contemplated the use of nanoparticles for labeling immunoreagents in order to develop multiplexed electrochemical immunosensors. Thus electrochemical metallic nanoprobe can be used for codifying different antibodies, producing signals at different redox potentials (see [40] for additional information). However, to our knowledge this approach has not been used to the analysis of aquatic environments.

1.3 Matrix of interest

When studying the impact of pollutants in the environment, the selection of the matrix is one step to consider. Having aquatic environments in mind; water, sediments and organisms (including fish or molluscs) are the three pillars at which contamination could have a great impact (see Figure 1.3).

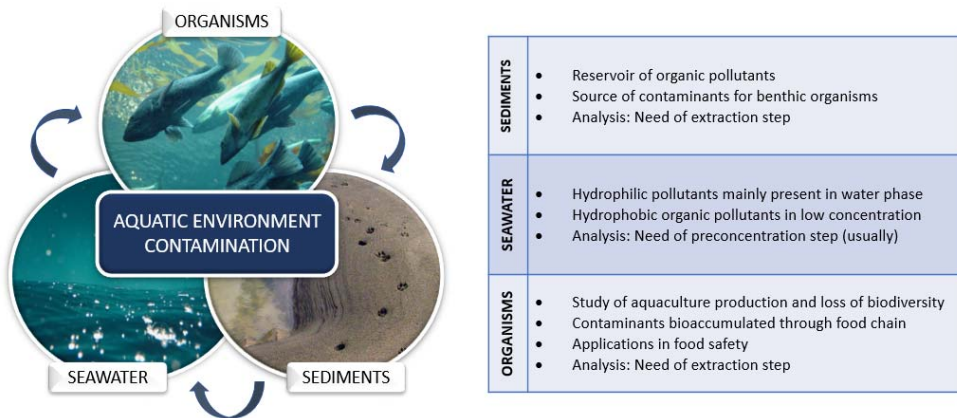


Figure 1.3. Relation between the different matrices of interest related to aquatic environmental pollution.

Oceans are under continuous stress from a huge variety of pollutants, resulting in a loss of species, physical damage to marine habitats or the variation of nutrients composition of waters. In parallel, aquaculture is growing more rapidly than all other animal food-producing areas.

Marine aquaculture is strongly dependent of environmental conditions, such as seawater quality, that can be affected by several classes of pollutants released to the environment by natural or anthropogenic sources. Therefore, the analysis of the seawater itself could present several advantages in comparison to other desired matrixes. Seawater is a complex matrix in which the proportion and concentration of salts is a key feature. Even though, excluding the need to ever do a filtration of the samples to remove suspension particles, direct analysis could be presented as a valid alternative. For that reason, seawater was selected as the target matrix for the development of this thesis.

1.4 Current trends: Alternatives and needs

Although the possibility to carry out measurements directly in the problematic scenario is an unmet need nowadays, the environmental monitoring field is evolving with the apparition of on-site testing devices. On-site testing could employ instruments, sample collection, and preparation with the goal of reducing the sample burden on the home laboratory. However, it also could

mean the development of platforms that could give real-time information directly from the field studied. The feasibility to implement different platforms for direct analysis of physical parameters (i.e. for water quality [43]) has been studied, however, the real application of devices for measuring on-site different features like the presence of pollutants in the environment have to face multiple troubles [44]. These platforms should be based in features such as miniaturization and multiplexation, and therefore be built mainly on the advances of two areas: nanotechnology and microfluidics.

Nanomaterials have been the focus of attention in several fields, including biomedicine, electronics, or catalysis, mainly due to the new properties materials gain when they are manufactured at the nanoscale [45, 46]. From different materials such as gold or silver, or with different intrinsic properties like magnetism or plasmonics, nanoparticles of different shapes, materials or sizes are being implemented in a wide range of applications (see Figure 1.4).

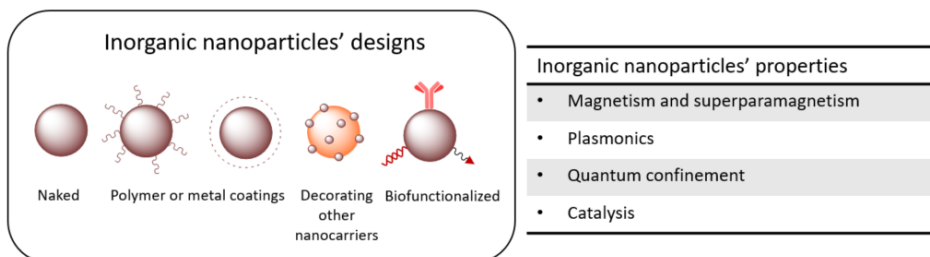


Figure 1.4. Scheme of inorganic nanoparticles as an example of nanomaterials applied in LOC systems, being magnetic and metallic the two majority groups.

On the other hand, microfluidics devices are characterized by the precise control and manipulation of fluids at the submillimetre scale. In most of the microfluidic platforms, fluids are manipulated through the existence of several pneumatic valves that can be integrated in flexible materials such as polydimethylsiloxane (PDMS)-based devices [47, 48]. Microfluidic technology promises to be a key element in order to convert bench-top laboratory protocols into low-cost and portable systems [49], and its combination with the great potential nanomaterials could offer in the field of biosensing and therapy, could revolutionize the field of environmental diagnosis and monitoring.

Having all these ideas in mind, the development of robust, multiplexed and real-time monitoring devices which can provide information on a continuous or semi-

continuous basis about the concentrations and fate of the numerous existing contaminants is clearly an urgent need to meet. Monitoring approaches and technologies for chemical pollutant analysis in the ocean should fulfill certain requirements as those listed below:

- 1) Simultaneous identification and quantification of several pollutants from distinct chemical families and origin.
- 2) Achieving levels of detectability in the range of nanograms or even picograms per liter in environmental samples.
- 3) Ability to provide reliable results with minimum or no need for sample treatment
- 4) Robustness considering the variety of aquatic environments, and therefore of different nature, in which those techniques are going to be applied.
- 5) Move from the proof-of-concept results towards well validated technologies from the analytical point of view.
- 6) Automated devices able to work autonomously for a certain period of time (ex. One month) reporting data to a central laboratory on a wireless mode.

Aiming to fulfill these requirements and monitoring objectives, innovative, efficient and reliable analytical techniques need to be developed, however, those platforms need to provide multiplexed capabilities without weakening their actual analytical features and advantages.

2 CONTEXT SCENARIO, OBJECTIVES AND STRUCTURE

2.1 CONTEXT SCENARIO

The present doctoral thesis has been developed within the framework of two different research projects:

1. **Biosensors for real time monitoring of biohazard and man made chemical contaminants in the marine environment, SEA-on-a-CHIP.** (FP7, OCEAN 2013. 1-614168). The focus of this european project is to develop a miniaturized, autonomous, remote, and flexible immunosensor platform based on a fully integrated array of micro/nanoelectrodes and a microfluidic system in a lab-on-a-chip configuration. The final prototype will be presented as a real-time platform for analysis of marine waters in multi-stressor conditions. This system will be developed for a concrete application in aquaculture facilities, including the rapid assessment of contaminants affecting aquaculture production and those produced by this industry.

2.2 Objectives and scientific strategy

The final goal of this thesis project has been the study, development and validation of multiplexed platforms and techniques for monitoring contamination in the oceans based on the use of antibodies as biorecognition elements. The strategy envisaged consisted on evaluating the performance of those antibodies on well-established and known multiplexed systems such as ELISA and fluorescent microarray for further on implementing them on novel technological approaches involving the use of plasmonic nanoparticles and optofluidic systems for the development of on-site analytical devices. Thus, the specific objectives proposed are

1. The evaluation of the performance of a selected panel of immunoreagents, addressed to the detection of environmental contaminants, for the development of multiplexed immunochemical techniques to assess the health status of the ocean

2. The development and analytical characterization of multiplexed immunochemical platforms and their implementation to the analysis of sweater samples.
3. The development of novel immuno-probe assays based on the possibility to specifically release fluorescent labels from plasmonic nanoparticles.
4. The study of a novel optofluidic sensor platform as a potential *on site* diagnostic device.

To address most of the objectives of the multiplexed platforms we have selected a panel of interested targets in respect of their impact on the health status of the oceans. Thus, important families of environmental and chemical pollutants such as triazine biocide (i.e. Irgarol 1051®), sulfonamide and chloramphenicol antibiotics, polybrominated diphenyl ether flame-retardant (PBDE, i.e. BDE-47), hormone (17 β -estradiol), and algae toxin (domoic acid) have been selected as target analytes for this thesis. For most of these contaminants, the Nb4D group had immunoreagents available except for pyrethroids.

2.3 Thesis structure

The main focus of this thesis (which includes chapters 3, 4 and 5), addresses all the work related to the development of multiplexed immunochemical techniques for the multidetection of the selected environmental pollutants, and it has involved the following tasks. Production and validation of different immunoreagents for the detection of pyrethroids.

1. Development of a multianalyte ELISA platform for the simultaneous detection of several classes of pollutants in seawater
2. Development of a protein microarray to detect some of the most important chemical contaminants of the seawaters.
3. Evaluation of the performance of the microarray platform using artificial seawater spiked samples.

Two annexes have been added to this thesis. The first one (chapter 7) describes the research done in respect of the possibility to exploit the plasmonic properties of the noble metal nanoparticles to develop a novel multiplexed platform based on the specific release of fluorescent labels. Main tasks addressed have been:

4. Preparation biofunctional nanoparticles on a reproducible manner.
5. Assessing the possibility to release the fluorescent dyes covalently attached to plasmonic particles using different types of lasers
6. Proof-of-concept of the possibility to develop a multiplexed platform based on this principle.

The second annex (chapter 8) describes the work related to the evaluation and validation of a new optofluidic sensor platform using non-rigid polymers and a photonic-based detection.

While chapter 6 includes the conclusions of this thesis, in chapter 9 the bibliography on which all the work developed has been supported can be found. Finally, in chapter 10 the section where all the acronyms used in this text are described is present.

The structure of the present thesis, including the content of each chapter is shown in Figure 2.1. Chapters are organized according to the different blocks explained, each one dedicated to a different final.

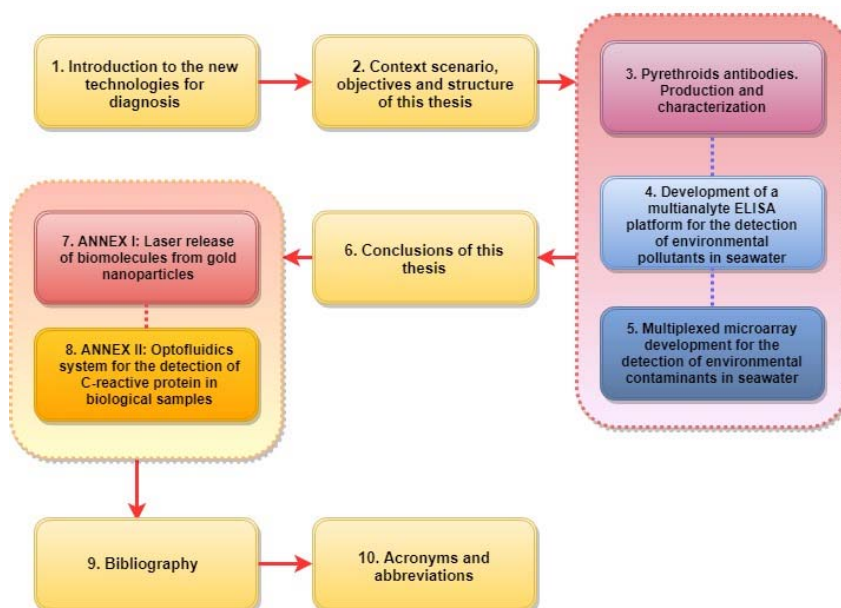


Figure 2.1. The structure of this thesis related to the different chapters and parts included in each one.

3 PYRETHROID ANTIBODIES. PRODUCTION AND CHARACTERIZATION

3.1 Introduction

Pyrethroids are synthetic chemicals modeled after the pyrethrin components of *pyrethrum*. The general mechanism of action of pyrethroids is the interference with normal production and conduction of nerve signals in the nervous system. Their contact with target organisms could delay the closing of the activation gate for sodium ion channels, affecting the correct transmission of nervous signals [50].

Two classes of pyrethroids, Type I and Type II, can be distinguished based on electrophysiological studies with nerves and symptoms of toxicity. Type II pyrethroids, including deltamethrin, have an α -cyano group that induces an inhibition of the sodium channel activation gate with a longer duration. Nowadays α -cyano pyrethroids are being extensively used as insecticides in domestic, agriculture, horticulture, public health, and veterinary applications, mainly due to its low mammalian toxicity and its activity against a broad range of pests [51, 52].

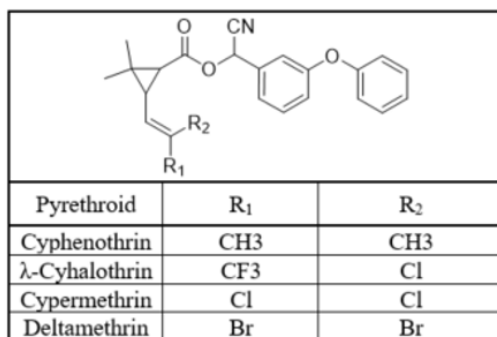


Figure 3.1. Chemical structures of some of the most used synthetic pyrethroids.

Cyphenothrin, λ -cyhalothrin, cypermethrin and deltamethrin (see Figure 3.1) among other synthetic pyrethroids have reported improved physicochemical properties and biological actions compared to their natural analogues. However, toxicological studies have shown the negative impact of these pyrethroids over invertebrates and fish [53-55]. Pyrethroids usually are considered to be less toxic

to mammals compared to insects due to mammals' higher body temperature, larger body size, and decreased sensitivity of the ion channel sites [56, 57].

Pyrethroids and also α -cyano pyrethroids are usually broken apart by sunlight in one or two days, however when associated with sediment they can persist for some time and contribute to toxicity in the surrounding watersheds. For that reason, and due to its non-specific toxic effects on fish, low levels of EQS (Environmental Quality Standard), between 8 and 80 $\mu\text{g L}^{-1}$, have been fixed for cypermethrin in surface waters. On the other hand, deltamethrin don't have yet a fixed EQS, although its presence in the environment have been found in soil, sediments, and surface water, with half-life valors depending on the pH and aerobic conditions of the substrate [50, 58].

3.1.1 PYRETHROIDS ROLE IN ENVIRONMENTAL MONITORING

The use of pyrethroids as insecticides has been increasing in recent years as a replacement for organophosphate insecticides that are being phased out because of water-quality concerns.

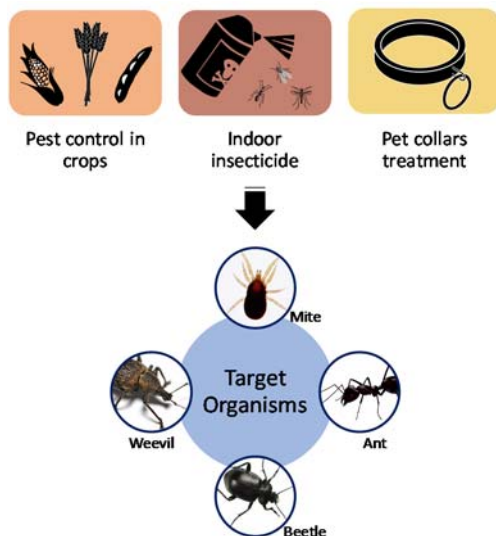


Figure 3.2. Main uses of the insecticides deltamethrin and cypermethrin, and its main target organisms.

Researchers first described deltamethrin in 1974 [59], however it was not registered in the United States Environmental Protection Agency (U.S. EPA) until 1994. Most synthetic pyrethroids are marketed as mixtures of optical and geometrical isomers. However, in contrast to that, deltamethrin is 1R-cis- in the dibromochrysanthemate moiety and S at the R-cyano carbon. Deltamethrin have been presented as one of the more lipophilic and stable insecticide-permethrins, and in consequence its residues have been detected in agricultural products, food, and surface waters [60-64]. As other family-compounds it is classified as a broad-spectrum insecticide and the main uses of deltamethrin as well as its specific target organism has been illustrated in Figure 3.2. This pyrethroid has been classified as highly toxic to aquatic life, especially fish, finally being classified as a neurotoxin [65]. However, and despite of the negative effects deltamethrin presents, it is commonly used as a treatment for sea lice. On the other hand, cypermethrin was introduced on the market in the late 1970s, registered in U.S. EPA in 1981 and has since been used on a wide range of crops due to its high pesticidal activity and low mammalian toxicity relative to other insecticides. As in the case of deltamethrin, this pyrethroid has been classified as highly toxic to aquatic life, affecting their movement, their fecundity rates or the larvae development, being finally classified as a neurotoxin [66].

Considering the classification of both pyrethroids, the study of these insecticides over aquatic organisms has been considered a priority in order to understand the possible secondary effects this kind of treatments could have. One of the effects documented is swimming performance of fishes is affected by deltamethrin at the range of ng L^{-1} . Model animal studies using zebrafish showed that the overall reproductive capability decreased due to a decreased fecundity, hatching rate and egg production [67]. Cypermethrin has been associated with behavioral changes such as loss of balance or swimming alteration in catfish species [68], but also induced oxidative stress and produce apoptosis through the involvement of caspases in zebrafish embryos [69]. For that reason, nowadays both cypermethrin and deltamethrin have been also classified as endocrine disruptor chemicals (EDC).

Several studies reported the presence of deltamethrin and cypermethrin in water and sediments, finding levels in the range of ng L^{-1} in different regions of the world. Concentrations up to 2 ng L^{-1} were detected in small and medium-sized rivers in Switzerland by passive sampling [70], and between 5 and 25 ng L^{-1}

were found in California during different years [71-73]. In Spain those concentrations were up to 60 ng L⁻¹ [74]. In the case of cypermethrin, its concentration can be as high as 194 µg L⁻¹ in the runoff of some farmed areas following pesticides applications [75, 76]. However, sporadically these levels could increase significantly as reported by the work of Bille et al [77] showing for the first time a fish kill episode reasonably linked to the exposure to high concentrations of pyrethroids in Italy freshwater. A highest concentration of 4317 µg L⁻¹ of deltamethrin (several orders of magnitude higher than the standard levels of deltamethrin reported), along with other pyrethroids such as cypermethrin, permethrin and tetramethrin, was detected on the first-day of a reported incident. Although α-cyano pyrethroids are thought to be safe for human health, some negative related-effects have been reported [62], and recent studies indicated that long-term exposure of humans to these pesticides causes reversible symptoms of poisoning and suppressive effects on the immune system. Thus, the toxic effects of these pesticides on the ecological, environmental, and human health aspects have elicited increasing concerns [78, 79] encouraging the need of creation of control and monitoring platforms.

3.1.2 DETECTION METHODS FOR PYRETHROIDS IN THE LITERATURE

Due to the hydrophobic profile of most of pyrethroids [80], including deltamethrin, these chemicals tend to bind to the particulate matter present in natural waters and are typically detected in sediments. However, it can also be detected in marine organisms and water itself. As pyrethroid use continues to increase in both urban and agricultural settings, it is important to have robust, sensitive methods that are capable of measuring these compounds at environmentally relevant concentrations (below acute toxicity levels) in both water and sediment samples. Although deltamethrin is not regulated by today's marine legislation, these regulations propose the control and quantification of cypermethrin by gas chromatography/high resolution mass spectrometry (HRGC/HRMS) [81]. As deltamethrin is a compound basically identical to cypermethrin only differing from the fact that it has bromine atoms instead of chlorine, it is likely possible that future regulations could advise analyzing deltamethrin with similar techniques. In the literature, the current analytical methods for deltamethrin detection are usually based on multistep cleanup

procedures followed by chromatographical techniques, including high-performance liquid chromatography (HPLC) [82-85], liquid chromatography combined with fluorescence detection (HPLC-FD) [86, 87], or gas chromatography coupled to mass spectrometry (GC-MS) [74, 88]. These methods reported good levels of sensitivity and accuracy of determination, but at the expense of being time-consuming, expensive, not suitable for the analysis of large numbers of samples and incapable of being easily field-deployable.

As nowadays both, environmental monitoring programs and current marine legislation are calling for analytical platforms to be used in case-study field studies providing near real-time information, the need for new analytical technologies complementary to the chromatographic techniques is clear. Following this trail, immunoassays have become great candidates to complement chromatographic techniques in environmental studies [60, 64]. Between the main benefits, there are their low cost, the possibility to directly analyze complex matrices without extensive pretreatment, their high flexibility and variety of analytical platforms possible and their high sample throughput capabilities. Additionally, since antibody-based microarrays and biosensors offer the possibility of multiplexed studies, on-site analytical devices with multiplexed capabilities for monitoring different environmental contaminants in a real-time manner could be possible.

3.2 Chapter overview

This chapter describes the preparation and characterization of immunoreagents for the detection of two different commonly used pyrethroids: cypermethrin and deltamethrin (Figure 3.3). Both pyrethroids are commonly used insecticides. Haptens have been designed and synthesized to produce antibodies that have been finally characterized by developing a competitive ELISA, before their implementation on the multiplexed immunochemical platforms described in chapters 4 and 5.

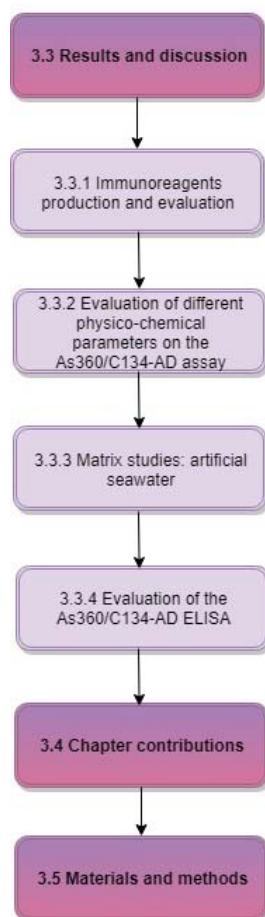


Figure 3.3 Structure of this chapter related to the different sections.

3.2.1 IMMUNOCHEMICAL ASSAYS

The basis of an immunochemical assay is the affinity of an antibody for a specific antigen. Usually in order to detect the immunochemical reaction between antibody and antigen a label is needed, except for a variety of label-free biosensor transducer schemes such as those based on SPR, impedance or certain grating couplers (for additional information see [89, 90]) Even though chemiluminescent and fluorescent labels have become a great label option for immunoassays in the environment field, enzyme labels such as horseradish peroxidase or alkaline phosphatase are still one of the most popular labels. Independently, both label-free and labelled immunochemical methods usually

rely on different configuration depending on the molecular weight of the target. Figure 3.4 shows these configurations in the case of an ELISA (enzyme-linked immunosorbent assay) method; however, these can be also extended to other immunochemical techniques, including immunosensors.

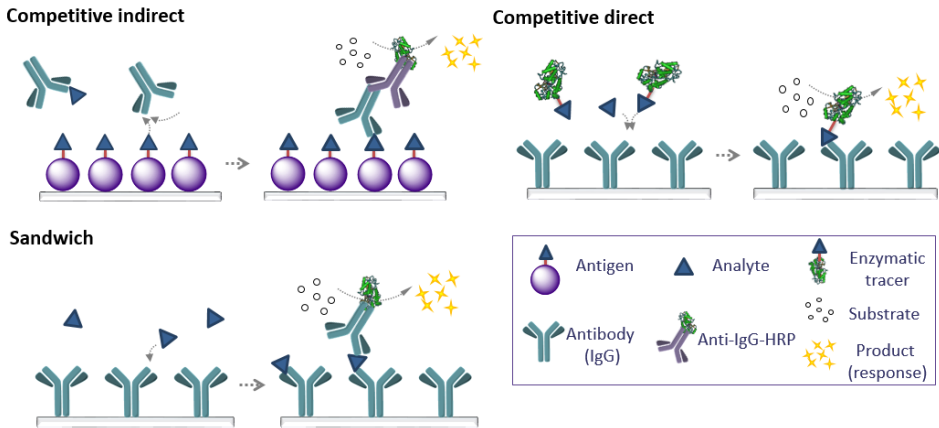


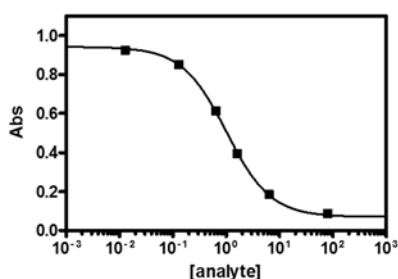
Figure 3.4. Schematic representation of the most common ELISA formats. In the first case, a competitive indirect ELISA is represented, in which coating antigen is immobilized in the plate, and the use of a secondary antibody is needed for obtaining the final signal. In the second case, a competitive direct ELISA is schematized, in which an antibody is the one immobilized in the plate, and the final signal is obtained through an enzyme tracer. Finally, a sandwich configuration shows the detection of an analyte using a pair of antibodies, a capture one and a detection one.

On an ELISA:

1. High molecular weight analytes, like whole proteins, are usually detected with sandwich ELISA, in which two antibodies, one immobilized in the plate (capture antibody) and another free in solution (detection antibody) allow the quantification of the target analyte
2. Low molecular weight molecules can't be detected directly in a sandwich format, and for that reason they need the presence of a competitor (Ag, a hapten coupled to a protein). This type of assay is called a competitive ELISA. Competitive assays can be direct, when the competitor is labelled with the enzyme that catalyse a colorimetric reaction; or indirect, when a secondary labelled antibody is required. This secondary antibody is specific for the constant fraction of the first antibody. Since deltamethrin is a low molecular weight pollutant, the most suitable assay format was the competitive one.

For high molecular weight analytes on label-free biosensors, often the detection antibody is not necessary, although in some cases is used for amplification purposes. For the case of small molecules, there are only few papers claiming direct detection of the analyte, without a competitive configuration [91].

In competitive assays, the concentration of the analyte is indirectly proportional to the colorimetric detection (see Figure 3.5). The representation of the logarithm of the analyte concentration in front of the measured signal gives the typical sigmoidal inhibition curve. This curve, fitted to a 4 parameters equation, will give the features of the assay.



$$f(x) = A_{max} \frac{(A_{min} - A_{max})}{\left(1 - \left(\frac{x}{IC_{50}}\right)^{Hillslope}\right)}$$

Figure 3.5. Inhibition curve of the competitive ELISA and its fitted equation. IC_{50} : half maximal inhibitory concentration, A_{max} : maximum absorbance, A_{min} : minimum absorbance, Hillslope: slope of the linear part of the curve.

3.3 Results and discussion

3.3.1 IMMUNOREAGENTS PRODUCTION AND EVALUATION

In order to establish an immunochemical assay for the detection of deltamethrin in environmental samples, it has been necessary to raise antibodies. Since small molecules do not elicit an immunological response, first task has been de design and synthesis of an immunizing hapten. Similarly, for developing a competitive immunochemical assay, also competitor haptens have been prepared.

3.3.1.1 Selection of the immunizing hapten

A hapten is a small molecule with similar physico-chemical properties to the analyte that wants to be measured, in which a linker with a chemical group is introduced for the coupling to the carrier protein.

The two basic ideas for doing a proper hapten design for the development of antibodies are:

1. Preserving the most characteristic epitopes of the target molecule.
2. Ensuring that the introduction of the linker does not affect the physical chemical properties of the analyte to be determined.

in order to become immunogenic, the hapten is usually conjugated to a highly immunogenic protein through its reactive groups such as the amines of the lysine residues or carboxylic acids of the glutamic or aspartic acid residues (see Figure 3.6).

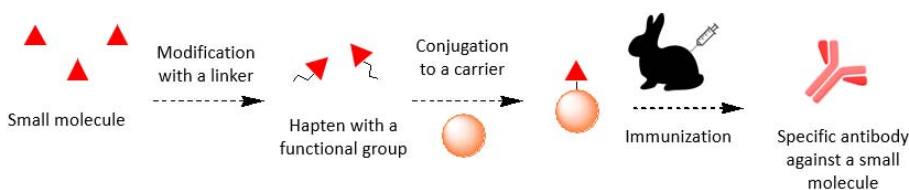


Figure 3.6. Scheme showing the procedure required for the production of antibodies against small molecules.

For the selection of the immunizing hapten in this case, a bibliographic research of already developed pyrethroid immunoreagents and the features of the corresponding immunoassays developed was made (see Table 3.1 for a summary). Some papers were found which described the production of antibodies for deltamethrin and other pyrethroids. However, the first criteria that was followed, was that all the epitopes of the desired molecules were conserved in the immunogen (see Figure 3.7).

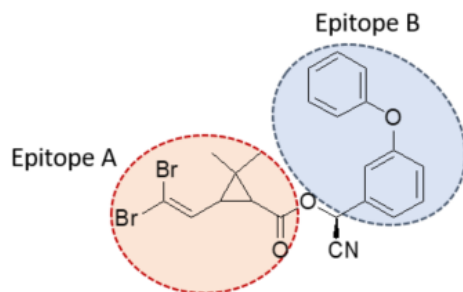







Figure 3.7. Chemical structure of deltamethrin. The most relevant epitopes are highlighted in red and blue.







For that reason, several strategies found in the literature were discarded [51, 60, 92, 93], because the haptens proposed lacked the double-aromatic ring, or the linker was introduced on a position that affected to the halogens atoms. In the case of the strategies followed by Hammock et. al [51] and Li et. al [94], although both epitopes were present, the introduction of a heteroatom in the aromatic ring for further derivatization, had the risk of introducing a significant change in the electronic configuration, being the reason why these strategies were not preferred. Instead, Skerrit et al. [95] proposed a hapten that preserved the two main molecule moieties (see Figure 3.7) by placing the linker through the cyano group. Therefore, this was the approach chosen in this work.

3.3.1.2 Hapten synthesis

The same synthetic approach as that used by Skerrit *et.al* [95] (see Figure 3.8) was followed with small modifications such as introducing the *tertbutyl*-3-aminopropionate. The synthesis of the different immunizing haptens was developed by the service of Synthesis of High added value Molecules (SIMchem) of the Institute of Advanced Chemistry of Catalonia (IQAC-CISC).

Table 3.1. Different immunogens found for the production of immunoreagents for deltamethrin, cypermethrin and cyhalothrin. Information regarding the IC_{50} , the % of cross—reactivity with other pyrethroids and the competitors produced is summarized here.

Immunogen	Competitor	Deltamethrin		Cypermethri		Cyhalothrin		Reference
		IC_{50} ($\mu\text{g L}^{-1}$)	CR, %	IC_{50} ($\mu\text{g L}^{-1}$)	CR, %	IC_{50} ($\mu\text{g L}^{-1}$)	CR, %	
	Homologous	2.61·106						[51]
	Homologous (exist others)	17	100		37			
	Homologous		0.04	13	100			[92]
	CYP-HRP	5		200				[95]
	CYP-HRP	2		8				

Immunogen		Competitor	Deltamethrin		Cypermethrin		Cyhalothrin		Reference
			IC ₅₀ ($\mu\text{g L}^{-1}$)	CR, %	IC ₅₀ ($\mu\text{g L}^{-1}$)	CR, %	IC ₅₀ ($\mu\text{g L}^{-1}$)	CR, %	
		CYP-HRP	4		22		11		[95]
		Homologous	7.08		10.72		>1000		[60]
		MAb, Homologous	500					<1 %	[96]
		MAb, Homologous	17	100	65.5	26			[94]
		Heterologous			49		58		[93]

Continuation Table 3.1.

Following this synthetic strategy, two haptens were synthesized: D133 (from deltamethrin r) and C134 (from cypermethrin).

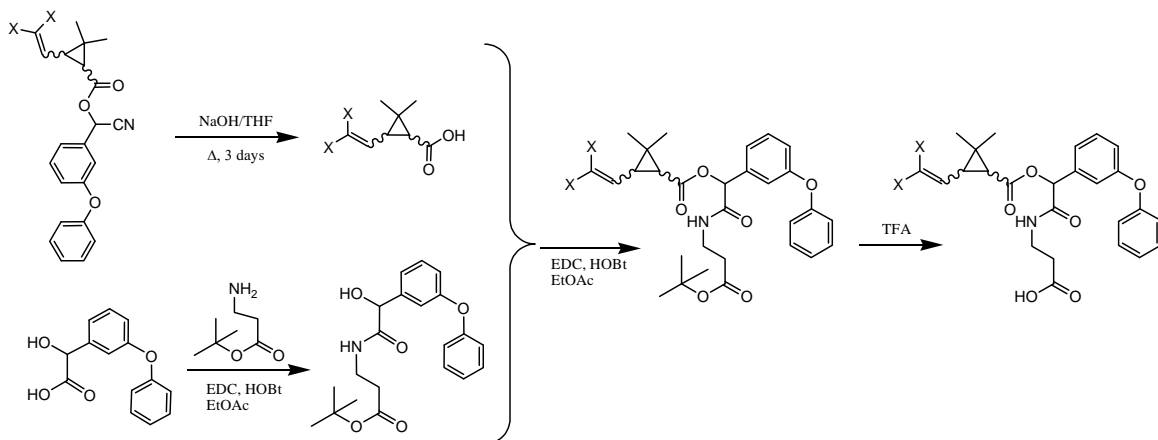


Figure 3.8. Reaction scheme for synthesis of haptens D133 and C134. The ester bond of both pyrethroids, deltamethrin (X=Br), and cypermethrin (X=Cl), was hydrolyzed. After that, the cyano group which was also hydrolyzed to a carboxylic group, was coupled to the protected spacer arm selected through a carbodiimide reaction. Finally, the spacer arm was deprotected with a TFA treatment.

3.3.1.3 Preparation of the immunogens

Once the haptens were synthesized, the immunogens were prepared by covalently coupling those haptens with horseshoe crab hemocyanin (HCH) via the mixed anhydride method using isobutylchloroformate/tributylamine. The evaluation of the conjugation was performed by MALDI-TOF-MS and the results can be found in Table 3.2. Due to HCH high molecular mass, the direct evaluation by MALDI-TOF-MS was not possible for which reason the assessment of the conjugation was performed by analyzing the corresponding bovine serum albumin (BSA) conjugate that had been prepared simultaneously under the same conditions.

Immunoreagents	δ -hapten ^b
C134-BSA	5 ^c
D133-BSA	4 ^c

^aThe BSA conjugates were prepared in parallel and under the same conditions as the HCH conjugates. Analyses were performed by MALDI-TOF-MS. ^bMols of hapten per mol of protein. ^cResidues of hapten per reference BSA.

3.3.1.4 Production of antibodies

Each of the immunogens prepared in the previous section were used for immunizing three New Zealand female rabbits. The ones immunized with C134-HCH were named 358-369-360, whereas the ones immunized with D133-HCH were named 361-362 and 363.

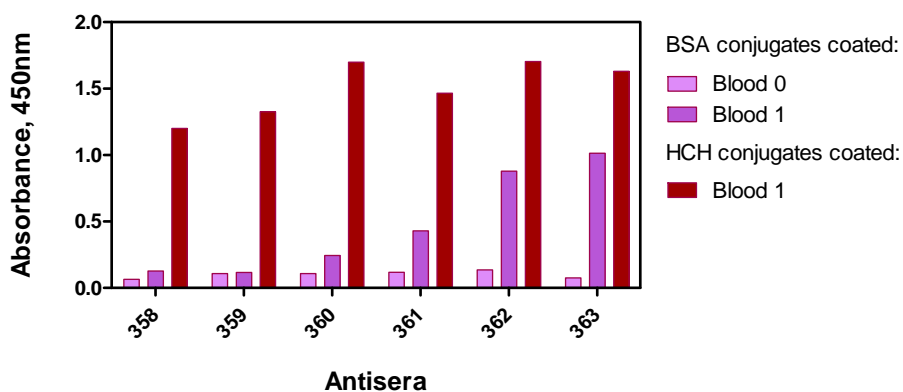


Figure 3.9. Evaluation of the antibody titer of the first blood obtained after the first boosting injection against the BSA (purple bars) HCH bioconjugates (red bars).

Antisera titers were evaluated along time with a non-competitive ELISA, measuring the absorbance related to the binding of serial dilutions of each antiserum with their corresponding BSA hapten conjugates. Unexpectedly, the antibody titers were very low. The first hypothesis for this lack of response was

to attribute the cause to a potential error or mistake during the immunization. However, D133- or C134-HCH was very well recognized since high absorbance values were achieved, which indicated that the immunization had taken place (see Figure 3.9). A second hypothesis for this lack of response was related to the BSA conjugates used to coat the microplates. The hydrophobic nature of the hapten (see Table 3.3, for the logP values of these insecticides) may have caused the hapten folding inside the protein, hindering in the way the recognition by the antibody. During the bibliographic research for the immunizing hapten design we noticed that most of the authors which decided to detect deltamethrin, were using BSA or OVA competitors for the competitive assay development. However, in most of the cases the competitor hapten was a derivative of the whole molecule of deltamethrin, lowering its LogP value, and therefore increasing its hydrophilicity [51, 60, 93, 96]. In those cases, it would not be expected a hapten folding, and therefore the conjugation to a protein carrier would not affect the antibody recognition. For the cases of the competitor with a higher LogP value, the add of an organic solvent (between 20 and 40% of methanol in most cases) was needed to develop the corresponding immunoassay [51, 92-94].

However, our approximation was focused on the preparation of new bioconjugates using more hydrophilic macrobiomolecules such as it could be dextrane.

Table 3.3. LogP_{ow} of different pyrethroids considered during the development of the deltamethrin ELISA

Pyrethroid	LogP _{ow} ^a
Deltamethrin	4.61
Cypermethrin	6.64

^aLogP_{ow} coefficient is related to the compound lipophilicity, differentiating 5 categories of lipophilicity degree: >5 very high; 3.5-5 high; 3-3.5 medium; 1-3 low; and <1 very low.
The parameter LogP_{ow} has been calculated using the software ACD/logP calculator.

For the HCH bioconjugates this behavior could not have had a significant impact because the immunological cascade involves a first step in which the molecules is digested by the macrophages to small peptide portions

3.3.1.4.1 Development of aminodextran bioconjugates as coating antigens

Aminodextran was selected as the carrier for C134 and D133 competitor's conjugation for being a hydrophilic polysaccharide, thus avoiding any hydrophobic nest for the hapten folding. Furthermore, the presence of amino groups in the polymer, allows the covalent coupling through the carboxylic groups on the haptens. AD could not be analyzed by MALDI-TOF-MS and for that reason, competitors linked to AD were further evaluated by checkerboard titration assays.

Higher responses at higher antisera dilutions were obtained when the non-competitive assays were performed against aminodextran conjugates, for which reason we decided to pursuit with further boosting injection until a total of six (see [section 3.6](#)). Figure 3.10 shows the evolution of the antibody titers recorded for both immunogens.

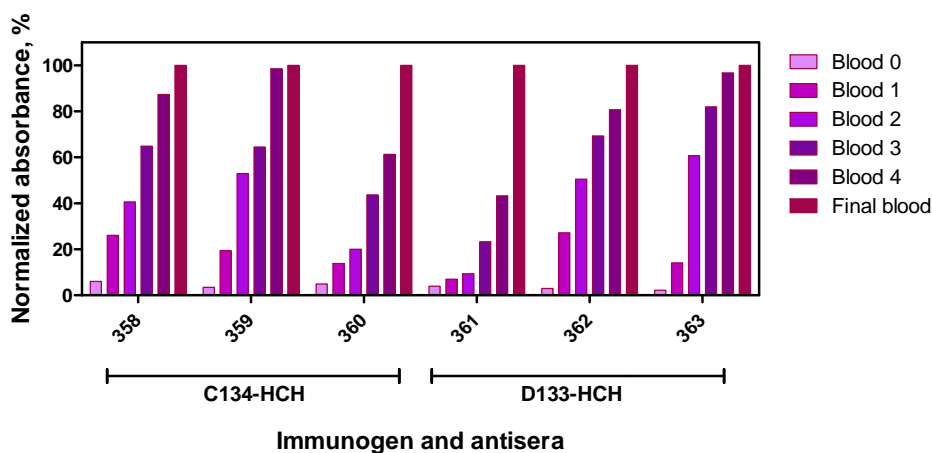


Figure 3.10. Antibody titer to evaluate the response of the antisera produced by non-competitive ELISA. Antigen had a concentration of $1 \mu\text{g mL}^{-1}$, antisera were used at a dilution of $1/32000$ for As358 and 359; and a dilution of $1/64000$ for As360-363.

3.3.1.5 Competitors conjugation

In addition to the homologous ones C134-AD and D133-AD, a set of other heterologous competitor haptens were prepared and conjugated to AD as well, with the aim to favour the competition of the target analyte for the binding sites of the antibody. It has been reported that the bioconjugate competitor can modulate parameters such as sensitivity and detectability [97]. Competitors with higher heterology could have lower affinity for the antibodies and then the equilibrium could be displaced favoring analyte detection. Heterologous competitor haptens based on cypermethrin moieties (F1-F3, for exploring the importance of the double ring structure on the antibody recognition profile), and 3-phenoxybenzaldehyde (3-PBA, molecule without the antigenic part of halogens presents in deltamethrin) were proposed [98] (see Figure 3.11).

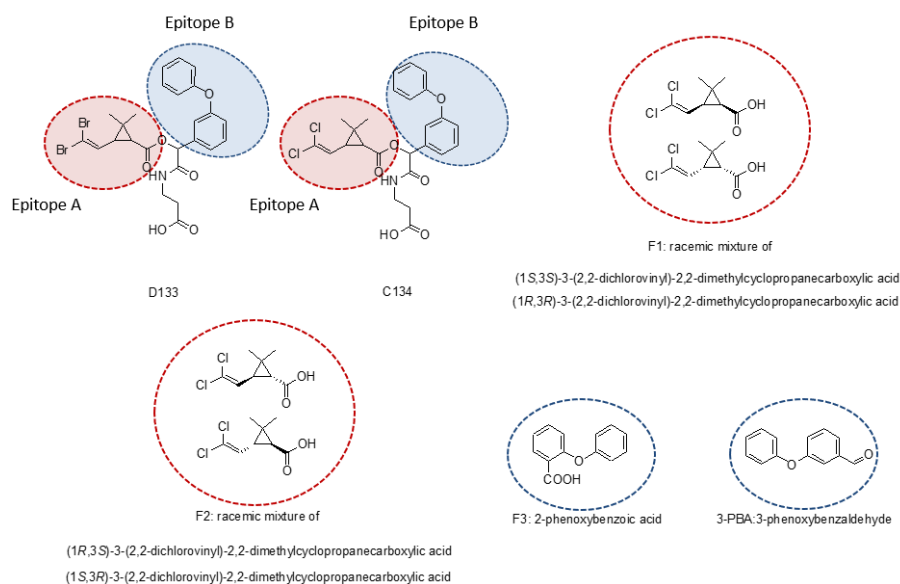


Figure 3.11. Structure of the haptens D133 and C134 with their different epitopes. Structures of the fractions F1-F3 and 3-PBA including the epitopes they resemble.

Since these haptens had medium values of $\log P_{ow}$ (between 1 and 3) their conjugation was performed directly to BSA instead of AD. The strategy selected for those conjugations was the active ester methods, using carbodiimide/N-hydroxysuccinimide chemistry. For each competitor hapten, distinct bioconjugates were prepared with different hapten densities (see Table 3.4), since it has also been described that lower hapten densities rend assays with better IC_{50} values.

Table 3.4. Densities of the heterologous competitors prepared ^a	
Immunoreagents	δ -hapten ^b
F1-BSA	16-10-8-7-4-2
F2-BSA	17-10-9-6-5-3-2
3-PBA-BSA	20-7-4-2
^a Analysis were performed by MALDI-TOF-MS. ^b Mols of hapten per mol of protein.	

All the combinations of antibodies raised, and newly heterologous competitors were tested in an inhibition assay in which the analytes, deltamethrin and cypermethrin, were added at a high concentration of 50 μ M to evaluate possible inhibition. The combinations which showed a minimum inhibition level (20%), were tested in a two-dimensional checkerboard titration format to select the appropriate concentration of the immunoreagents and subsequently on competitive assays by building calibration curves. Unfortunately, as it can be seen in Table 3.5 any heterologous antisera/antigen combination showed detectabilities in the low nanomolar range. In contrast, the homologous aminodextran bio conjugates performed much better, even though the detectability achieved was not in the low nM range as it was expected.

The combination which showed the best sensitivity and detectability parameters were As360 (raised against C134-HCH, cypermethrin) and its homologous coating antigen C134-AD. The fact that the antiserum raised against a chlorinated compound (cypermethrin) recognize better the brominated derivative (deltamethrin) has been previously reported [99, 100]. Between the hypotheses to explain this fact there is the size of the bromine atoms, bigger than the chlorine atoms, and therefore, fitting better into the antibody binding cavities, favoring the antibody recognition of the deltamethrin. Another explanation relies in the differences of the electronic distribution between chlorinated and brominated analogues, which could create differences in dipole-dipole interactions in the antigen-antibody complex.

Table 3.5. Immunoassay features of some competitive ELISA combinations for cypermethrin and deltamethrin detection.^a

Assay	Immunogen	Analyte	A _{max}	A _{min}	IC ₅₀ , nM	Slope	R ²
As360/D133-AD	C134-HCH	Deltamethrin	0.753	0.157	1504	-0.959	0.994
As360/C134-AD			0.987	0.05	332.5	-0.834	0.999
As361/ 3-PBA ₇ -BSA	D133-HCH		1.730	0.329	11211	-1.063	0.996
As361/F1 ₂ -BSA			0.813	0.195	3191	-0.968	0.969
As361/F2 ₃ -BSA			0.713	0.114	3014	-0.765	0.977
As360/D133-AD	C134-HCH		Cypermethrin	0.721	0.06	1130	-1.020
As360/C134-AD		0.858		0.001	1334	-0.996	0.995
As361/ 3-PBA ₇ -BSA	D133-HCH	1.728		0.061	5732	-0.881	0.996
As361/F1 ₂ -BSA		0.926		0.079	3325	-1.133	0.987
As361/F2 ₅ -BSA		0.875		0.089	3110	-1.008	0.997

^aOnly the best assay for each heterologous competitor is shown.

This pair of immunoreagents produced an ELISA assay capable of detect deltamethrin directly in seawater with an IC₅₀ around 330 nM (166 µg L⁻¹), and cypermethrin with an IC₅₀ around 1330 nM (553 µg L⁻¹), values far away from the detectability achieved by other assays reported in the literature (see Table 3.1 above). For that reason, some physicochemical parameters (Tween20 concentration, pH, conductivity, competence time and the option of add a preincubation step of the assay) were assessed. with the aim of trying to improve the features of the final ELISA.

However, at this point, and although the two pyrethroids were interesting to monitor, in order to to meet the requirements of the european project to which the thesis is associated, only the ELISA development for deltamethrin was continued.

3.3.2 EVALUATION OF DIFFERENT PHYSICO-CHEMICAL PARAMETERS ON THE AS360/C134-AD ASSAY

Standard calibration curves were built and measured in the ELISA under different conditions, varying one parameter individually each time. The Tween20 concentration in the assay buffer was tested at concentrations between 0 and 0.1%, the conductivity from 5.4 to 93 mS cm⁻¹, the pH value was studied from 2.5 to 11.5, competition time was tested between 5 and 60 min and the effect of the preincubation of the antibody with the analyte was evaluated from 5 to 60 min. The value that gave a lower IC₅₀ maintaining good levels of absorbance was selected for each and used in the next assay.

Figure 3.12 shows the result of these studies. The sensibility of the assay was improved up to an order of magnitude, reducing the concentration of Tween20 down to 0.005% and increasing the conductivity of the buffer up to 28.5mS/cm. An improvement on the IC₅₀ was observed when reducing the time of competence, but this improvement was related to the absorbance decrease, so finally it was decided to maintain this parameter at the standard value, 30 minutes. No improvement was observed when a preincubation step of the analyte with the antibodies was introduced. Regarding pH, the assay was very stable between 4.5 and 10.5, without significant variations in the IC₅₀ or in the Amax of the assay.

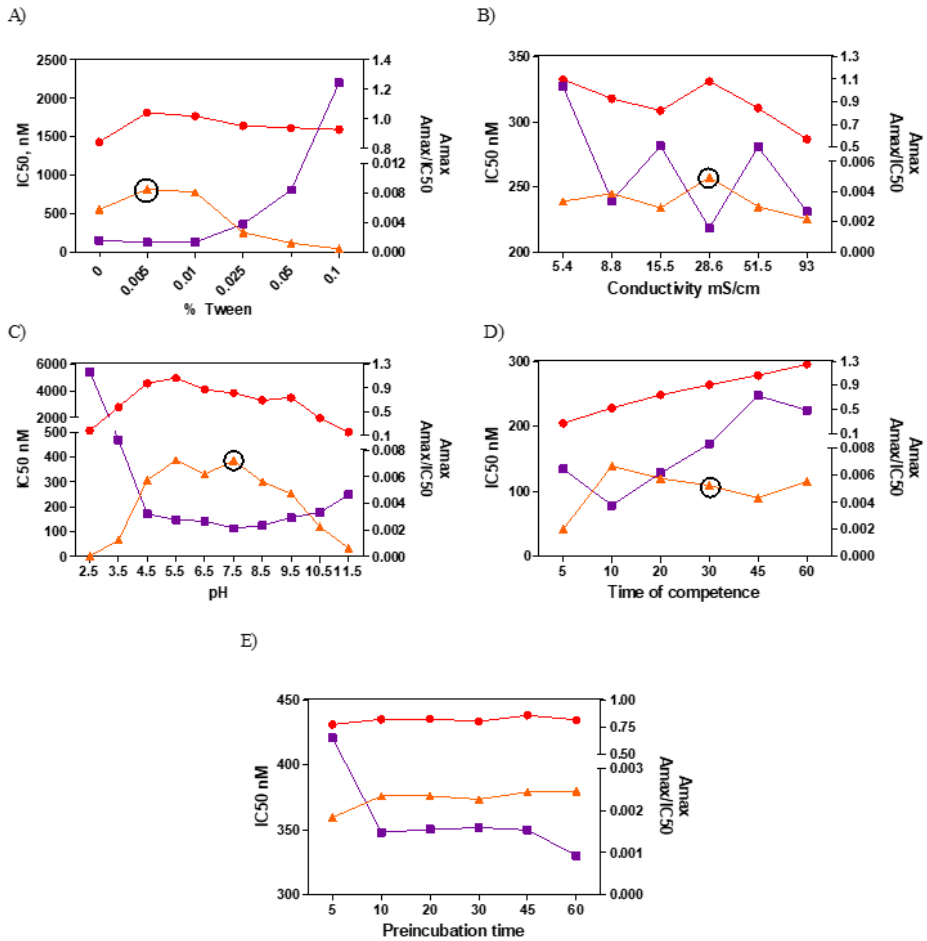


Figure 3.12. Effect of different physico-chemical parameters on the As360/C134-AD immunoassay. Effect of: A) Concentration of Tween20; B) Conductivity (ionic strength); C) pH; D) Competition time; E) Preincubation time. At least three-well replicates were employed for each assay. Left axis indicates the value of the IC₅₀. Right axis indicates the difference of absorbance and the ratio (A_{max}/IC_{50})*100. The IC₅₀ values are expressed in nM.

3.3.3 MATRIX STUDIES: ARTIFICIAL SEAWATER

Because of the low detectability of the assay, our goal was to be able to analyze seawater without the need to dilute the sample or to carry out a sample pre-treatment to minimize the matrix effect. Therefore, the assay was carried out directly in artificial seawater, a matrix characterized by high concentration of salts and therefore a high conductivity. Previously, we have already seen that

the assay performs quite well within 8 and 90 mS cm⁻¹ (only a mild loss of the maximum signal was observed at the conductivity levels associated with the artificial seawater used during the matrix effect studies, which were around 50 mS cm⁻¹).

As it can be observed in Figure 3.13, maintaining the same antibody dilution only a mild signal loss was observed as expected by the previously explained. Furthermore, the sensibility of the assay was in the same range that the buffer assays, demonstrating a practically null matrix effect on the detection of deltamethrin.

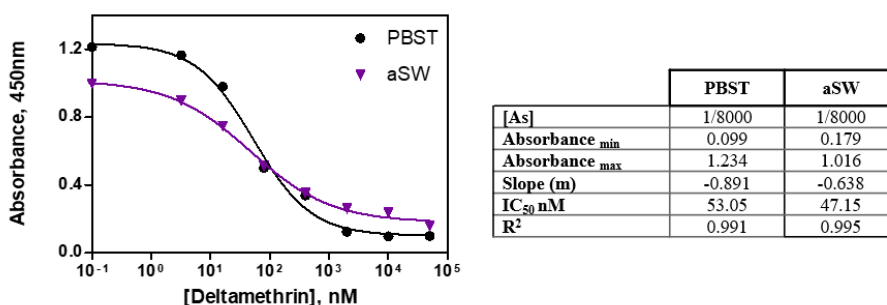


Figure 3.13. Performance of the As360/C-134-AD assay in artificial seawater. The calibration curve was built in DMSO 200 times concentrated and finally diluted in sea water prior the assay. The antiserum was diluted in PBT optimized buffer. Two replicates were assayed in each curve.

3.3.4 EVALUATION OF THE AS360/C134-AD ELISA

Figure 3.14 shows the calibration of the assay corresponding to the average of 3 assays performed on different days using three-well replicates. The final features of the assay regarding immunoreagents concentrations or physicochemical parameters are also listed. As it can be observed the variability between days was very low, obtaining a final IC₅₀ value of 21.4 ± 0.3 µg L⁻¹ and a limit of detection of 1.2 ± 0.04 µg L⁻¹, similar to the ones described in the literature, but without the need of adding solvents nor cleanup's samples procedures. Moreover, the average of %CV in the linear range (2.97 to 854 µg L⁻¹) is less than 15% in all the cases, demonstrating the robustness of the assay.

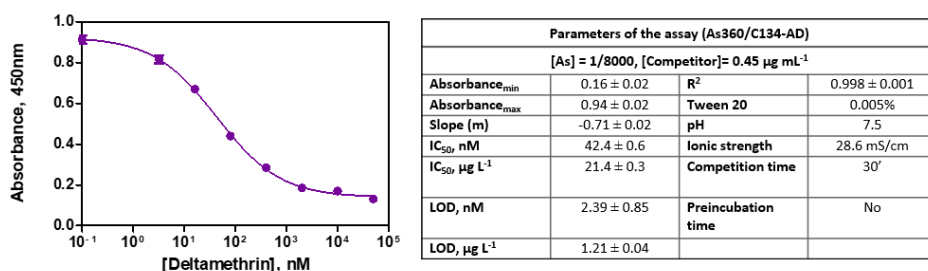


Figure 3.14. Analytical features for As360/C134-AD assay. The data showed correspond to the average of three assays performed on three different days. Each assay was built using three well replicates. LOD corresponds to limit of detection, calculated as the concentration given at 90% of the maximum signal.

3.3.4.1 Selectivity studies

With the aim of study the specificity of the ELISA assay established, compounds which are structurally related to deltamethrin as well as other pyrethroids like cypermethrin, esfenvalerate, permethrin, 3-phenoxybenzaldehyde and λ-cyhalothrin were tested as target analytes (see Figure 3.15).

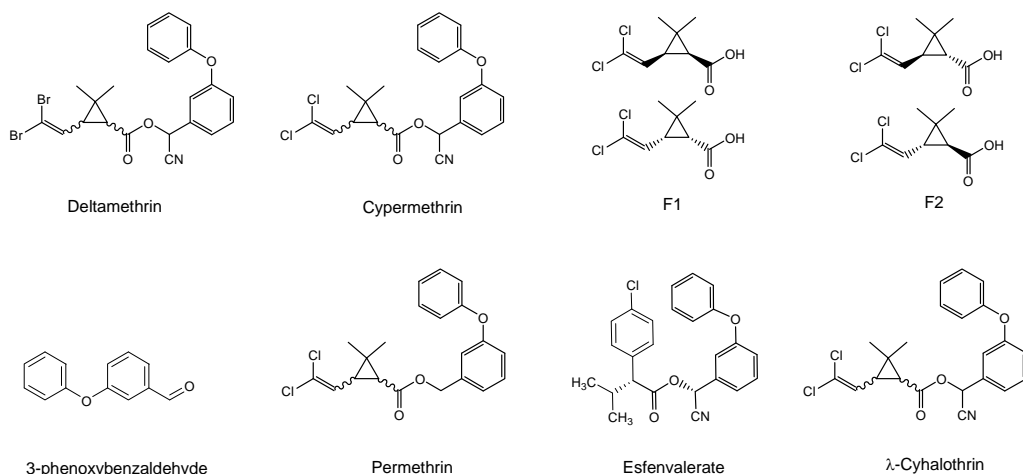


Figure 3.15. Chemical structure of similar compounds to deltamethrin used in cross-reactivity studies. F1 and F2 corresponds to different fractions purified after the hydrolysis of cypermethrin (described in Figure 4.3).

Table 3.6 summarizes the IC_{50} and cross-reactivity results for each compound, showing that the antibody raised and selected for this study presented high specificity for deltamethrin, but recognizes all the pyrethroids that share the 2,2-dimethyl-ciclopropane group, or one of the terminal halogens atoms. Additionally, other contaminants usually found in environmental samples, such as antibiotics, pesticides, or toxins, were also tested. Other environmental pollutants were tested such as Irgarol 1051[®], sulfapyridine, chloramphenicol, BDE-47, 17 β -estradiol and domoic acid, the pollutants selected for the development of the multiplexed microarray platform explained in [Chapter 5](#), but any of them reported significant cross-reactivity levels.

3.3.4.2 Accuracy assays of the final platform

Accuracy assays were carried by preparing blind samples spiking artificial seawater with 9 different concentrations of deltamethrin (Figure 3.16) which were analyzed blindly by ELISA. As it can be observed, spiked values closely match the results obtained plotting a linear regression of a slope of 0.904, close to the perfect correlation.

Table 3.6. Cross-reactivity of related compounds in the As360/C134-AD assay.

Compound	IC_{50} (nM)	% CR
Deltamethrin	42	100
Permethrin	307	13
Cypermethrin	189	22
Esfenvalerate	218	19
λ -Cyhalothrin	185	22
3-Phenoxybenzoic acid	> 10000	<0.05
F1	> 10000	<0.05
F2	> 10000	<0.05
Irgarol 1051 [®]	> 10000	<0.05
Sulfapyridine	> 10000	<0.05

Chloramphenicol	> 10000	<0.05
BDE-47	> 10000	<0.05
17 β estradiol	> 10000	<0.05
Domoic acid	> 10000	<0.05
^a Cross-reactivity is expressed as a percentage of the relation between the IC ₅₀ (nM) of deltamethrin and the IC ₅₀ (nM) of the other compounds tested.		

The results demonstrate that the assay is suitable for the detection of trace levels of deltamethrin in water without any sample cleanup nor pretreatment.

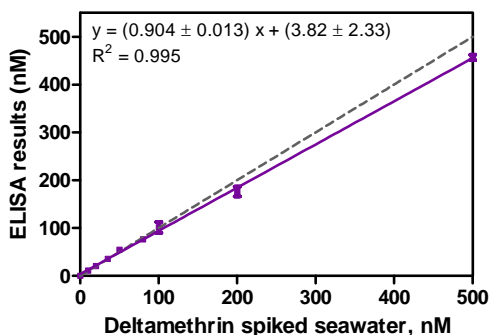


Figure 3.16. Results from the accuracy study performed in artificial seawater in the ELISA format. The graph shows the correlation between the spiked and measured concentration values. The dotted line corresponds to a perfect correlation ($m = 1$). The data correspond to the average of at least three-well replicates from 3 different days.

3.4 Chapter contributions

- Aminodextran conjugates have been reported as a great proposal in comparison to standard carrier proteins in dealing with high lipophilic haptens such as the pyrethroids studied in this chapter. Lower concentrations of immunoreagents could be used if the hapten is forced to be accessible during immunorecognition's events.

- Although any heterologous competitor could be used for the development of an ELISA assay for the detection of deltamethrin, a final immunoassay with a LOD of $1.2 \mu\text{g L}^{-1}$, a value in the range of the ones reported in the literature has been established using the homologous competitor.

3.5 Materials and methods

Reagents, materials and equipment. The chemical reagents used were obtained from Aldrich Chemical Co. (Milwaukee, WI, USA) and from Sigma Chemical Co. (St. Louis, MO, USA). The preparation of the immunoreagents used is described below. The matrix-assisted laser desorption ionization time-of-flight mass spectrometer (MALDI-TOF-MS) was a Bruker autoflex III Smartbeam spectrometer (Billerica, Massachusetts). The pH and the conductivity of all buffers and solutions were measured with a pH-meter pH 540 GLP and a conductimeter LF 340, respectively (WTW, Weilheim, Germany). Polystyrene microtiter plates were purchased from Nunc (Maxisorp, Roskilde, Denmark). Dilution plates were purchased from Nirco (Barberà del Vallés, Spain). Washing steps were performed on a Biotek ELx465 (Biotek Inc.). Absorbances were read on a SpectramaxPlus (Molecular Devices, Sunnyvale, CA, USA). The competitive curves were analyzed with a four-parameter logistic equation using the software SoftmaxPro v4.7 (Molecular Devices) and GraphPad Prism 5.03 (GraphPad Software Inc., San Diego, CA, USA). For the matrix studies, artificial seawater (aSW) was purchased from Sigma Chemical Co. (St. Louis, MO, USA), prepared at 40 mg mL^{-1} in MilliQ water; its pH and conductivity were monitored being 8.14 ± 0.27 and 49.69 ± 1.51 respectively ($n=20$).

C134-HCH and D133-HCH preparation by mixed anhydride method. C134 and D133 ($10 \mu\text{mol}$ s) were dissolved in $100 \mu\text{L}$ DMF anh. Then, a solution of tributylamine ($12 \mu\text{mol}$ s) and isobutylchloroformate ($11 \mu\text{mol}$ s) were added to the hapten, dropwise, under N_2 atmosphere and in an ice bath. The mixture was stirred for 30 minutes. The activated haptens were added dropwise to a solution of 10 mg of hemocyanin from *limulus polyphemus hemolymph* (HCH) in 1.8 mL borate buffer. The reaction mixture was gently stirred for 4 hours at r.t.

C134-BSA, D133-BSA, F1-BSA and F2-BSA preparation by active ester method.

Each hapten (C134, D133, F1 and F2; 10 μmol s) were dissolved in 100 μL DMF anh. A solution of N, N'-dicyclohexylcarbodiimide (DCC) (50 μmol s) in 50 μL DMF and a solution of N-hydroxysuccinimide (NHS) (25 μmol s) in 60 μL DMF were added sequentially. The mixture was stirred for 3 hours for either cases, or until a white precipitate appeared. The suspension was centrifuged at 10000 rpm for 10 min. The supernatant was added dropwise to a solution of 10 mg of albumin from bovine serum (BSA) in 1.8 mL borate buffer. The reaction mixture was gently stirred for 4 hours at r.t.

3-PBA-BSA preparation by reductive amination method. 3-PBA (10 μmol s) were dissolved in 100 μL DMF anh. The hapten was added dropwise to a a solution of 10 mg of albumin from bovine serum (BSA) in 1.8 mL carbonate buffer., followed by 50 μL of sodium cyanoborohydride (NaBH_3CN) (40 mg mL^{-1} in NaOH 1M). The solution was allowed to react 4.5 hours at r.t.

C134-AD and D133-AD. These competitors were prepared by both, mixed anhydride and active ester methods, already described.

All the protein conjugates were purified by dialysis against 0.5 mM PBS (4 \times 5 L) and Milli-Q water (1 \times 5 L) and were stored frozen at -40 $^{\circ}\text{C}$. Unless otherwise indicated, working aliquots were stored at 4 $^{\circ}\text{C}$ in 0.01 M PBS at 1 mg mL^{-1} . Hapten densities of the bioconjugates were estimated by measuring the molecular weight of the native proteins and the MW of the conjugates by MALDI-TOF-MS. Because HCH is not able to be analyzed by MALDI, simultaneously to preparing the immunogen, the hapten was also conjugated to BSA. However, we assume that this result can be correlated with the hapten density of the immunogen. The mass spectrum was obtained by crystallization of the corresponding matrix (sinapinic acid, 2 μL of 10 mg mL^{-1} in a 70:30 solution of ACN / H₂O and 0.1% in HCOOH), followed by 2 μL of sample, or 2 μL of the reference sample (BSA, 5 mg mL^{-1} in 50:50 ACN / H₂O and 0.1% in HCOOH). Finally, after evaporation of the solution deposited on the plate, 2 μL of the matrix was added again. The hapten densities (δ hapten) were calculated according to the following equation: $[\text{MW}(\text{conjugate}) - \text{MW}(\text{protein})] / \text{MW}(\text{hapten})$.

Buffers. Unless otherwise indicated, phosphate buffer saline (PBS) is 0.01 M phosphate buffer in a 0.8% saline solution, pH 7.5. Coating buffer is a 0.05 M carbonate-bicarbonate buffer, pH 9.6. PBST is PBS with 0.05% Tween 20, pH 7.5.

PBST optimized is PBS with 0.005% Tween 20, 1.6% saline solution, pH 7.5. Citrate buffer is 0.04 M sodium citrate, pH 5.5. The substrate solution contains 0.01% 3,3',5,5'-tetramethylbenzidine (TMB) and 0.004% H₂O₂ in citrate buffer. Borate buffer is 0.2 M boric acid/sodium borate, pH 8.7.

Polyclonal antisera. Antisera were obtained by immunizing female white New Zealand rabbits with C134-HCH were named As358, As359 and As360 and with D133-HCH were named As361, 362 and 363. Evolution of the antibody titer was assessed on a non-competitive indirect ELISA, by measuring the binding of serial dilutions of the different antisera to microtiter plates coated with a fixed concentration of hapten-AD (1 µg mL⁻¹). After 6 immunizations, the animals were exsanguinated, and the blood was collected in vacutainer tubes provided with a serum separation gel. Antisera were obtained by centrifugation at 4°C for 10 min. at 10000 rpm and stored at -80 °C in the presence of 0.02% NaN₃. Unless otherwise indicated, working aliquots were stored at 4 °C.

Non-competitive indirect ELISA. The screening of the avidity of the antisera (As358-363) with the different antigens (C134-AD, D133-AD, F1-BSA, F2-BSA, F3-BSA, and its corresponding densities varieties) was evaluated. Two-dimensional titration assays (2D-assay) were carried out based on the measurement of the binding of serial dilutions of the antisera (1/1000 to 1/64000, and zero, 100 µL well⁻¹) against different concentration of the antigens (10 µg mL⁻¹ to 10 ng mL⁻¹, and zero; 100 µL well⁻¹). From these experiments, optimum concentrations for coating antigens and antisera dilutions were chosen to generate around 0.7-1 units of absorbance.

Competitive ELISA C134-AD/As360 for the detection of Deltamethrin. Microtiter plates were coated with the antigen C134-AD (0.45 µg mL⁻¹ in coating buffer, 100 µL well⁻¹), overnight at 4 °C and covered with adhesive plate sealers. The next day, the plates were washed four times with PBST (300 µL well⁻¹), and the solution of deltamethrin (stock from 2000 to 0 µM in DMSO and diluted 200 times in PBST or aSW) or the samples, were added (50 µL well⁻¹), followed by the solution of antisera As360 (1/8000 both in PBST, and PBT2x, 50 µL well⁻¹). After 30 min at r.t., the plates were washed as mentioned before, and a solution of anti-IgG-HRP (1/6000 in PBST) was added to the wells (100 µL well⁻¹) and incubated for 30 minutes at r.t. The plates were washed again, and the substrate solution was added (100 µL/well). Color development was stopped after 30 min at r.t. with 4 N H₂SO₄ (50 µL/well), and the absorbance was read at 450 nm. The

standard curves were fitted to a four-parameter equation according to the following formula: $y = (A - B/[1 - (x/C)^D]) + B$, where A is the maximal absorbance, B is the minimum absorbance, C is the concentration producing 50% of the maximal absorbance, and D is the slope at the inflection point of the sigmoid curve. Unless otherwise indicated, data presented correspond to the average of at least three wells replicates.

Physicochemical parameters optimization. The effects of different physicochemical parameters related to the final matrix and the buffer selected for the development of the assays were tested introducing variations in the initial conditions of the assay. The study included Tween 20 concentration, pH, ionic strength, pre-incubation time and competition time.

Specificity studies. Solutions of different structurally-related compounds such as cypermethrin, cypermethrin fractions (F1 and F2), λ -cyhalothrin, esfenvalerate, permethrin, 3-phenoxybenzaldehyde, (see Figure S3). The standard curves were performed following the protocol described before. The cross-reactivity (CR) values were calculated according to the equation: IC_{50} [nM] (Deltamethrin)/ IC_{50} [nM] (cross-reactant) $\times 100$.

Matrix Effect Studies. Non-specific interferences produced by the parameters associated with the matrix of interest were studied by preparing a standard curve directly in seawater. During the development of the deltamethrin assay in seawater, the As concentration was optimized. The antiserum dilution for the Competitive ELISA C134-AD/As360 in aSW, was tested again, in a non-competitive indirect ELISA; from 1/1000 to 1/64000 dilution in PBT 2x. Thereafter, all immunoassays performed were done with a 1/8000 antisera dilution in PBT2x for calibration curves in aSW.

Reproducibility studies. The assays were carried out three times within three different days, with three replicates for each one. The main features of the final assay were described as the mean of all the replicates.

Recovery studies. The recovery of the analyte concentration after the sample treatment was assessed by spiking blank aSW at 9 different concentrations (from 10 to 500 nM, including a zero). The sample concentrations were calculated interpolating the results to deltamethrin standard curves prepared in aSW. The

results were fitted to a linear regression curve between the spiked concentrations and the measured ones

4 DEVELOPMENT OF A MULTIANALYTE ELISA PLATFORM FOR THE DETECTION OF ENVIRONMENTAL POLLUTANTS IN SEAWATER

4.1 Introduction

Nowadays, because of the high variety of human activities, a huge variety of contaminants can be found in aquatic environments.

4.1.1 POLLUTANTS IN AQUATIC ENVIRONMENTS

Since some years a great effort has been invested to understand the origin, fate and levels of pollutants in aquatic environments. In this context, the European Commission establishes EQS, to limit the concentrations of certain chemical substances that pose a significant risk to the environment or to human health in surface waters in the European Union (EU). However, a great challenge is that most of the concerning chemical pollutants are found at very low concentrations in marine environments (see Table 4.1).

Among the great different groups of pollutants that can arrive to the ocean, some of them are of relevance because of their negative impact in offshore aquaculture; such is the case of the endocrine disruptor chemicals (EDCs). EDCs are substances that can interfere with the endocrine system and the hormonal activity of the aquatic organisms and have been linked to damages at the larval and adult stages of fishes, disrupting their sexual development, behaviour and fertility.

Another group of interests are the so called persistent organic pollutants (POPs), contaminants that due to their chemical properties are persistent in the environment and can bioconcentrate in certain organisms and be toxic. In fact, these persistent and bioaccumulative substances are becoming a great concern within the marine initiatives developed towards the protection of the marine seawater and biodiversity due to its long-time linked consequences.

Antibiotics and pesticides are classes of concerning pollutants which are indiscriminately used in intensive production in aquaculture to ensure the growth and survival of fishes and seafood. These chemicals not only can have a

Table 4.1. Examples of analytes with different chemical natures (represented by their LogP values), their environmental quality standard (EQS) and their reported levels in aquatic environments.

Analyte	Contaminant type	EQS ^b	ACD/LogP	Levels reported ($\mu\text{g L}^{-1}$)
Irgarol 1051 [®]	Herbicide	2.5 ng L ⁻¹	3.27	0.013 – 2 [101, 102]
Sulfapyridine	Antibiotic	-	0.03	0.05 - 0.3 [103, 104]
Chloramphenicol	Antibiotic	-	1.02	0.001 - 0.2 [105, 106]
Polybrominated diphenyl ether: BDE-47	POP ^a	2.4 fg L ⁻¹	7.39	0.004 - 0.11 [107, 108]
17 β - Estradiol	Hormone	80 pg L ⁻¹	4.13	0.004 - 0.016 [109, 110]
Domoic acid	Algal toxin	-	0.61	0.02 – 13 [111, 112]

^a Persistent Organic Pollutant.
^b Set by Water Framework Directive 2000/60/EC (WFD).

negative environmental effect, but also can be absorbed by fish and finally enter into the food chain. Furthermore, these non-natural conditions produced within the aquaculture facilities have been related to the proliferation of algal blooms. Some algae under certain temperature, light, deprivation of nutrients or competition against microorganisms can produce toxins that can be accumulated in seafood or fish and cause several negative effects such as intoxications or even deaths.

Due to the huge variety of pollutants to be monitored, we have been used certain criteria to establish the most important priorities. These principles have been:

1. Their impact in offshore aquaculture.
2. Their actual use in aquaculture facilities.

4. Development of a multianalyte ELISA platform for the detection of environmental pollutants in seawater.

3. The possibility of using them as markers of water quality.
4. Their persistence in the environment and bioaccumulation possibilities

Following these criteria, a panel of chemical pollutant families was initially proposed as priority to be monitored under regular manner in the marine environment. Within each family, a representative congener was selected also based in the above-mentioned criteria together with the frequency of use or based on the reported cases in which these chemicals have been detected (see Table 4.2). Within the next sections, the environmental relevance of each of these chemicals selected will be explained.

Table 4.2. Selection of chemicals for monitoring

Contaminant family	Target selected
Biocide (antialgae)	Irgarol 1051®
Antibiotic	Sulfapyridine
Antibiotic	Chloramphenicol
Insecticide	Deltamethrin
Industrial contaminant	Polybrominated diphenyl ether: BDE-47
Hormone	17 β - Estradiol
Algal toxin	Domoic acid

4.2 Chapter objective

With this scenario, the goal of the research reported in this chapter (Figure 4.1) has been the development of a multiplexed bioanalytical platform to detect a panel of the some of the most representative or relevant pollutants in the marine environment. To achieve this purpose, we have first performed a literature research on the contaminants with a more negative impact in the environment and aquaculture facilities (see section 4.3, below). Subsequently, we have identified potential sources of immunoreagents targeting these substances. Prior developing the multiplexed platform, individual ELISAs have been

established in order to assess their analytical performance in seawater samples and developing compatible immunochemical protocols. Finally, the immunoreagents selected have been used in combination to develop a multiplexed ELISA.

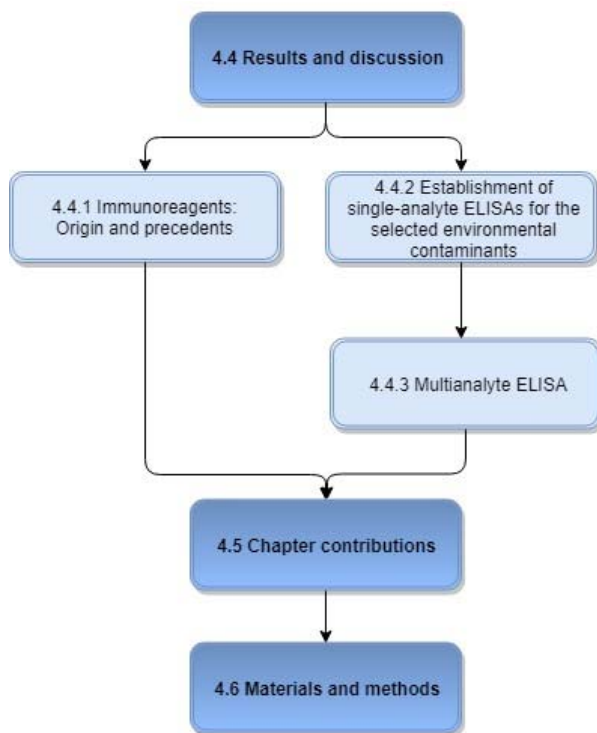


Figure 4.1. Structure of this chapter related to the different sections

4.3 Target Selection: Environmental Candidates

4.3.1 HERBICIDES: IRGAROL 1051®

Irgarol 1051® (see Figure 4.2) is an algaecide, an herbicide specifically designed for its use in marine antifouling coatings in combination with copper and zinc-based agents. Irgarol 1051® has a very low water solubility, a seawater half life

of 100 to 273 days [113] and a high partition coefficient, therefore having an extended antifouling action, and the ability to remain associated with sediments.

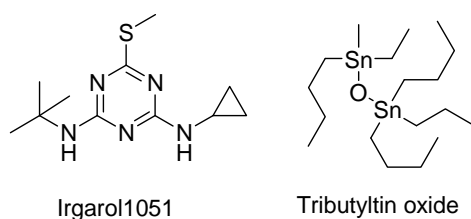


Figure 4.2. Irgarol 1051[®] and Tributyltin oxide chemical structures.

Historically, Irgarol 1051[®] was presented as a substitute of the agent Tributyltin (TBT). TBT, used as biocide and especially as a wood preservative had been one of the most recognized marine anti-fouling agent, but nowadays it is currently banned by the European Commission in the Mediterranean region. Before 1992, contamination of coastal waters by Irgarol 1051[®] was unknown, however, several studies revealed the presence of this herbicide across Europe after that. The EQS fixed for both fresh and salt water for Irgarol is 2.5 ng L⁻¹ [81] but higher levels have been detected in natural environments [102, 114, 115]. However, the most critical zones to consider are seaports, where the concentration of Irgarol 1051[®] can achieve levels up to 2000ng L⁻¹. [101, 116].

4.3.2 ANTIBIOTICS: SULFAPYRIDINE AND CHLORAMPHENICOL

The European Union has listed the antibiotics that can be used in aquaculture which include tetracyclines, penicillins, quinolones, trimethoprim and sulfonamides (EC Regulation n. 37/2010 of 22 Dec. 2009) [117]. Among all them, sulfonamides (SAs) (see Figure 4.3) are between the most frequently used in aquaculture. They are a group of synthetic antimicrobial agents that contain a sulfamide group, and have been detected at significant levels in many biological samples such as cow's milk [118, 119] and in superficial water resources [120].

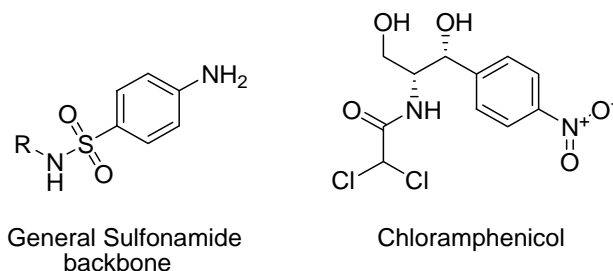


Figure 4.3. Sulfonamide general structure and Chloramphenicol chemical structure.

The second antibiotic selected for its detection in seawater samples is chloramphenicol. Chloramphenicol is a broad-spectrum antibiotic exhibiting activity against both gram-positive and gram-negative bacteria. As opposed to sulfapyridine, chloramphenicol is banned in the European Union, mainly due to its serious toxic effects in aquatic environments [121, 122] and in human health. Among the serious adverse effects chloramphenicol can have over human health the most important is bone marrow toxicity [123].

4.3.3 HORMONES: 17-B ESTRADIOL

There is a growing alarm about the potential effects of endocrine-disrupting pollutants in wildlife and humans. 17 β -Estradiol (E2) (see Figure 4.4) is the predominant natural female sex hormone and is the most active from the naturally occurring estrogenic hormones; being involved in mammalian prenatal development, growth, reproduction and sexual behaviour [124-126]. Furthermore, estradiol is one of the most active EDC, acting as an estrogen receptor agonist. The effect of such hormone-like compounds has been extensively studied in aquaculture. It is known that E2 at levels from 1 to 10 ng L⁻¹ have been linked to feminization of fishes [110], and even more disturbing, steroidal estrogens, including estradiol, can bioaccumulate in fish exposed to contaminated water [127, 128] and then arrive to the food chain. The EU has set-up as safe levels values which are much lower than those; thus, EQS concentrations of 80 and 400 pg L⁻¹ has been fixed in seawater and freshwater respectively [129].

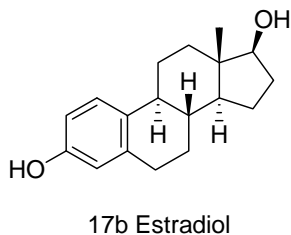


Figure 4.4. 17-β Estradiol chemical structure.

4.3.4 INDUSTRIAL CONTAMINANTS: POLYBROMINATED DIPHENYL ETHERS

Polybrominated diphenyl ethers (PBDEs) (see Figure 4.5) are brominated flame retardants consisting of a mixture of compounds used as additives for electronic equipment, plastics and even textiles since a long time ago. Polybrominated diphenyl ethers (PBDEs) [130, 131]. PBDEs are ubiquitous environmental contaminants and can bioaccumulate in wildlife, being classified as persistent organic pollutants.

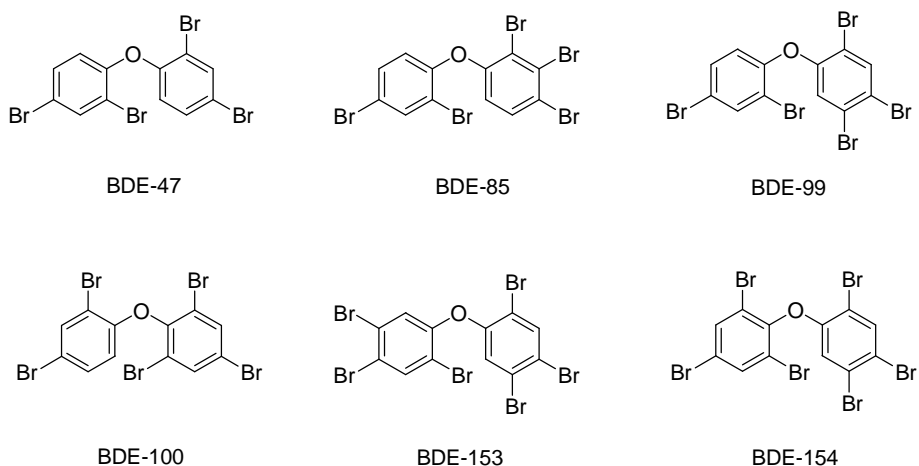


Figure 4.5. PentaBDEs formulation's composition: chemical structures of the mixture of PBDE congeners.

During several years, due to the similarities in chemical and structural features with polychlorinated biphenyls (PCBs), compounds known to be toxic, PBDEs

have been the focus of many studies [132, 133]. }. And although their use has been or banned or severely restricted several years ago, their persistence in the environment make them detectable even nowadays [134].

EQS of 49 fg L⁻¹ and 2.4 fg L⁻¹ in fresh and salt water respectively have been set [81], which indicates that its toxicity is remarkable. Some data suggest that the less bromo-substituted congeners are more toxic than the higher brominated [135, 136], and that together with being the most predominant BDE in pentaBDE formulation, makes BDE-47 an interesting candidate to be monitored.

4.3.5 ALGAL TOXINS: DOMOIC ACID

Toxic algal blooms are becoming an emerging problem for offshore aquaculture. These toxins can arrive to the consumers by the ingestion of the farmed fish or molluscs, causing a public health problem that must be minimized.

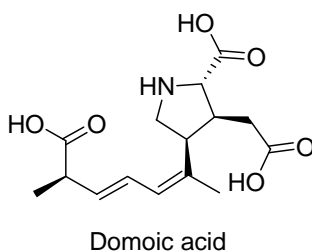


Figure 4.6. Domoic acid chemical structure

Domoic acid (DA) (see Figure 4.6) is a toxin produced by a few marine algae, including microalgae of the genus *Pseudo-nitzschia*, and is accumulated by shellfish filter-feeding during blooms [137]. DA and its isomers bind to and activate kainate receptors, causing neurological symptoms such as amnesia as well as gastrointestinal effects [138, 139]. For that reason, DA has been classified as an Amnesic Shellfish Poisoning [ASP] toxin. In 1987 in Canada occurred a food poisoning incident due to ingestion of mussel contaminated with DA. Since then, global awareness of DA has been raised [140]. Monitoring programs and control measures have been implemented around the world to prevent foodborne illness associated with DA in bivalves. Although these measurements have been successful in preventing other episodes of ASP, there are reports of intoxication

in wild animals, including sea lions and whales [141, 142]. During several years and periodically, reports of coastal water contamination in many world regions have been presented [143-145]. Therefore, early warning systems for monitoring the presence of this toxin in water samples are required.

4.4 Results and discussion

4.4.1 IMMUNOREAGENTS: ORIGIN AND PRECEDENTS

The immunoreagents for Irgarol 1051[®] (Irg)[146, 147], sulfonamide (SA)[148, 149] and chloramphenicol antibiotics have been developed previously by our group[147, 150]. Based in the literature, we identified several deltamethrin immunoreagents [51, 60, 92-96]. Although initial experiments were performed using the immunoreagents kindly given by Prof. Bruce Hammock (UC Davis, CA, USA), their performance in the multiplexed platform was not satisfactory. This is the reason because we addressed the development of antibodies and the corresponding ELISA as it has been described in [Chapter 3](#). For the case of BDE-47, the immunoreagents were kindly provided by Dr. Shelver (USDA- ARS, Fargo, North Dakota, USA) and its preparation has been described before [151]. The monoclonal antibodies for 17 β -estradiol were purchased from Fitzgerald Industries International (North Acton, Massachusetts, USA) and those used for domoic acid (DA) were kindly provided by the group of Prof. Chris Elliot (Queen's University, Belfast, UK) [152]. Finally, the corresponding bioconjugate competitors 6E2BSA (estradiol) and DABSA (DA) was performed in our laboratory as described below.

4.4.2 ESTABLISHMENT OF SINGLE-ANALYTE ELISAS FOR THE SELECTED ENVIRONMENTAL CONTAMINANTS

4.4.2.1 Bioconjugate preparation

As mentioned above, most of the immunoreagents (antibody and bioconjugate competitor) for the selected targets were already available, except for 17 β estradiol and DA, for which only the antibodies were found. Thus, we addressed the preparation of these bioconjugate competitors, as described in [section 4.6](#), by preparing the corresponding active esters using the carbodiimide/N-hydroxysuccinimide (NHS) chemistry. In both cases, 3 conjugates (A, B and C) with different hapten densities were prepared varying the quantity of activated hapten that was added to the BSA solution during the conjugation process. Hapten densities were measured by MALDI-TOF and are listed in Table 4.3.

Table 4.3. Hapten densities of different competitors produced				
Compound	Hapten	δ^a		
		A	B	C
17 β estradiol	6-OCMO	7	5	4
Domoic acid	DA	8	5	3
^a The hapten densities (δ hapten) were calculated according to the following equation: $\frac{[MW(\text{conjugate}) - MW(\text{protein})]}{MW(\text{hapten})}$				

The avidity of the antibodies for the bioconjugate competitors prepared was assessed by two-dimensional titration experiments. Finally, using competitive immunochemical conditions, the most suitable bioconjugate competitors were selected, being those with 4 and 5 hapten residues for 17 β estradiol and DA, respectively.

4.4.2.2 Single-analyte ELISAs.

Appropriate immunoreagent concentrations were selected by two-dimensional titration experiments for all the antibody/bioconjugate competitors to develop ELISAs with a maximum absorbance of around 1, selecting conditions in which the binding of the antibodies to the bioconjugate competitor is between 70- 80%. Using these concentrations, competitive ELISAs were established in both, buffer and in artificial seawater (aSW).

Although seawater is a matrix characterized by its particular mixture of salts providing a pH of 8.1 ± 0.2 ($N=20$) and a conductivity of 49.6 ± 1.5 mS cm⁻¹ ($N=20$), much higher than the conductivity of the PBS buffer used in most of the assay (10 mM PBS, 16.0 ± 0.5 mS cm⁻¹), as it can be observed in Table 4.4, the seawater did not affect significantly the performance of the assays. In the case of sulfonamide, a reduction in the maximum signal was observed, however the sensibility of the assay was maintained. In the case of chloramphenicol, a higher concentration of antibody was needed to obtain an absorbance similar to 1, and a great improvement in the assay's slope was observed. Finally, in the case of estradiol, also an improvement of the IC₅₀ was observed, however this improvement could be attributed to the lower signal obtained in the seawater assay.

Although the detectability achieved is quite good, as discussed previously, an important challenge of assessing marine contamination is to reach the detectability levels at which usually most of the organic pollutants are present (see table 4.1 above for EQS values and environmental levels reported for some of these pollutants). Half of the analytes detected in this chapter have not an EQS value set in the actual legislation, however, for the ones with existing EQS, the limits established by Marine legislations are far below the ones achieved in this work (see Table 4.1), and even for the reference techniques which has been proposed as standard detection methods [81].

Considering the potential use of the technologies developed in a real environment, to achieve the detectabilities required, it seemed clear that a preconcentration step had to be introduced. For this reason, in collaboration with the department of Environmental Chemistry from the Institute of Environmental Assessment and Water Research (IDAEA-CSIC), also participating in the Sea-on-a-Chip project, it was developed a solid-phase extraction (SPE)

procedure aimed at increasing the concentration of these pollutants in the seawater samples to be analysed.

Table 4.4. Analytical parameters for all the target assays in an ELISA format, performed both in buffer and directly in seawater.

	Irgarol 1051®		Sulfapyridine		Chloramphenicol	
ELISA	4eBSA/ As87		SA2BSA/ As155		CA6BSA/ As226	
Condition	PBST	aSW	PBST	aSW	PBST	aSW
[CA], $\mu\text{g mL}^{-1}$	0.25	0.25	0.25	0.25	0.0625	0.0625
[As] dilution	1/16000	1/16000	1/16000	1/16000	1/64000	1/32000
Abs_{min}	0.03 ± 0.02	0.04 ± 0.004	0.03 ± 0.02	0.019 ± 0.015	0.030 ± 0.01	0.03 ± 0.02
Abs_{max}	1.47 ± 0.09	1.46 ± 0.17	1.34 ± 0.08	0.839 ± 0.097	0.809 ± 0.02	0.984 ± 0.1
Slope	-0.98 ± 0.22	-1.06 ± 0.06	-0.784 ± 0.09	-0.95 ± 0.15	-0.60 ± 0.05	-0.82 ± 0.1
IC₅₀ (nM)	0.58 ± 0.19	0.43 ± 0.11	6.58 ± 1.73	7.41 ± 1.6	0.59 ± 0.05	0.94 ± 0.07
IC₅₀ ($\mu\text{g L}^{-1}$)	0.145 ± 0.05	0.111 ± 0.03	1.43 ± 0.23	1.84 ± 0.39	0.192 ± 0.09	0.324 ± 0.09
LOD ($\mu\text{g L}^{-1}$)	0.012 ± 0.007	0.015 ± 0.007	0.08 ± 0.02	0.12 ± 0.07	0.004 ± 0.01	0.019 ± 0.01
R²	0.996 ± 0.002	0.994 ± 0.004	0.992 ± 0.006	0.991 ± 0.005	0.995 ± 0.003	0.994 ± 0.004
	BDE-47		17β-Estradiol		Domoic acid	
ELISA	2,2,4triBDEBSA/ As122		6-OCMOBSA/MAb_E2		DABSA/MAb_DA	
Condition	PBST	aSW	PBST	aSW	PBST	aSW
[CA], $\mu\text{g mL}^{-1}$	1.25	1.25	0.3	0.3	0.6	0.6
[As] dilution	1/16000	1/16000	1/64000	1/64000	1/16000	1/16000
Abs_{min}	0.03 ± 0.001	0.04 ± 0.005	0.013 ± 0.003	0.012 ± 0.006	0.038 ± 0.01	0.07 ± 0.001
Abs_{max}	1.46 ± 0.19	1.34 ± 0.38	1.36 ± 0.20	0.902 ± 0.16	0.935 ± 0.12	1.08 ± 0.16
Slope	-0.720 ± 0.04	-0.720 ± 0.06	-1.01 ± 0.07	-0.958 ± 0.04	-0.866 ± 0.13	-0.788 ± 0.15
IC₅₀ (nM)	30.75 ± 5.18	24.41 ± 6.27	4.01 ± 0.74	2.84 ± 0.05	9.69 ± 1.05	9.77 ± 0.87
IC₅₀ ($\mu\text{g L}^{-1}$)	14.97 ± 2.52	11.86 ± 3.05	1.09 ± 0.20	1.02 ± 0.02	3.02 ± 0.33	2.82 ± 0.14
LOD ($\mu\text{g L}^{-1}$)	0.95 ± 2.52	0.593 ± 0.08	0.11 ± 0.03	0.10 ± 0.007	0.24 ± 0.02	0.17 ± 0.07
R²	0.998 ± 0.001	0.999 ± 0.001	0.990 ± 0.012	0.985 ± 0.023	0.996 ± 0.005	0.997 ± 0.002

^aThe parameters (Abs_{max}, Abs_{min}, slope, IC₅₀) were extracted from the four-parameter logistic equation used to fit the standard curves. The LOD was estimated as the concentration providing 90% of the maximum signal of the assay. The assays were performed using three-well replicates.

4.4.2.3 Improvement of the detectability required: Pre-concentration step.

SPE is the most frequently used procedure for clean-up, extraction and pre-concentration [153] of trace of pollutants from environmental [154], clinical [155], biological, food and beverages samples [156, 157]. In fact, most of the US Environmental Protection Agency (EPA) approved analytical methods for chemical residues [158] include SPE as recommended procedure for pre-treatment of organic pollutants.

The basic SPE protocol consists on:

1. Conditioning the column: usually the elution solvent followed by water, in case of aqueous samples
2. Sample loading
3. Washing.
4. Elution of the retained pollutants using the proper eluting phase, consisting on pure solvents or mixtures of them.

Between the advantages of SPE is worth to mention the possibility to perform rapid clean-up/preconcentration methods for an extensive diversity of substances (polar, non-polar, weak, or strong cationic or anionic substances, etc) and samples (biological fluids, water, aqueous or organic tissue extracts, etc) based on the wide variety of stationary phases (reversed- and normal phase, ion exchange, affinity, etc) nowadays available from several suppliers. Moreover, SPE methods are usually reproducible, providing high recoveries and clean extracts. The selectivity can be modulated by playing with different solvent mixtures, but in respect to classical liquid extraction methods, SPE uses low organic solvent volumes and do generate less waste. Nowadays, parallel and automated SPE methodologies allow establishing high-sample treatment throughput methodologies increasing the efficiency of the chromatographic technologies employed in most of the European Reference Laboratories. However, there has also been reported the use of SPE methods coupled to immunochemical assays [159, 160] (see Figure 4.7). The only limitation in such case, is to ensure the compatibility between the movil phase used for eluting the retained substances and the usual aqueous media of the immunochemical assay,

unless the SPE used is based on bioaffinity interaction with the targets, in which case the elution is usually performed with aqueous solvents.

In this work, considering the wide variety of chemical compounds with different chemical properties (In ex. Irgarol 1051[®] (ACD/LogP, 3.27) chloramphenicol (ACD/LogP, 1.02) brominated flame retardant BDE-47 (ACD/LogP, 7.39), etc.) that had to be analysed simultaneously and the high volume of seawater that will have to be used in order to accomplish pre-concentration of sometimes up to several orders of magnitude, the researchers of the department of Environmental Chemistry (IDAEA-CSIC) proposed to use two modules of SPE with different stationary phases: ISOLUTE[®] ENV+ with an hydroxylated polystyrene-divinyl benzene copolymer as the stationary phase; and OASIS HLB with a specific ratio of two monomers (the hydrophilic N-vinylpyrrolidone and the lipophilic divinylbenzene), a support characterized by a neutral polar profile. These stationary phases usually employ methanol, acetonitrile or some mixtures of them as solvents. For our purposes, it was mandatory to select solvents that were miscible in water for further analysis of the eluate in the multianalyte ELISA.

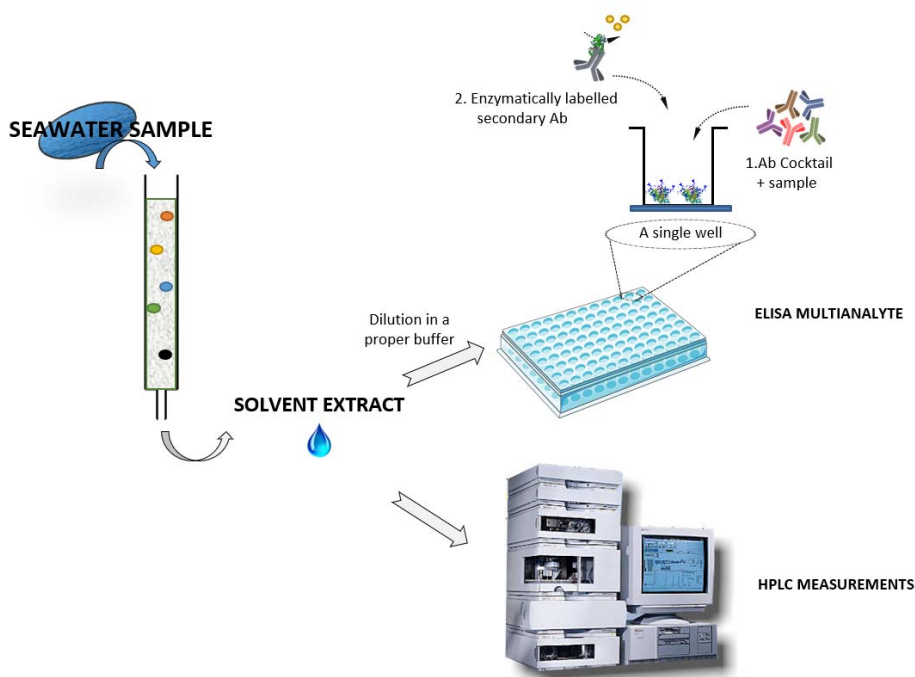


Figure 4.7. Left: Solid-phase extraction columns for the pre-concentration of the target analytes. Right: Analytical methods to be use within this study: multianalyte ELISA and HPLC for validation

Thus, it was proposed to use either DMSO or methanol, but there existed the risk that those solvents would have a negative effect on the performance of the assays. For this reason, first studies were addressed to investigate the tolerance of the immunochemical assays established to these organic solvents.

4.4.2.4 Solvent effect in the different ELISA assays

The SPE module selected was an ISOLUTE® ENV+ (220 mg, 6 ml, Biotage) for Irgarol 1051® and OASIS HLB (200 mg, 6ml, Waters) for the rest.

According to previous studies of the department of Environmental Chemistry (IDAEA-CSIC), the cartridge allowed to load up to 500 mL of environmental seawater and elute the target pollutants with a good recovery (76 to 98 %) in just 0.8 mL of pure organic solvent (DMSO or methanol) achieving a preconcentration factor of 625. However, usually immunoassays are not able to work in pure organic solvent, although there have been reported some cases in which it was possible to measure analytes in media of up to 50% organic solvent, this is not common. Thus, it is necessary to dilute the eluate in the assay buffer prior the quantification of the analytes by ELISA. Therefore, first studies were addressed to determine the percentage of solvent tolerated by the immunochemical assays for the different families, without a significant decrease of their performance in terms of detectability and maximum absorbance.

4.4.2.4.1 Effect of Methanol

The graphs in Figure 4.8 show the effect of increased concentrations of methanol in the assay buffer over the maximum signal and the detectability of the assays.

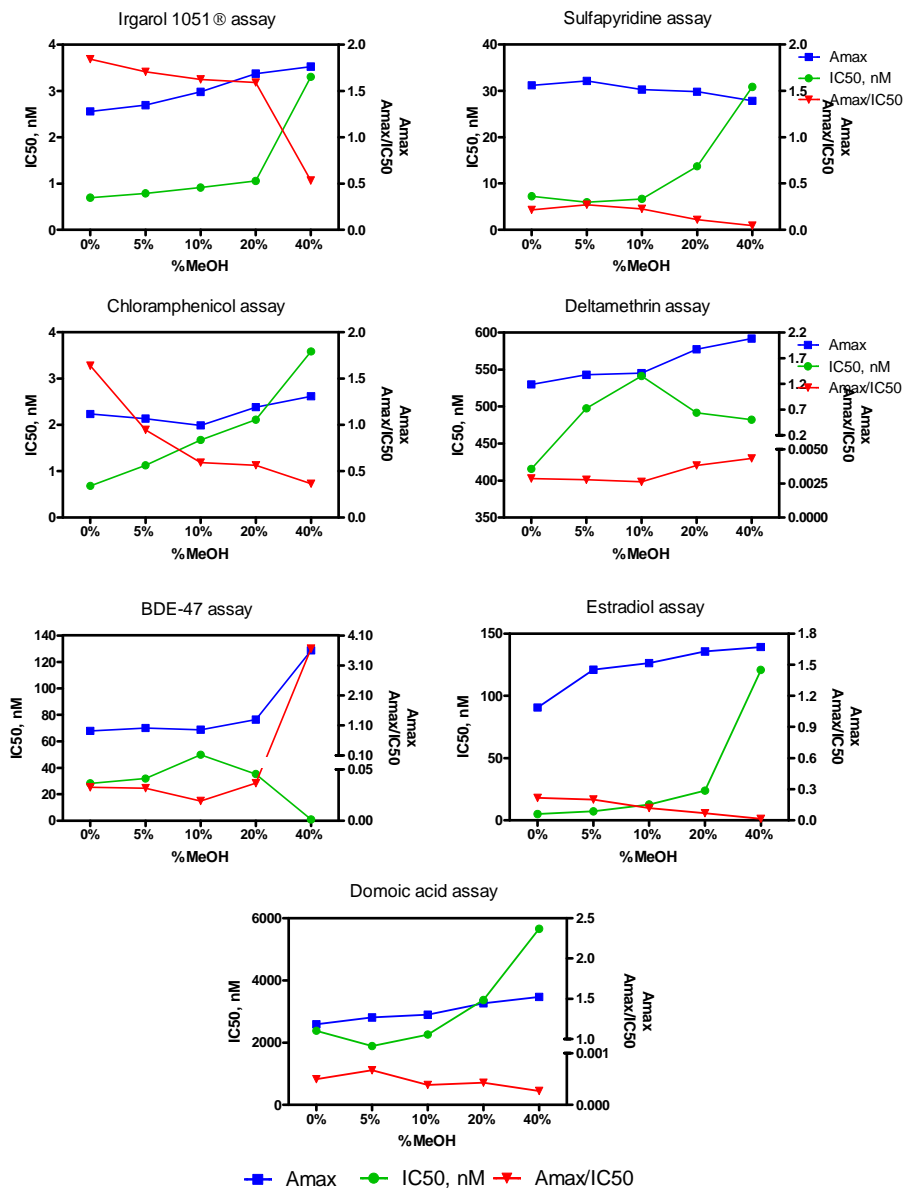


Figure 4.8. Effect of different percentages of methanol over the maximum signal and the detectability of the different ELISAs. The values of % of methanol in the x-axes correspond to the concentration of solvent in the standards used to prepare the calibration curves of each assay.

With small differences, all the assays tolerated quite well samples of up to 20% of methanol. Except for deltamethrin and BDE-47, for whose an improvement was observed at 40% of methanol, a significant drop in the detectability was observed. These two compounds (Deltamethrin (ACD/LogP, 7.39) and BDE-47 (ACD/LogP, 7.39)) are the ones which a more hydrophobic profile, and the addition of an organic solvent has been demonstrated to increase the solubility of hydrophobic compounds, improving the detectability of immunochemical techniques [161, 162]. In fact, it was relevant the improvement in the performance of the assay of BDE-47 in the present of 40 % of methanol, increasing both the maximum signal and the detectability.

Since the final aim of this work was to implement these procedures on a multiplexed format, it was decided to select a percentage of methanol that was well tolerated by all assays. Thus, it was decided that the samples (and standards) had to be measured in the multiplexed ELISA at 20% methanol (final concentration in the assay 10% after mixing the samples with the antibody solution). Therefore, prior the ELISA the pure methanolic eluates had to be diluted five times with the assay buffer. The dilution of the extract has an effect on the established SPE procedure, that under these conditions would allow achieving a preconcentration factor of $625/5 = 125$ times, which for most analytes would be sufficient to reach the environmental levels usually found. However, this value should be corrected with the real recovery obtained after the SPE column treatment (see Table 4.5.)

Table 4.5. SPE recoveries obtained for the different pollutants			
Pollutant	SPE cartridge	Recovery (%)	Preconcentration factor
Irgarol 1051®	ISOLUTE® ENV+	96.7	120.8
Sulfapyridine	OASIS HLB	99	123.8
Chloramphenicol	OASIS HLB	76	95
Estradiol	ISOLUTE® ENV+	72	90
Domoic acid	OASIS HLB	98	122.5
*BDE-47 and Deltamethrin didn't have an optimized protocol for their analysis by HPLC-MS/MS.			

Thus, for example, the detectability of the ELISA for the detection of Irgarol 1051® with a LOD of 0.015 µg L⁻¹, would be enhanced reaching a LOD of 0.124 ng L⁻¹ after the SPE treatment, which is below to the levels often found in the environment (see Table 4.1) and meet the EQS criteria fixed by the actual legislation (see Table 4.6).

Table 4.6. Analytical parameters for the target assays after the SPE treatment.			
	Irgarol 1051®	Sulfapyridine	Chloramphenicol
ELISA	4eBSA/ As87	SA2BSA/ As155	CA6BSA/ As226
Condition	aSW treated with SPE	aSW treated with SPE	aSW treated with SPE
IC₅₀ (ng L⁻¹)	0,918 ± 0,02	14.86 ± 0,42	3.41 ± 0,11
LOD (ng L⁻¹)	0.124 ± 0.006	0.969 ± 0.09	0.2 ± 0.05
	17β-Estradiol	Domoic acid	
ELISA	6-OCMOBSA/MAb_E2	DABSA/MAb_DA	
Condition	aSW treated with SPE	aSW treated with SPE	
IC₅₀ (ng L⁻¹)	11.33 ± 0.05	23.02 ± 0.16	
LOD (ng L⁻¹)	1.11 ± 0.012	1.39 ± 0.09	
The values of each parameter were obtained correcting with the real preconcentration factor (i.e. 120.8 for Irgarol 1051®; 123.8 for sulfapyridinde; 95 for chloramphenicol; 90 for 17β-estradiol; and 122.5 for domoic acid) the values of each individual assay for three days.			

To ensure this new assay conditions, the accuracy was studied for three ELISAs: Irgarol 1051®, sulfapyridine and domoic acid. With this aim, four environmental seawater blank samples and six blind spiked seawater samples, including two blanks, were passed through the solid-phase cartridge and the methanolic eluates measured with the corresponding ELISAs, after dilution with assay buffer, and the results compared with those obtained by HPLC- MS/MS.

The results from Figure 4.9 showed that the ELISA results match very well the spiked concentration values (slopes near 1), pointing at the high chances to develop a multiplexed platform able to quantify accurately these analytes in seawater samples after SPE. Only for the sulfapyridine ELISA it was observed a

4. Development of a multianalyte ELISA platform for the detection of environmental pollutants in seawater.

slight overestimation of the concentrations (slope= 1.262). The environmental blank samples additionally measured also with the chloramphenicol ELISA, as expected, were negative in the four assays.

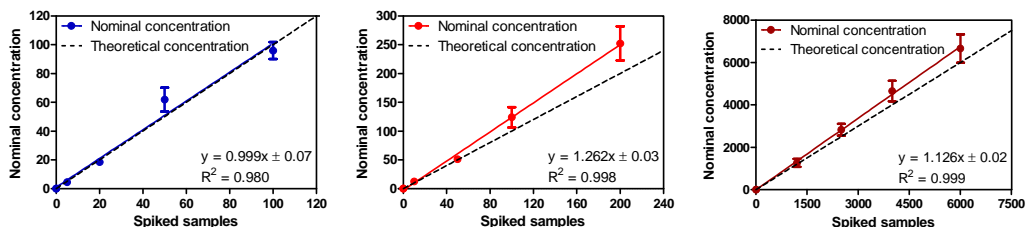


Figure 4.9. Correlation between the methanolic extracts nominal values and the measurements obtained by ELISA for Irgarol 1051[®] (blue), Sulfapyridine (red) and Domoic acid (brown). All the concentrations are expressed in nM.

Surprisingly, the correlation with the HPLC values was not completely satisfactory for domoic acid (see Figure 4.10). During the analysis of domoic acid samples there were some problems related to the equipment, and the analysis was postponed. This fact could have induced the degradation of the domoic acid present in the samples, explaining the subestimation of the HPLC method. For the Irgarol 1051[®] and sulfapyridine samples the results were much better, with only a slight underestimation for the first one and a slight overestimation for the second. The underestimation found for the Irgarol 1051[®] ELISA could have a negative impact on the reliability of the multiplexed platform due to the higher chances for false negative results. However, considering the high detectability that could be reached by the SPE-ELISA method (LOD 4.9 ng L⁻¹) is very much unlikely that contaminated samples could not be detected.

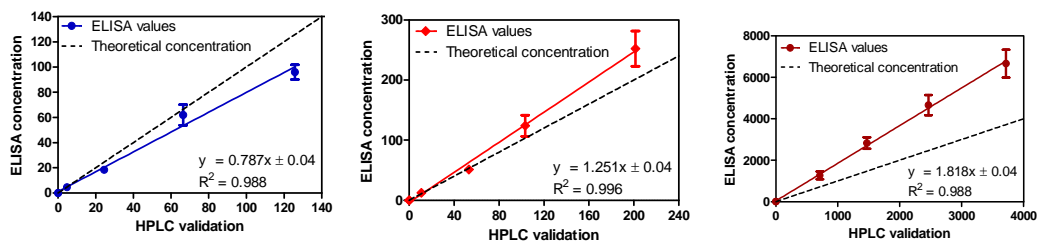


Figure 4.10. Correlation between the values of methanolic extracts quantification obtained by HPLC and ELISA for Irgarol 1051[®] (blue), Sulfapyridine (red) and Domoic acid (brown). All the concentrations are expressed in nM.

4.4.2.4.2 Effect of DMSO

Some problems were detected when the SPE module had to be implemented in the final multisensing platform proposed within the European Project SEA-on-a-CHIP, regarding the correct elution of some pollutants selected. For that reason, other solvents such as DMSO were considered. However, in order to consider DMSO as a good option, a comparison between the reference assays, the assays in presence of the 20% of methanol (the solvent and concentration previously selected) and the assays in presence of a 20% of DMSO was considered necessary (see Table 4.7).

Table 4.7. Comparison between the effect of methanol and DMSO in the analytical parameters of the different ELISA developed.

	Irgarol 1051®			Sulfapyridine			Chloramphenicol		
ELISA	4eBSA/ As87			SA2BSA/ As155			CA6BSA/ As226		
Condition	PBST	Methanol	DMSO	PBST	Methanol	DMSO	PBST	Methanol	DMSO
Slope	-1.15	-0.983	-1.33	-0.749	-0.869	-0.844	-0.823	-0.627	-1.02
IC ₅₀ (nM)	1.78	3.59	4.06	18.2	58.0	18.2	0.286	1.79	0.188
LOD (nM)	0.204	0.434	0.597	0.413	0.627	0.772	0.022	0.087	0.025
	BDE-47			17β-Estradiol			Domoic acid		
ELISA	2,2,4triBDEBSA/ As122			6-OCMOBSA/MAb_E2			DABSA/MAb_DA		
Condition	PBST	Methanol	DMSO	PBST	Methanol	DMSO	PBST	Methanol	DMSO
Slope	-0.794	-0.902	-0.687	-1.01	-0.898	-0.913	-1.09	-0.794	-1.04
IC ₅₀ (nM)	48.1	80.7	39.4	15.3	93.8	15.1	14.5	14.8	15.5
LOD (nM)	0.764	4.15	0.881	1.61	6.01	1.26	1.96	0.784	1.31

^aThe parameters (Slope and IC₅₀) were extracted from the four-parameter logistic equation used to fit the standard curves. The LOD was estimated as the concentration providing 90% of the maximum signal of the assay. The assays were performed using three-well replicates.

4. Development of a multianalyte ELISA platform for the detection of environmental pollutants in seawater.

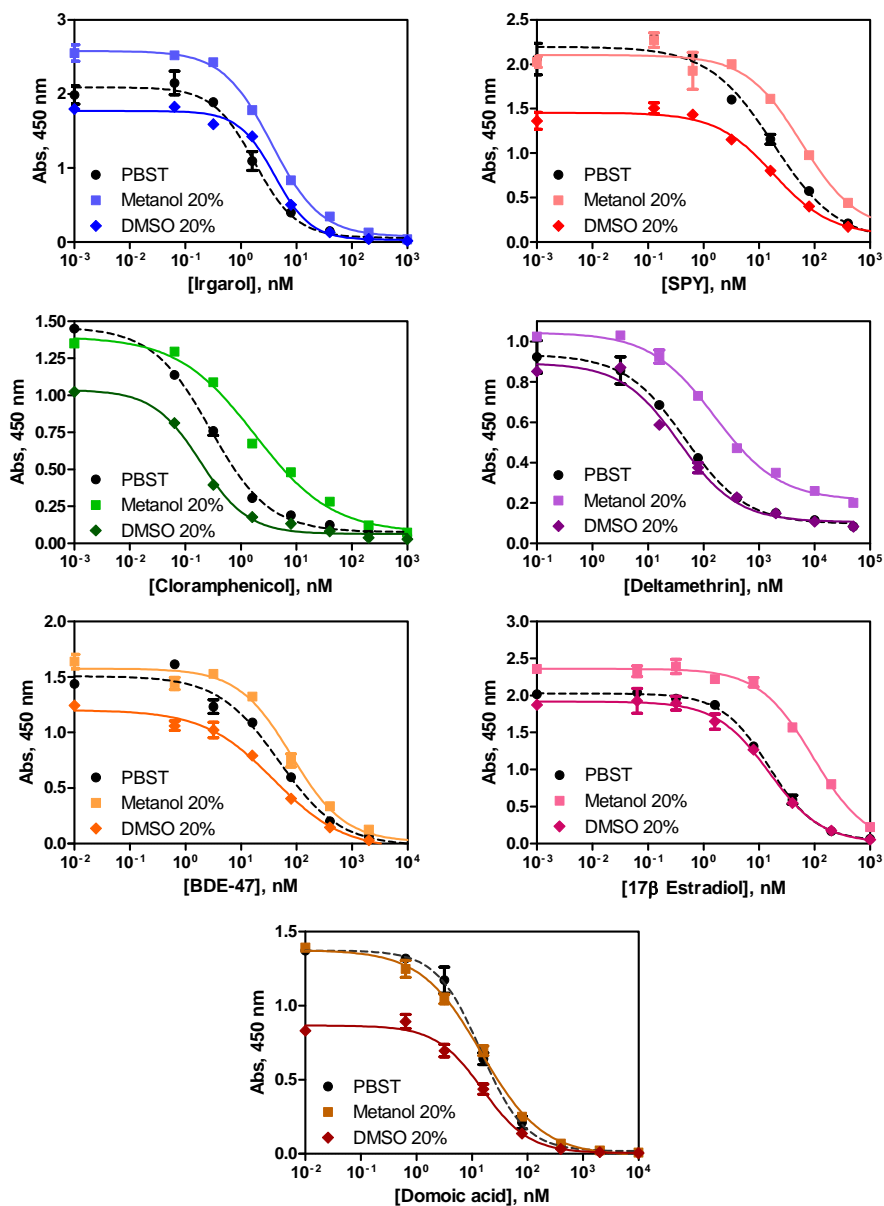
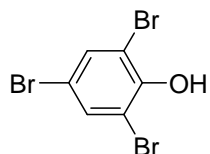


Figure 4.11. Comparison between the effect of methanol and DMSO over the different ELISA assays at the percentage selected for the SEA-on-a-CHIP project.

As it can be observed in Figure 4.11, not only most of the parameters were maintained when using DMSO in comparison to the reference assays, but when comparing against the methanol alternative, although in some cases the maximum signal slightly decreased, the sensibility of the assays was improved (see Table 4.7). Based on these results, the eluent selected for the pollutants elution from the SPE columns was changed to DMSO provisionally, until the accuracy studies and the validation by HPLC were completed.



2,4,6-Tribromophenol

Figure 4.12. Chemical structure fo 2,4,6-tribromophenol.

Table 4.8. Analytical parameters for the 2,4,6-Tribromophenol ELISA performed both in buffer and directly in seawater.		
	2,4,6-Tribromophenol	
Microarray	29BSA/ As43	
Condition	PBST	aSW
[CA], $\mu\text{g mL}^{-1}$	0.25	1.25
[As] dilution	1/8000	1/4000
Abs _{min}	0.09 ± 0,05	0.05 ± 0,04
Abs _{max}	1.29 ± 0.07	1.20 ± 0.07
Slope	-1.43 ± 0.14	-1.38 ± 0.07
IC ₅₀ (nM)	0.55 ± 0.04	0.56 ± 0.08
IC ₅₀ ($\mu\text{g L}^{-1}$)	0.175 ± 0.02	0.185 ± 0,02
LOD ($\mu\text{g L}^{-1}$)	0.032 ± 0.016	0.024 ± 0.015
R ²	0.998 ± 0.02	0.997 ± 0.03

The parameters are extracted from the four-parameter equation used to fit the standard curve. The calibration curve was run in the ELISA using three-well replicates.

Unfortunately, at this point of the research some problems started to appear with the BDE-47 ELISA which were attributed to the estability of the

4. Development of a multianalyte ELISA platform for the detection of environmental pollutants in seawater.

immunoreagents. For this reason, this assay was substituted by another ELISA develop in our group against tribromophenol (see Figure 4.12) [163]. The analytical parameters of the assay can be found in Table 4.8.

As before, fortified seawater samples were passed through the SPE module and the fractions eluted were analyzed by ELISA and by HPLC-MS/MS. In this occasion, all the ELISAs developed were evaluated.

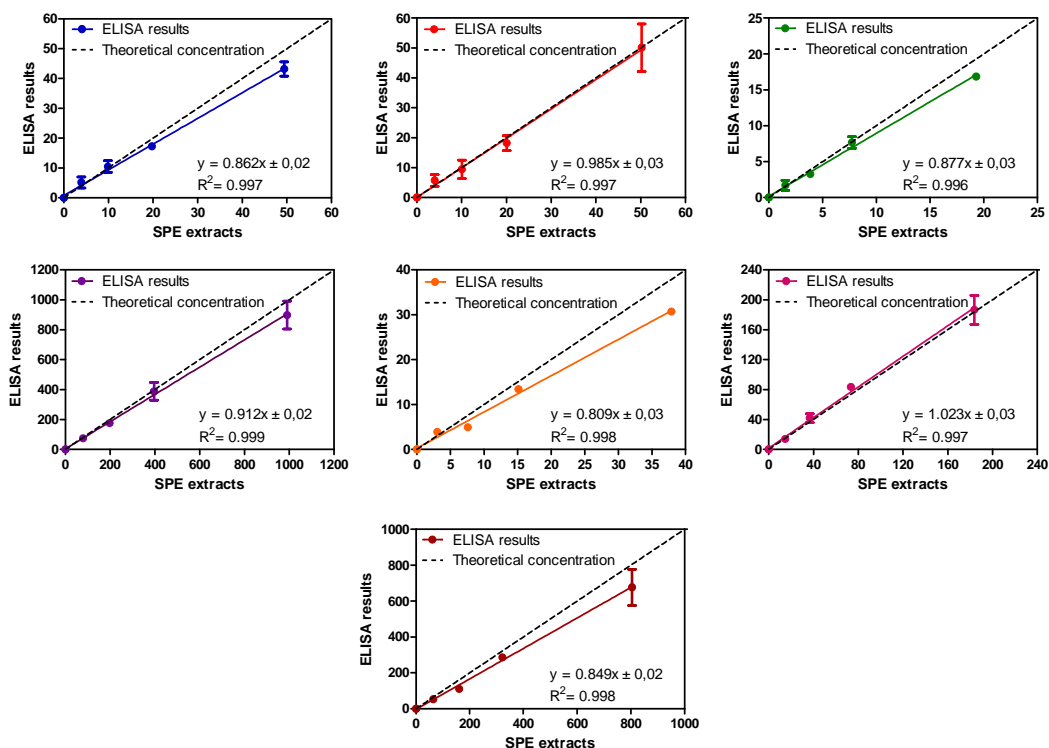


Figure 4.13. Correlation between the DMSO extracts nominal values and the measurements obtained by ELISA for Irgarol 1051® (blue), Sulfapyridine (red), Chlroamphenicol (green), Deltamethrin (purple), Tribromophenol (orange), 17β Estradiol (pink) and Domoic acid (brown). All the concentrations are expressed in nM. The results are the average and standard deviation of the samples measured in three-well replicates.

As it can be observed in Figure 4.13, in all the cases good levels of accuracy were obtained with slopes near 1 (being $m=1.00$ the perfect correlation with theoretical concentrations). and very good coefficients of regression. Only TBP and DA showed slopes below 0.9 pointing to a slight underestimation of the concentration by these assays.

Some of these blind samples were measured in parallel by the ELISA platforms and by HPLC for validation purposes. As it can be observed in Table 4.9, the results obtained by ELISA were very close to those provided by the HPLC, except for the case of chloramphenicol for which the HPLC gave a higher concentration, and for 17 β -estradiol for which the HPLC provided a lower value. The spiked value was in fact, in between the results provided by both technologies. Only TBP could not be analyzed by HPLC.

Table 4.9. Comparison of the results obtained by ELISA and HPLC-MS/MS.

Blind sample	Nominal concentration	Measured concentration ($\mu\text{g L}^{-1}$)	
		ELISA measurement	HPLC measurement
Irgarol 1051 [®]	3	4.2 \pm 0.7	3.4
Sulfapyridine	3	4.1 \pm 0.4	3.4 \pm 0.2
Chloramphenicol	6	2.2 \pm 0.2	9.0 \pm 1.4
Deltamethrin	139	87.9 \pm 5.6	105
Tribromophenol	4	3.8 \pm 0.7	Not analysed
17 β estradiol	14	17.1 \pm 2.5	10.0 \pm 1.1
Domoic acid	70	50.6 \pm 1.5	62.9

The ELISA results were obtained as a result of three different assays in different days. The HPLC measurements were obtained from different laboratories during the samples' validation process within the SEA-on-a-CHIP project.

4.4.3 MULTIANALYTE ELISA

The multiplexed ELISA was developed using the same protocol as for the single-ELISAs but using the antibodies in a mixture. This was possible because of the lack of cross-recognition between the different immunoreagents as it was shown on microarray experiments (see [section 5.1 in the next chapter](#)). Moreover, as it can be observed in Table 4.10, the analytical features of the multiplexed ELISA for each target were very similar to those accomplished by the corresponding single-analyte assays, achieving excellent LOD values in spite of the presence of a 10% of DMSO in the assay.

4. Development of a multianalyte ELISA platform for the detection of environmental pollutants in seawater.

Table 4.10. Analytical parameters of the multiplexed ELISA in comparison with the corresponding single-analyte assays^a.

	Irgarol 1051[®]		Sulfapyridine		Chloramphenicol	
ELISA	4eBSA/ As87		SA2BSA/ As155		CA6BSA/ As226	
Condition	PBST	Multiplexed ELISA	PBST	Multiplexed ELISA	PBST	Multiplexed ELISA
[CA], $\mu\text{g mL}^{-1}$	0.25	0.078	0.25	0.156	0.0625	0.0625
[As] dilution	1/16000	1/32000	1/16000	1/8000	1/64000	1/32000
Abs_{min}	0.03 ± 0.02	0.108 ± 0.02	0.03 ± 0.02	0.076 ± 0.05	0.030 ± 0.01	0.102 ± 0.03
Abs_{max}	1.47 ± 0.09	1.65 ± 0.22	1.34 ± 0.08	1.64 ± 0.16	0.809 ± 0.02	1.39 ± 0.22
Slope	-0.98 ± 0.22	-1.21 ± 0.16	-0.784 ± 0.09	-0.729 ± 0.11	-0.60 ± 0.05	-0.736 ± 0.04
IC₅₀ (nM)	0.58 ± 0.19	3.47 ± 0.11	6.58 ± 1.73	10.7 ± 2.64	0.59 ± 0.05	2.16 ± 0.16
IC₅₀ ($\mu\text{g L}^{-1}$)	0.145 ± 0.05	0.879 ± 0.16	1.43 ± 0.23	2.64 ± 0.66	0.192 ± 0.09	0.699 ± 0.05
LOD ($\mu\text{g L}^{-1}$)	0.012 ± 0.01	0.106 ± 0.02	0.08 ± 0.02	0.115 ± 0.06	0.004 ± 0.01	0.034 ± 0.01
R²	0.996 ± 0.002	0.995 ± 0.003	0.992 ± 0.006	0.990 ± 0.011	0.995 ± 0.003	0.997 ± 0.003
	Deltamethrin		17β-Estradiol		Domoic acid	
ELISA	C134-AD/As360		6E2BSA/Mab_E2		DABSA/Mab_DA	
Condition	PBST	Multiplexed ELISA	PBST	Multiplexed ELISA	PBST	Multiplexed ELISA
[CA], $\mu\text{g mL}^{-1}$	0.45	0.45	0.3	0.3	0.6	0.6
[As] dilution	1/8000	1/8000	1/64000	1/64000	1/16000	1/16000
Abs_{min}	0.089 ± 0.03	0.097 ± 0.02	0.013 ± 0.003	0.125 ± 0.09	0.038 ± 0.01	0.128 ± 0.05
Abs_{max}	1.09 ± 0.25	1.10 ± 0.06	1.36 ± 0.20	1.17 ± 0.19	0.935 ± 0.12	0.826 ± 0.01
Slope	-0.795 ± 0.08	-0.731 ± 0.08	-1.01 ± 0.07	-1.07 ± 0.02	-0.866 ± 0.13	-1.24 ± 0.13
IC₅₀ (nM)	104.7 ± 15.6	65.27 ± 8.98	4.01 ± 0.74	4.20 ± 0.30	9.69 ± 1.05	6.48 ± 0.36
IC₅₀ ($\mu\text{g L}^{-1}$)	52.9 ± 7.9	32.96 ± 4.54	1.09 ± 0.20	1.06 ± 0.08	3.02 ± 0.33	2.02 ± 0.11
LOD ($\mu\text{g L}^{-1}$)	3.45 ± 0.69	1.51 ± 0.43	0.11 ± 0.03	0.149 ± 0.002	0.24 ± 0.02	0.40 ± 0.03
R²	0.998 ± 0.001	0.997 ± 0.010	0.990 ± 0.012	0.989 ± 0.015	0.996 ± 0.005	0.998 ± 0.003

^aThe assays were performed in PBST with a 10 % of DMSO in order to mimic the conditions to be used when analyzing seawater samples using the SPE procedure. The results shown are the average a standard deviation of assays performed in three different days. On each day the assays were run using three-well replicates.

As discussed above, the detectability will be even better when the ELISA will be coupled to the SPE module, multiplying the detectability by a factor of 125. The reproducibility of the assays is also very good. Thus, on experiments performed

during different days the following percentages of interday coefficient of variation (%CV) for the IC₅₀ values were obtained: <25% for sulfapyridine, <15% for deltamethrin and <8% for the rest of pollutants.

Table 4.11. Results of the accuracy quantification of the different seawater samples spiked with all the target analytes simultaneously.

		Measured concentration ($\mu\text{g L}^{-1}$)		
Blind sample		Nominal concentration	ELISA quantification	HPLC quantification
High level	Irgarol 1051®	1.25	1.25 ± 0.01	1.82 ± 0.04
	Sulfapyridine	2.5	2.48 ± 0.08	2.94 ± 0.02
	Chloramphenicol	2.5	2.58 ± 0.17	2.44 ± 0.21
	Deltamethrin	250	248.9 ± 27.6	277.2 ± 19.9
	17β estradiol	2.5	2.49 ± 0.11	2.24 ± 0.14
	Domoic acid	12.5	13.16 ± 0.82	17.2 ± 0.84
Medium level	Irgarol 1051®	1	1.01 ± 0.01	1.46 ± 0.01
	Sulfapyridine	1.25	1.34 ± 0.20	1.00 ± 0.09
	Chloramphenicol	1	1.10 ± 0.06	1.61 ± 0.75
	Deltamethrin	100	102.0 ± 7.39	80.04 ± 0.13
	17β estradiol	1.25	1.23 ± 0.12	1.61 ± 0.52
	Domoic acid	10	10.72 ± 0.58	15.8 ± 1.19
Low level	Irgarol 1051®	0.5	0.56 ± 0.05	2.00 ± 0.04
	Sulfapyridine	1	1.12 ± 0.07	0.81 ± 0.19
	Chloramphenicol	0.5	0.58 ± 0.2	0.39
	Deltamethrin	25	24.58 ± 2.5	32.2 ± 1.17
	17β estradiol	1	0.95 ± 0.03	1.22 ± 0.59
	Domoic acid	5	5.89 ± 0.82	5.72 ± 0.57

The ELISA results were obtained as a result of three different assays in different days. The HPLC measurements were obtained from the department of Environmental Chemistry (IDAEA-CSIC).

Finally, the accuracy of the multiplexed ELISA to analyze seawater samples was assessed by preparing blind spiked environmental seawater samples, treating

them with the SPE module and analyzing them by the multiplexed ELISA and by HPLC-MS/MS. Three samples containing the six analytes at three concentration levels (high, medium and low) were analyzed. Table 4.11 shows the results of these studies. As it can be observed the multiplexed ELISA performed very well. The concentration values matched the spiked values and those were in agreement with the results obtained by HPLC-MS/MS. These experiments demonstrate that the presence of other analytes in a sample do not affect the accurate quantification of each individual pollutant.

Finally, 6 environmental seawater samples obtained from different locations over the Catalonia coasts were also measured following the same procedure as described above for the spiked samples. The results shown in Table 4.12 demonstrate that the multiplexed ELISA developed could be an excellent and reliable tool for analyzing pollutants in environmental seawater samples. As it can be observed, there was found a very good agreement between the SPE-multiplexed ELISA and the SPE-HPLC-MS/MS.

The multiplexed ELISA here presented can become an efficient and reliable analytical tool for screening contaminants in the ocean with a very good accuracy and reaching excellent limits of detection, particularly if coupled to SPE. In respect to the HPLC-MS/MS method, the ELISA has a higher sample throughput capability being able to analyze more than 100 samples in parallel in just about 1.5h, with the same accuracy. Therefore, we can conclude that we have developed a bioanalytical tool with a great potential for screening contamination of natural environmental waters since the limits of detection accomplished are close to the environmental levels usually reported for these contaminants in ocean waters. This is the first time that a multiplexed bioanalytical technology with analytical features suitable to measure simultaneously 6 families of relevant pollutants in seawater samples has been reported. In most of the cases the platform is enough to detect the concentrations of pollutants often found in the environment (see Table 4.1), and in some cases such as with Irgarol 1051[®], the platform proposed couple to the SPE column could fulfill the needs presented by actual legislation. Furthermore although other reported multiplexed systems address detection of different contaminants, usually they are from the same family, such as pesticides [164], toxins [165] or from restricted families [166], but in any case a wide selection of pollutants from different families and chemical nature as in our approximation.

Table 4.12. Results from the preliminary validation studies of the SPE-multiplexed ELISA using environmental seawater samples^a

		Measured concentration ($\mu\text{g L}^{-1}$)											
		Sample A				Sample B				Sample C			
		ELISA quantification	HPLC quantification	ELISA quantification	HPLC quantification	ELISA quantification	HPLC quantification	ELISA quantification	HPLC quantification	ELISA quantification	HPLC quantification	ELISA quantification	HPLC quantification
Irgarol 1051 [*]		<LOQ	<LOQ	<LOQ	<LOQ	<LOQ	<LOQ	<LOQ	<LOQ	<LOQ	<LOQ	<LOQ	<LOQ
Sulfapyridine		<LOQ	<LOQ	<LOQ	<LOQ	<LOQ	<LOQ	<LOQ	<LOQ	<LOQ	<LOQ	<LOQ	<LOQ
Chloramphenicol		nd	nd	nd	nd	nd	nd	nd	nd	nd	nd	nd	nd
Deltamethrin		10.04 ± 0.97	9.52	nd	nd	nd	nd	nd	nd	nd	nd	nd	nd
17 β estradiol		nd	nd	nd	nd	nd	nd	0.011 ± 0.04	nd	0.012	nd	0.012	nd
Domoic acid		<LOQ	<LOQ	<LOQ	<LOQ	<LOQ	<LOQ	<LOQ	<LOQ	<LOQ	<LOQ	<LOQ	<LOQ
		Sample D				Sample E				Sample F			
		ELISA quantification	HPLC quantification	ELISA quantification	HPLC quantification	ELISA quantification	HPLC quantification	ELISA quantification	HPLC quantification	ELISA quantification	HPLC quantification	ELISA quantification	HPLC quantification
Irgarol 1051 [*]		<LOQ	<LOQ	<LOQ	<LOQ	<LOQ	<LOQ	<LOQ	<LOQ	<LOQ	<LOQ	<LOQ	<LOQ
Sulfapyridine		<LOQ	<LOQ	<LOQ	<LOQ	<LOQ	<LOQ	<LOQ	<LOQ	<LOQ	<LOQ	<LOQ	<LOQ
Chloramphenicol		nd	nd	nd	nd	nd	nd	nd	nd	nd	nd	nd	nd
Deltamethrin		4.26 ± 0.99	3.777	<LOQ	0.415	<LOQ	0.415	1.77 ± 0.99	nd	1.981	<LOQ	1.981	<LOQ
17 β estradiol		<LOQ	nd	nd	nd	nd	nd	<LOQ	nd	<LOQ	<LOQ	<LOQ	<LOQ
Domoic acid		<LOQ	<LOQ	<LOQ	<LOQ	<LOQ	<LOQ	<LOQ	<LOQ	<LOQ	<LOQ	<LOQ	<LOQ

Seawater samples collected from different location in the Catalanian Coast were passed through the SPE module, eluted with DMSO and the eluate splitted in two parts, one for analysis with the multiplexed ELISA and the other for the analysis by HPLC-MS/MS. For the case of the ELISA, the results shown are the average a standard deviation of three-well replicates and the experiments was repeated 3 days.

4.5 Chapter contributions

- Single ELISAs for seven families of relevant pollutants regarding contamination of natural waters have been established and evaluated in comparison with HPLC-MS/MS. All the assays were found to perform very well, showing excellent analytical features (see Table 4.4), even when analysing directly seawater samples without any clean-up step.
- A multiplexed ELISA has been developed by just using the antibodies as cocktail. The analytical features of this multiplexed bionalytical methods are very close to those obtained by the single-analyte ELISAs and has been found to work very well in seawater samples.
- The combination of the single-analyte or the multiplexed ELISAs here reported with a SPE module to pre-concentrate the pollutants potentially present in the ocean has allow multiplying by a factor of 125 the detectability accomplished, which is then closed to the environmental levels usually reported for these contaminants. Performance of the multiplexed ELISA has been evaluated and validated by HPLC-MS/MS using spiked and environmental waters.

4.6 Materials and methods

Reagents, materials and equipment. The chemical reagents, materials and equipment used are the same than in [section 3.6](#).

Immunoreagents. The immunoreagents for Irgarol 1051[®] (Irg), Sulfapyridine (SPy), Chloramphenicol (CAP) and Tribromophenol (TBP) detection used for the development of the competitive assays in the ELISA platform have been described before [147, 150, 163]. In the case of BDE-47, the immunoreagents were described before [151], and were provided by the group of Dr. Li. For Estradiol (E2), the coating antigen was purchased from Sigma-Aldrich and conjugated to BSA trough the active ester method. The monoclonal antibody used on the estradiol assay was purchased from Fitzgerald Industries International. Finally, Domoic acid (DA) was purchased from Sigma-Aldrich and

conjugated to BSA through the active ester method while Queen's University provided the monoclonal antibody. The secondary antibody marked with HRP was purchased from Sigma Chemical Co. (St. Louis, MO, USA). The target analytes in this chapter were Irgarol 1051® (Irg), Sulfapyridine (SPy), Chloramphenicol (CAP), BDE-47, 2,4,6-Tribromophenol (TBP) 17 β -estradiol (E2), and Domoic acid (DA), all purchased from Sigma Chemical Co. (St. Louis, MO, USA), except for BDE-47 (provided by Plymouth University). Stock solutions of each analyte were prepared at 10 mM concentration in DMSO and stored at 4°C until its use.

Buffers. The buffers used are the same than in [section 3.6](#).

Bioconjugate competitors' preparation. The preparation of the bioconjugate competitors for Irgarol 1051® [147], sulfonamides [148, 149] and BDE-47 [151] has been already been reported, while that of the chloramphenicol will be described elsewhere. The preparation of the bioconjugates for estradiol (6E2₄BSA) and DA (DA₅BSA) was performed using the following general procedures. Briefly, a solution of N, N'-dicyclohexylcarbodiimide (DCC; 50 μ mol) in anhydrous DMF (50 μ L) was added to a solution of the hapten (100 μ L) in the same solvent followed by a solution of N-hydroxysuccinimide (NHS, 25 μ mol, 50 μ L) also in DMF [167]. The mixture was stirred for approximately 3 hours at RT until a white precipitate appeared. The suspension was then centrifuged (10000 rpm for 10 min) and the supernatant (25 μ L for 6E2 and 50 μ L for DA₅) was added dropwise to a solution of bovine serum albumin (BSA, 10 mg, 1.8 mL borate buffer) and the mixtures kept under gently stirred for 4 hours at RT. The protein bioconjugates were purified by dialysis against 0.5 mM PBS (4 \times 5 L) and ultrapure water (1 \times 5 L) and finally stored frozen at -40 °C. Unless otherwise indicated, working aliquots were stored at 4 °C in 0.01 M PBS at 1 mg mL⁻¹.

Non-competitive indirect ELISA. The screening of the avidity of all the antisera and monoclonal antibodies with the corresponding antigens was evaluated. Two-dimensional titration assays (2D-assay) were carried out, based on the measurement of the binding of serial dilutions of the antisera (1/1000 to 1/64000, and zero, 100 μ L well⁻¹) against different concentration of the antigens (1 μ g mL⁻¹ to 0.5 ng mL⁻¹, and zero, 100 μ L well⁻¹). From these experiments, optimum concentrations for coating antigens and antisera dilutions were chosen to generate around 0.7-1 units of absorbance.

Competitive ELISA assay. The plates were coated with the proper concentration of competitor antigen in coating buffer ($\mu\text{L well}^{-1}$), overnight at 4°C and covered with adhesive plate sealers. e times with PBST. The next day, the plates were washed four times with PBST ($300 \mu\text{L well}^{-1}$), each analyte was added (in buffer or seawater, $50 \mu\text{L well}^{-1}$) followed by the specific antibody ($50 \mu\text{L well}^{-1}$ in PBST or PBT 2x). After 30 min at r.t., the plates were washed as before, and a solution of anti-IgG-HRP (1/6000 in PBST) was added to the wells ($100 \mu\text{L well}^{-1}$) and incubated for 30 minutes at r.t. The plates were washed again, and the substrate solution was added ($100 \mu\text{L well}^{-1}$). Color development was stopped after 30 min at r.t. with $4 \text{ N H}_2\text{SO}_4$ ($50 \mu\text{L well}^{-1}$), and the absorbances were read at 450 nm . The standard curves were fitted to a four-parameter equation according to the following formula: $y = (A - B/[1 - (x/C)^D] + B$, where A is the maximal absorbance, B is the minimum absorbance, C is the concentration producing 50% of the maximal absorbance, and D is the slope at the inflection point of the sigmoid curve. Unless otherwise indicated, data presented correspond to the average of assays performed during three different days with at least two well replicates each day.

Accuracy studies for each analyte detection. The accuracy of each ELISA assay for its specific analyte was assessed by analyzing 5 different SPE extracts spiked at 5 different concentrations within the working range of each curve's analyte. The results were fitted to a linear regression curve between the spiked concentrations and the measured ones.

Solid-phase extraction. Solid phase extraction (SPE) was employed as method of extraction and concentration for every compound. Different conditions were considered for the extraction of Irgarol 1051[®] and the rest of compounds. With minor modifications, the extractions were proceeded following the previously developed and optimized methods [168],[169],[170],[171],[172] with recoveries ranging from 76 to 98 %. Briefly, cartridges were conditioned with 6 ml of methanol and equilibrated with 6 ml of pure water. For Irgarol 1051[®], ISOLUTE[®] ENV+ (220 mg, 6 ml) cartridges were employed, whereas cartridges of OASIS HLB (200 mg, 6ml) were used for the rest of compounds. 500 ml of seawater were loaded into the cartridges at approximately 1 ml/min. Cartridges were then washed with 6 ml of pure water to remove the interferences and salts and dried under vacuum for 20 minutes. Lastly, 6 ml of methanol was used for the elution. All extracts were concentrated through a flow of N_2 steam of an evaporator

Reacti –Therm III of Pierce (Rockford, IL, USA) and then reconstituted to 1 ml of solvent. The extracts analysed by ELISA were reconstituted with DMSO and those by HPLC-HRMS with the initial chromatographic conditions of mobile phase, (9:1) methanol/water.

HPLC validation of the multianalyte ELISA format. The accuracy of the multiplexed ELISA assay for all analyte concentrations was assessed by analyzing 6 different real SW samples pre-concentrated through an SPE column, altogether with 3 more SPE extracts which contained all the analytes spiked at three different levels of concentration (high, medium and low) within the working range of each curve's analyte. All the samples were eluted in pure DMSO and for its analysis were diluted in PBST, obtaining final samples of only a 10% of solvent. For each sample, 500 mL of seawater was treated through the SPE system mentioned before, and the elute obtained was 1mL, applying therefore a preconcentration factor of 1/500. All the samples were analyzed in parallel by high performance liquid chromatography (HPLC) as a reference technique

4. Development of a multianalyte ELISA platform for the detection of environmental pollutants in seawater.

**5 MULTIPLEXED MICROARRAY DEVELOPMENT FOR THE
DETECTION OF ENVIRONMENTAL CONTAMINANTS IN
SEAWATER**

5.1 Introduction

As explained in the general introduction of this thesis, there is a need for multiplexed analytical techniques in several fields including clinical diagnostics, food safety or environmental monitoring. These platforms should be fast, robust, easy-to-use and be able to measure a high number of samples and compounds of different chemical nature simultaneously.

5.1.1 MICROARRAYS PLATFORMS IN ENVIRONMENTAL APPLICATIONS

Nowadays, due to the increasing number of contaminants in the environment, most of them being organic compounds, the samples needed to be analysed along with the number of target pollutants has increased. Not only one of the goals in the environmental monitoring programs and current marine legislation is the possibility to establish platforms that could work on-field allowing near real-time information, but also further studies focused in, the establishment of screening methods that can answer the problems presented are needed (see Figure 5.1).

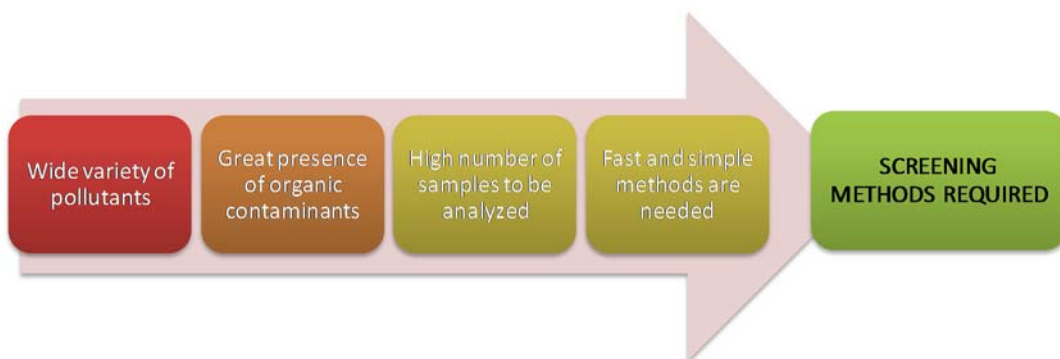


Figure 5.1. Scheme of the reasons why the development of environmental screening techniques is a today's need.

Amongst the platform that could fulfill these demands, one of the most exploited for environmental monitoring [165, 173-175] are microarrays [176]. A microarray can be defined as a set of miniaturized bio/chemical reaction areas, where reagents are immobilized in an organized manner on solid surfaces such as glass slides or silicone thin films [177]. They are characterized by being a great

tool for high throughput screening, thanks to their multiplexation and miniaturization capabilities, offering the possibility to perform the analysis minimizing the amount of sample required [176]. Furthermore, they offer flexibility in terms of solids supports. In most of the mono- or multiplex microarray assays, proteins are covalently immobilized in glass slides or silicone films, but some examples have also been reported using alternative supports such as digital disks [178].

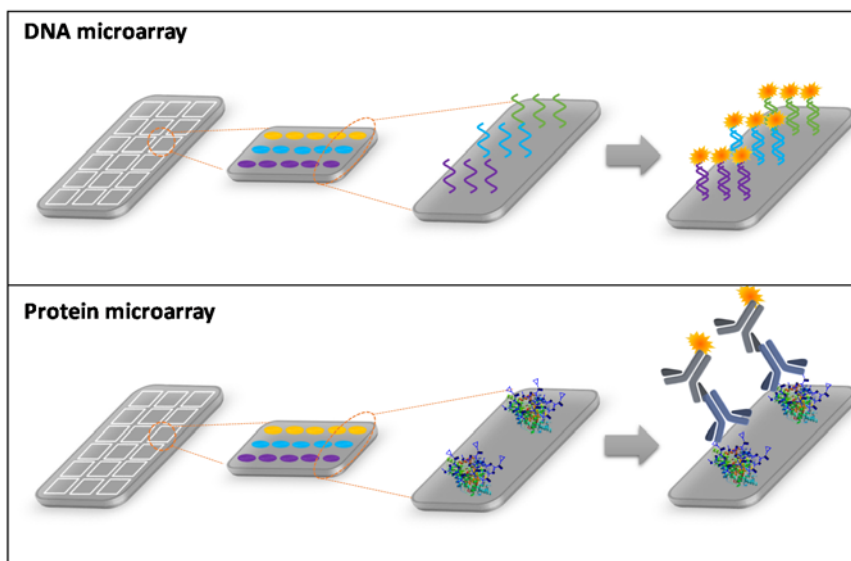


Figure 5.2. Schematic representation of common configuration of DNA and protein microarrays. The schemes are based on the use of glass slides for the immobilization of A) Nucleic acids for a hybridization assay or B) Protein for a competitive indirect assay

Microarrays appeared in the decade of the 80s, being the first ones' DNA microarrays (see Figure 5.2). DNA microarrays have revolutionized the diagnostics area due to their great stability and elevated specificity related to the hybridization process which takes place between complementary strands [179]. These microarrays have been commonly used to measure the expression levels of large numbers of genes simultaneously [180, 181] or to genotype multiple regions of a genome [182]. However, although DNA microarray usually offer major stability in comparison to the ones based on proteins, and the level of specificity related to the binding of nucleotides is not easily reproducible in the protein's platforms, great expectations regarding the potential of protein

Table 5.1. Summary of some multiresidue and multiplexed platforms applied to water monitoring.

Substances class	Substances analyzed	LOD ($\mu\text{g L}^{-1}$)	Assay format	Matrices analyzed	Reference
Sulfonamides	Sulfamethoxazole	0.255	Multiresidue ELISA Competitive direct	Wastewater River water	[183]
	Sulfamethoxy-pyridazine	0.146			
	Sulfachloropyridazine	0.180			
	Sulfadimethoxine	0.420			
	Sulfamethazine	0.880			
Pyrethroids	Deltamethrin	1.8 ± 0.30	Multiresidue ELISA Competitive direct	River water	[184]
	Cypermethrin	1.5 ± 0.42			
	Fluvalinate	2.0 ± 0.58			
	Fenvalerate	2.0 ± 0.35			
	Phenothrin	2.2 ± 0.64			
	Flucythrinate	2.4 ± 0.40			
	Fenpropathrin	3.0 ± 0.45			
Permethrin	5.0 ± 0.38				
Algal toxins	Microcystin-RR	0.32	Multiresidue ELISA Competitive direct (commercial)	Drinking water Surface water	[185]
	Microcystin-YR	0.38			
Multiclass	Atrazine	0.06	Microarray format Competitive indirect Gold labeled secondary antibody Polycarbonated DVD as support Sample filtration	River water Spring water	[186]
	Chlorpyrifos	0.25			
	Metolachlor	0.37			
	Sulfathiazole	0.16			
	Tetracycline	0.10			

Continuation Table 5.1.						
Substances class	Substances analyzed	LOD ($\mu\text{g L}^{-1}$)	Assay format	Matrices analyzed	Reference	
Multiclass	2,4-Dichlorophenoxyacetic acid 2,4,6-Trinitrotoluene Okadaic acid	1 1.000 0.02	Microarray format Competitive indirect Optical clear pressure sensitive adhesive as support Colorimetric detection	Spiked water samples	[18]	
Herbicides	Mesotrione Paraquat Diquat Hexaconazole	0.04 0.06 0.09 0.10	Four-band capillary optical immunosensor Protein conjugates immobilized in plastic capillary Competitive indirect format	Spiked deionized water	[187]	
Multiclass	Propanil Atrazine Isoproturon Sulfamethizole Bisphenol A Estrone	0.019 0.010 0.020 0.018 0.008 0.007	AWACSS (Automated Water Analyser Computer Supported System) Total internal reflection fluorescence immunosensor Competitive indirect format	MiliQ water Groundwater Surface water Mixed municipal / industrial waste water	[188]	
Multiclass	Estrone Isoproturon Atrazine	0.084 0.046 0.155	RIANA Total internal reflection fluorescence immunosensor Competitive indirect format	Spiked river water samples	[189]	

microarray is usually expected. Its easy way of preparation and their fast and simple assays protocols make protein microarrays useful platforms for answering the need of real time analysis of marine waters in multi-stressor conditions and the monitoring of pollutant's levels. For that reason, this platform was chosen as a set-up for the multiplexed detection of the environmental pollutants studied in [Chapter 4](#).

Even though, protein microarrays present a variety of limitations, mainly related to the great diversity of chemical structures and functions. Sometimes, poor reproducibility and lack of homogeneity of the spots have been reported, mainly due to the great diversity and complexity of their chemical structures. In spite of the drawbacks commented before, some multiplexed microarray platforms have been reported for environmental monitoring due to their excellent throughput screening capabilities (see Table 5.1).

5.2 Chapter objective

The goal of this chapter (see Figure 5.3) is the development of a fluorescent multiplexed microarray platform for the multidetection of environmental pollutants. Main advantages of this technology are the possibility to expand the number of analytes measured in the same chip thanks to the possibility to print matrices with a high density of spots and the chance to run multiple samples simultaneously using hardware that allows running several chips at the same time.

A difference to ELISA, for the microarray technology, in this case, the bioconjugate competitors will be immobilized covalently on glass slides. Since the conditions are different to the microplate-based ELISA described in the previous chapter, there will be necessary to evaluate the performance of the individual fluorescent immunoassays, before integrating them in the multiplexed format. Thus, the following studies will be performed:

1. **Biofunctionalization of the glass slides** selecting the appropriate chemistry and setting up the appropriate conditions for the competitive fluorescent immunoassays

2. **Development and analytical characterization of single-analyte microarray competitive fluoroimmunoassays** in buffer and in seawater,
3. **Ensuring the lack of shared reactivity**, mean that each antibody should recognize specifically only its bioconjugate competitor and no other bioconjugates immobilized in other spots of the same chip.
4. **Development of the multiplexed fluorescent microarray** and evaluation of its performance in seawater.

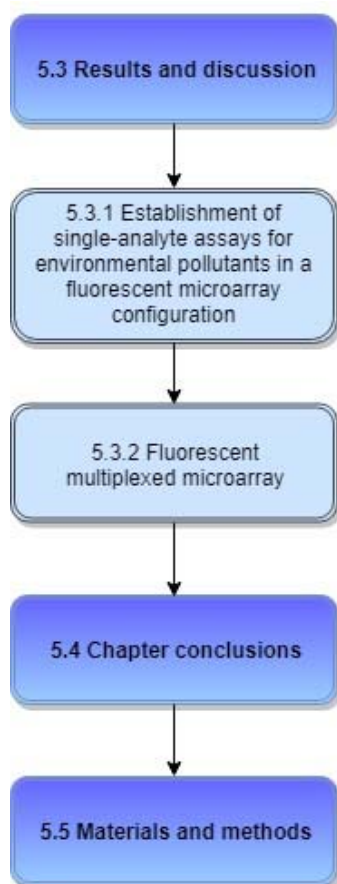


Figure 5.3. Structure of this chapter related to the different sections

5.3 Results and discussion

5.3.1 ESTABLISHMENT OF SINGLE-ANALYTE ASSAYS FOR ENVIRONMENTAL POLLUTANTS IN A MULTIPLEXED FLUORESCENT MICROARRAY CONFIGURATION.

5.3.1.1 Protein microarray: Immobilization protocol

Glass slides were selected as microarray support due to the high chemical and physical resistance of this material. Plain glass has low intrinsic fluorescence and high transmission, two crucial parameters when the final readout selected is fluorescence. Glass is an inexpensive and easy to obtain material, its surface is normally flat with few wrinkles, rigid, transparent and without pores. Finally, it offers the possibility to immobilize biomolecules covalently, through its hydroxyl groups that could be activated with a variety of silanizing reagents with different types of chemical groups [190].

In this case, activation of the surfaces with 3-(glycidyloxypropyl) trimethoxysilane (GPTMS) was selected (Figure 5.4). GPTMS provides epoxy groups that react with nucleophiles such as for example the amino groups from the proteins. For this purpose, the slides were first activated by treating them with piranha solution, washed with water and finally immersed in a 10% NaOH solution to deprotonate hydroxyl groups. Afterwards, the slides were treated with pure GPTMS was used to introduce epoxy groups and subsequently washed with absolute ethanol to eliminate the excess GPTMS. The epoxy activated glass slides could be stored in a desiccator until use for up to a month, without losing activity.

Biofunctionalization of the glass slides was performed with the aid of a nanodrop dispenser, under controlled temperature (20°C) and humidity (65%) conditions; forming a matrix of micrometric active zones (spots) of around 300 µm each. The biofunctionalized slides were kept at RT in a desiccator until use for up to 1 week without any loss of activity.

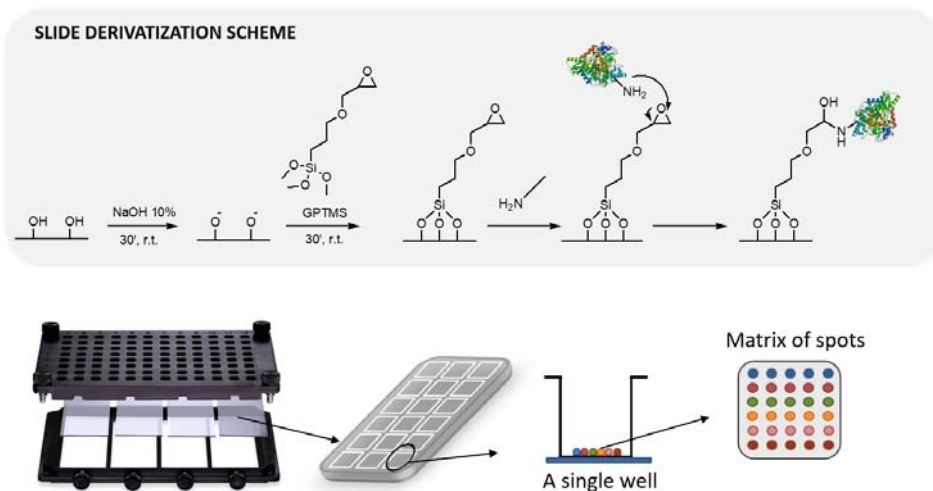


Figure 5.4. TOP: Scheme of the chemistry used to functionalize with GPTMS and subsequently with the bioconjugate competitors. BOTTOM: Scheme of the microarray hardware platform used to hold four glass slides. Each glass slide could be printed with 24 different microarrays. In this study, each microarray contained a matrix of 5x6 spots for the multiplexed assays.

The microarray assay was run by placing the slides in an ArrayIt® hardware multi-well platform (see Figure 5.5). In this manner, each slide was divided in 24 (8 x 3) wells; each well sealing a microarray chip printed with a variable number of spots depending on the type of experiment.



Figure 5.5. All material needed for the different steps involved in fluorescent microarray development: print, assemble, measure, analyze and data treatment.

5.3.1.1 Single-analyte microarray assays for seawater analysis

Two dimensional assays in microarray format were performed for each pair antibody/bioconjugate competitor to select the appropriate concentrations of the immunoreagents in buffer and seawater. As mentioned in the previous chapter, this is a matrix characterized by its particular mixture of salts providing a pH of 8.1 and a conductivity much higher than the conductivity of the PBS buffer used in most of the assay. For setting up the assays in seawater the antibody solution was dissolved in PB2T (0.02 M phosphate buffer, no saline solution, 0.1% Tween 20, pH 7.5) instead of the usual PBS (0.01 M phosphate buffer, 0.8% saline, 0.05 % Tween20) in order to achieve the similar buffer conditions when mixed with the seawater sample at 1:1 ratio.

Despite the particularities of the seawater, it was possible to set-up six fluorescent microarray assays with good analytical features (LODs in the ppb or sub-ppb level) performing quite similar both, in buffer and in seawater; only for some analytes (sulfonamides and 17 β -estradiol) it was necessary to modify slightly the concentration of the antibody to accomplish the same analytical features as in PBST (see Table 5.2).

These results demonstrated that the fluorescent microarray assays are robust in respect to their potential application to the analysis of seawater samples and that the biofunctionalization procedure employed has worked properly. Only some problems were encountered for deltamethrin due to the fact that the bioconjugate competitor was made with aminodextran instead of BSA. The spots in that case, presented problems in homogeneity and morphology (see Figure 5.6).

Table 5.2. Analytical parameters for all the target assays in an individual fluorescent microarray format performed both in buffer and directly in seawater.

	Irgarol 1051®		Sulfapyridine		Chloramphenicol	
Microarray	4eBSA / As87		SA2BSA / As155		CA6BSA / As226	
Condition	PBST	aSW	PBST	aSW	PBST	aSW
[CA], $\mu\text{g mL}^{-1}$	25	25	12.5	12.5	25	25
[As] dilution	1/8000	1/8000	1/2000	1/1000	1/12000	1/12000
RFUmin	331	276	344	215	3643	2772
RFUmax	10855	9753	13223	11226	12529	11323
Slope	-1.45	-1.95	-1.14	-1.51	-1.19	-0.997
IC₅₀ (nM)	2.29	2.19	15.23	18.90	10.25	9.89
IC₅₀ ($\mu\text{g L}^{-1}$)	0.579	0.554	3.79	4.71	3.00	3.19
LOD ($\mu\text{g L}^{-1}$)	0.135	0.162	0.397	0.991	0.453	0.268
R²	0.997	0.998	0.983	0.999	0.988	0.995
	BDE-47		17β-Estradiol		Domoic acid	
Microarray	2,2,4triBDEBSA / As122		6E2 ₄ BSA /Mab_E2		DA ₅ BSA /Mab_DA	
Condition	PBST	aSW	PBST	aSW	PBST	aSW
[CA], $\mu\text{g mL}^{-1}$	25	25	25	25	50	50
[As] dilution	1/2000	1/2000	1/16000	1/25000	1/1000	1/1000
RFUmin	459	971	13.6	97.1	328	6.99
RFUmax	13825	15748	25671	24704	14810	20004
Slope	-0.733	-1.07	-1.24	-1.55	-1.20	-0.829
IC₅₀ (nM)	7.96	18.71	9.671	11.84	19.21	25.30
IC₅₀ ($\mu\text{g L}^{-1}$)	3.87	9.09	2.63	3.22	5.97	7.88
LOD ($\mu\text{g L}^{-1}$)	0.216	1.24	0.362	0.463	1.26	0.709
R²	0.995	0.998	0.998	0.989	0.989	0.996

The assays presented correspond to assays performed in one-day using at least 3 replicates of each concentration value, both in buffer and in seawater conditions. Microarray chips for single analyte analysis were contained 5 spots of the specific bioconjugate for each assay.

To overcome these problems, we attempted to find out other more suitable printing conditions by changing the buffer composition, the conductivity, the type of detergents such as Tween 20, the pH or even using additives such as

glycerol or DMSO in the printing buffer: However, any of these initiatives provided an improvement of the quality of the spots.

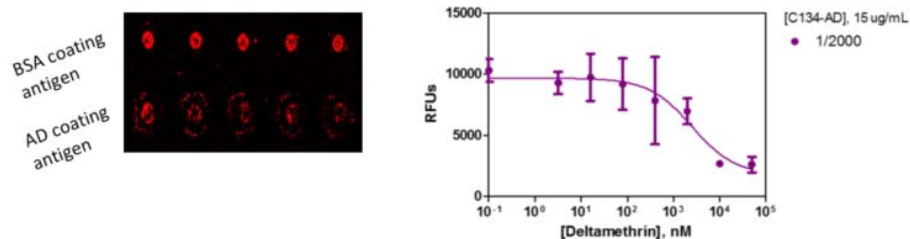


Figure 5.6. Comparison between the spots observed in the case of BSA conjugates immobilized and aminodextran (AD) conjugates (both 50 $\mu\text{g mL}^{-1}$). **Right:** Calibration curve for the assay C134-AD/As360 (15 $\mu\text{g mL}^{-1}$ of antigen, 1/2000 of antiserum) (5 replicates/value).

At the light of these problems, we searched in the literature microarray examples based on dextran derivatives [191, 192]. In most of these examples, the immobilization strategies used were not based on the use of GPTMS. Certain alternatives involved the oxidation of the sugars of the AD [193], or using other supports such as nitrocellulose [194]. However, since our final goal was to develop a multiplexed microarray platform with 6 other pollutants using protein bioconjugates, the strategy of using a different chemistry or support material for this particular analyte was not suitable. On the other hand, as it has been shown in chapter 2, protein-based bioconjugates did not provide good results when detecting deltamethrin using the whole molecule of deltamethrin as the competitor, due to its hydrophobicity. For this reason, at this stage we decided to discard the deltamethrin assay in the microarray multiplexed platform to pursuit with the investigation for perhaps further on trying to investigate other strategies allowing the immobilization of this analyte.

5.3.2 FLUORESCENT MULTIPLEXED MICROARRAY

It has been described that the probability of shared reactivity ((recognition of a bioconjugate competitor by more than one antibody) grows exponentially with the increase of the multiplexation [195]. Thus, on a first instance, the possibility of cooperative phenomena or shared reactivity was assessed to ensure that the

signal recorded on each spot is only due to the binding of the corresponding specific antibody. Although the chemical structures of the selected targets are very different, the use of the same bioconjugation procedure could have led to undesired common epitopes [195]. With this purpose, experiments were carried out to test the binding of each antibody to the different bioconjugates spotted on the glass slides.

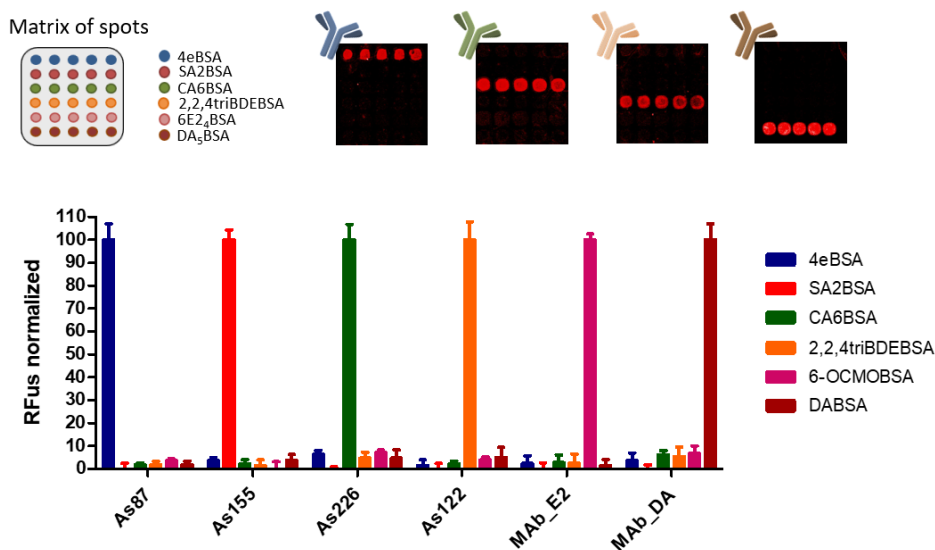


Figure 5.7. Specificity of the antibodies used towards all the bioconjugate competitors spotted on microarray chip. The signal presented corresponds to the average and standard deviation of five spots replicates. Concentrations of the different immunoreagents are summarized in Table 5.2.

As it can be seen in Figure 5.7, any non-specific recognition between each specific antibody and the matrix of antigens selected for the multiplexed microarray platform was detected, demonstrating the strictly specific profile of the immunoreagents selected.

Next step consisted on ensuring the lack of cooperative phenomena recognizing the target analytes by comparing the response of the assays when the antibodies were used individually or as a cocktail composed of 6 antibodies (Irg: As87, diluted 8000 times; SPy: As155 diluted 1000 times; CAP: As226 diluted 12000 times, BDE-47: As122 diluted 2000 times, E2: MAb_E2 diluted 25000 times, DA: MAb_DA diluted 2000 times; all in PBT2x). see Figure 5.9 for an scheme of the performance of the multiplexed microarray.

Figure 5.8 shows the comparison of the standard curves of each analyte in individual format and multiplexed format. Although there were observed slight differences in shape, the analytical features summarized in Table 5.3 show that most of the assays maintain the same parameters once have been multiplexed demonstrating that the use of the antibody cocktail does not affect the detectability of the selected analytes and that those can be quantified individually in the multiplexed platform. Thus, Irgarol 1051®, sulfapyridine, chloramphenicol, BDE₄₇, 17β-estradiol and domoic acid can be detected in the multiplexed format at $0.190 \pm 0,06$, 0.17 ± 0.07 , 0.11 ± 0.03 , 2.71 ± 1.13 , 0.94 ± 0.30 and $1.71 \pm 0.30 \mu\text{g L}^{-1}$ (N=3), respectively, also very close to the reported environmental levels for these pollutants (see Table 4.1 in chapter 4).

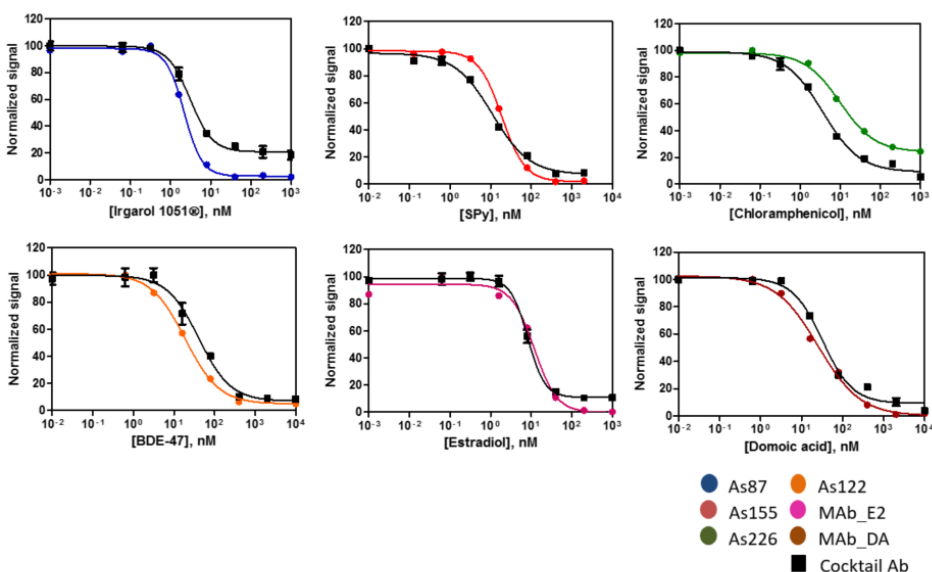


Figure 5.8. Calibration curves obtained when using single antibody solutions (colored curve) or the cocktail of antibodies (black curve). As it can be observed, no significant differences were found. See Table 5.3 for the analytical parameters of the calibration curves of the multiplexed microarray assay. For the multiplexed data, each analyte concentration, was measured using five-spot replicates on each chip. The results are the average of 3 assays performed on 3 different days. The standard curves obtained using single antibody solutions are experiments recorded using at least 3 spot replicates for each concentration value.

In Figure 5.8 can be observed the comparison of the standard curves of each analyte in individual format and multiplexed format. Most of the assays maintain

the same parameters once multiplexed (and being analyzed with the antibody cocktail), consistent results given the cross-reactivity profile obtained previously.

The development of a multiplexed fluorescent microarray platform for the detection of different classes of environmental contaminants was addressed once all the individual assays were established, and the cross-reactivity profile of all the immunoreagents was studied. For the development of the microarray assay an antisera cocktail composed of the 6 antibodies needed was used, and the fact of using a cocktail of antibodies and its possible effect over the parameters of all the assays developed was explored (see Figure 5.9).

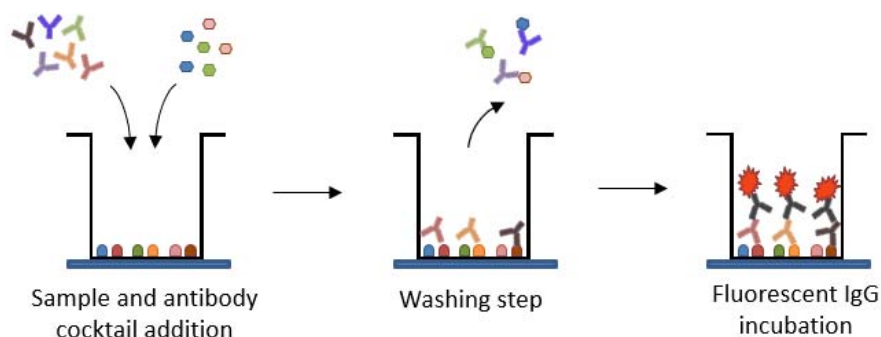


Figure 5.9. Scheme of the multiplexed competitive assay. The printed glass slides are placed in the ArralT hardware and the assay performed as described in the experimental section (see [Materials and methods](#)), by adding the sample followed by the mixture of the antibodies. Finally, a secondary antibody labelled with a fluorophore is added.

The final features of each assay regarding immunoreagents concentrations are summarized in Table 5.3. In respect to the multiplexed ELISA (see Table 4.10) the parameters of IC_{50} and LOD are maintained in the same range (except in the case of domoic acid in which the multiplexed ELISA was slightly better). However, the great features of microarray protocols present some advantages in comparison to the multiplexed ELISA approach. The assay protocol is faster, because as the secondary antibodies are labelled with a fluorophore, no substrate is needed to obtain the final signal. Furthermore, the possibility to analyze simultaneously several samples using the necessary multi-well holder allows running 96 microarrays in parallel, obtaining information of all the pollutants from each measurement.

Although the EQS (environmental quality standard) values set by the Water Framework Directive 2000/60/EC are not reached, the detectability achieved without any sample treatment or preconcentration step is very close to the concentrations found in the environment for most of the pollutants selected. Furthermore, as the different immunoassays have been characterized in the presence of solvents, and their IC_{50} and LOD parameters improved when coupling the SPE column as a preconcentration treatment, it is expected that the detectability of this platform could also greatly improve when choosing the same approximation.

5.3.2.1 Accuracy of the multiplexed microarray

The objective of these experiments was to assess accuracy and to prove that the presence of more than one contaminant in the sample did not affect the quantification. For this purpose, 30 blind spiked samples were prepared in seawater containing the selected analytes at different concentrations, including zero and 5 different concentrations for each analyte. All the samples were analyzed during three different days using five-spot replicates of the multiplexed microarray chips.

As it can be observed in Figure 5.10, the linear regression studies provided slopes near 1 in all cases (being $m=1.00$ the perfect correlation) with very good

Table 5.3. Analytical parameters for all the target assays in a multiplexed fluorescent microarray format performed directly in seawater (n=3). Each analyte was detected a cocktail antibody following the concentrations described in Table 5.2.

	Irgarol 1051®	Sulfapyridine	Chloramphenicol
Microarray	4eBSA / Cocktail antibodies	SA2BSA / Cocktail antibodies	CA6BSA / Cocktail antibodies
[CA], µg mL⁻¹	25	12.5	25
[As] dilution	1/8000	1/1000	1/12000
RFUmin	2214 ± 481	854 ± 467	877 ± 257
RFUmax	10662 ± 459	11985 ± 186	9477 ± 257
Slope	-1.62 ± 0.38	-0.944 ± 0.080	-0.951 ± 0.040
IC₅₀ (nM)	3.05 ± 1.01	11.14 ± 1.61	3.66 ± 0.45
IC₅₀ (µg L⁻¹)	0.773 ± 0.257	2.775 ± 0.404	1.184 ± 0.147
LOD (µg L⁻¹)	0.190 ± 0.06	0.171 ± 0.071	0.105 ± 0.035
R²	0.995 ± 0.005	0.994 ± 0.003	0.992 ± 0.001
	BDE-47	17β-Estradiol	Domoic acid
Microarray	2,2,4triBDEBSA / Cocktail antibodies	6E2 ₄ BSA /Cocktail antibodies	DA ₅ BSA /Cocktail antibodies
[CA], µg mL⁻¹	25	25	25
[As] dilution	1/2000	1/25000	1/2000
RFUmin	907 ± 161	2281 ± 417	1016 ± 212
RFUmax	13025 ± 1111	20653 ± 942	11197 ± 193
Slope	-1.12 ± 0.22	-2.17 ± 0.50	-1.18 ± 0.05
IC₅₀ (nM)	40.77 ± 4.46	8.22 ± 1.30	32.40 ± 0.98
IC₅₀ (µg L⁻¹)	19.81 ± 2.17	2.95 ± 0.47	10.08 ± 0.30
LOD (µg L⁻¹)	2.71 ± 1.13	0.936 ± 0.298	1.71 ± 0.30
R²	0.991 ± 0.005	0.998 ± 0.001	0.990 ± 0.003

Table 5.4. Multiplexed microarray accuracy and precision studies

Analyte	Sample	Spiked value (nM)	Multiplexed quantification	CV (%)	Analyte	Sample	Spiked value (nM)	Multiplexed quantification	CV (%)	Analyte	Sample	Spiked value (nM)	Multiplexed quantification	CV (%)
IRGAROL 1051®	I1	1	1.38 ± 0.27	19.3	SULFAPYRIDINE	S1	3	2.99 ± 0.74	24.8	CHLORAMPHENICOL	C1	2	2.50 ± 0.09	3.8
	I2	2	2.72 ± 0.27	9.8		S2	5	7.05 ± 1.50	21.3		C2	4	4.12 ± 0.78	18.9
	I3	3	3.30 ± 0.14	4.2		S3	10	10.34 ± 1.35	13.1		C3	5	5.53 ± 0.98	17.7
	I4	4	4.04 ± 0.31	7.6		S4	20	18.01 ± 1.57	8.7		C4	8	8.15 ± 1.11	13.7
	I5	5	5.49 ± 0.13	2.4		S5	30	34.3 ± 4.22	12.3		C5	10	11.50 ± 1.48	12.9
BDE-47	B1	20	17.09 ± 2.56	15.0	17β ESTRADIOL	E1	5	5.91 ± 0.88	14.8	DOMOIC ACID	D1	20	17.60 ± 1.01	5.7
	B2	25	27.74 ± 3.98	14.3		E2	6	6.48 ± 0.08	1.2		D2	30	32.17 ± 5.21	16.2
	B3	40	42.58 ± 3.17	7.5		E3	7	7.56 ± 0.24	3.1		D3	50	49.90 ± 2.13	4.3
	B4	75	75.96 ± 4.60	6.1		E4	8	9.85 ± 0.82	8.4		D4	80	83.35 ± 4.54	5.5
	B5	100	102.2 ± 9.10	8.9		E5	10	11.07 ± 1.00	9.1		D5	100	102.85 ± 13.68	13.3

The different samples were analyzed in the multiplexed assay format for the detection of all the target analytes, however only the values of the specific analytes spiked are shown. In all the cases the results obtained for non-specific analytes were lower than the LOD of the assay (i.e. LOD of Irgarol 1051®, sulfapyridine, chloramphenicol, BDE-47, 17β-estradiol and domoic were 0.190 ± 0.06, 0.17 ± 0.07, 0.11 ± 0.03, 2.71 ± 1.13, 0.94 ± 0.30 and 1.71 ± 0.30 µg L⁻¹).

Table 5.5. Complex samples and blanks analyzed by the final multiplexed microarray platform.

Sample	Irgarol 1051 [®]		Sulfapyridine		Chloramphenicol		BDE-47		17 β -estradiol		Domoic acid	
	Multiplexed quantification	CV (%)	Multiplexed quantification	CV (%)	Multiplexed quantification	CV (%)	Multiplexed quantification	CV (%)	Multiplexed quantification	CV (%)	Multiplexed quantification	CV (%)
M1	3.44 \pm 0.14	4.0	10.77 \pm 2.23	20.7	4.25 \pm 0.92	21.7	42.25 \pm 5.21	12.3	7.92 \pm 0.33	4.2	35.74 \pm 7.26	20.3
M2	3.29 \pm 0.32	9.8	11.75 \pm 0.61	5.2	4.14 \pm 1.04	25.1	43.14 \pm 4.35	10.1	7.96 \pm 0.47	5.9	35.58 \pm 3.78	10.6
B1	<LOD	-	<LOD	-	<LOD	-	<LOD	-	<LOD	-	<LOD	-
B2	<LOD	-	<LOD	-	<LOD	-	<LOD	-	<LOD	-	<LOD	-
B3	<LOD	-	<LOD	-	<LOD	-	<LOD	-	<LOD	-	<LOD	-
B4	<LOD	-	<LOD	-	<LOD	-	<LOD	-	<LOD	-	<LOD	-
B5	<LOD	-	<LOD	-	<LOD	-	<LOD	-	<LOD	-	<LOD	-
B6	<LOD	-	<LOD	-	<LOD	-	<LOD	-	<LOD	-	<LOD	-

Two complex samples containing all the analytes at different concentrations (Irg:3nM; SPy:10nM; GAP:4nM; BDE-47:40nM; E2:7nM and DA:30nM) were analyzed by the multiplexed platform. Each sample was detected using a cocktail antibody following the concentrations described in Table 2, during three different days using at least 3 replicates for each concentration value. Microarray chips for multiplexed analysis were spotted in a matrix of 5 x 6 spots (6 analytes, 5 replicates).

regression coefficients ($R^2 > 0.95$), indicating the excellent assay accuracy. On the other hand, the coefficients of variation were below of the 20% pointing to a good microarray assay precision (see Table 5.4).

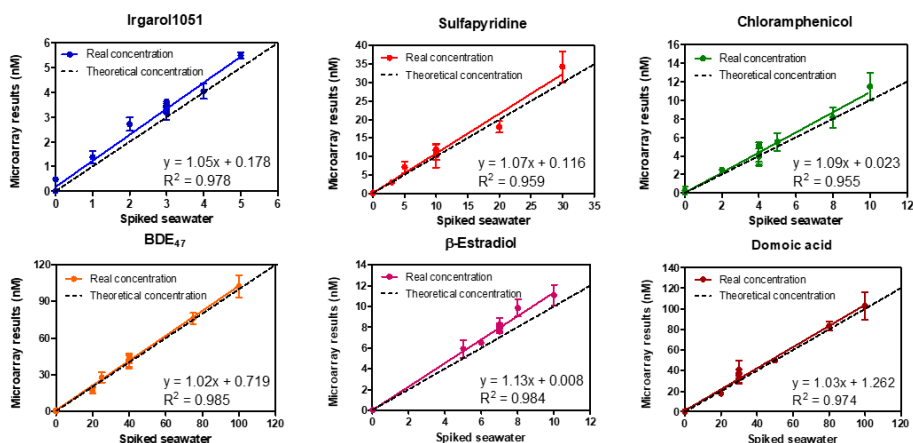


Figure 5.10. Results from the accuracy studies performed in artificial seawater in the multiplexed microarray format. The graph shows the correlation between the spiked and measured concentration values. The dotted line corresponds to a perfect correlation ($m = 1$). The data correspond to the average of at least three-well replicates from 3 different days.

Finally, blank seawater samples and spiked with mixtures of analytes were also quantified, to demonstrate the reliability of the platform. Table 5.5 summarizes the results obtained showing that when several analytes were present it was possible to obtain good levels of accuracy and precision. The coefficients of variation are almost in all cases below 20% and never greater than 25%. No false positives were observed since all the blank samples were negative for the six families of analytes. These experiments illustrated the possible implementation of the platform in environmental monitoring as a screening technique, complementing standard methods such as those based in chromatography.

5.4 Chapter contributions

- A fluorescent microarray for the multiplexed determination and quantification of six different families of potential pollutants of the

ocean has been developed and its suitability to analyze seawater samples has been demonstrated

- The microarray chips consisted on a matrix of 6x5 spots, which allow quantification of each pollutant using five-spot replicates. Seawater samples can be measured directly without any sample treatment in just about 1:30h, being possible to analyze simultaneously several samples using the necessary multi-well holder, which allows running 96 microarrays in parallel.
- Due to the wide selectivity of some of the immunoreagents used in this study is very much likely that the present microarray chip would be able to detect a significant number of chemical congeners of the families selected.
- In spite of the different chemical structures, different antibiotic families, hormones, industrial contaminants, and toxins can be simultaneously quantified with good accuracy and precision.

5.5 Materials and methods

Reagents, materials and equipment. The chemical reagents used are the same than in [section 4.6](#). The plain microscope slides were purchased from Corning Inc (Corning, NY, USA). Fluorescence was read on a ScanArray Gx PLUS (Perkin Elmer, USA).

Immunoreagents. The immunoreagents are the same than in [section 4.6](#). The analytes used in this platform were Irgarol 1051[®] (Irg), Sulfapyridine (SPy), Chloramphenicol (CAP), BDE-47, 17 β -estradiol (E2), and Domoic acid (DA), all purchased from Sigma Chemical Co. (St. Louis, MO, USA), except for BDE-47 (provided by Plymouth University). Stock solutions of each analyte were prepared at 10 mM concentration in DMSO and stored at 4°C until its use. For the development of the microarray assays an antisera cocktail composed of 6 antibodies was used (Irg: As87, diluted 8000 times; SPy: As155 diluted 1000 times; CAP: As226 diluted 12000 times, BDE-47: As122 diluted 2000 times, E2: MAb_E2 diluted 25000 times, DA: MAb_DA diluted 2000 times; all in PBT2x). The anti-rabbit IgG-TRITC and anti-mouse IgG-TRITC were purchased from Sigma-Aldrich.

Buffers. The buffers used are the same than in [section 3.6](#). The printing buffer (PrB) was PBST with 0.005% Tween 20 at pH 7.5. PBT2x is PB (0.02 M phosphate buffer, no saline solution) with 0.1% Tween 20 at pH 7.5.

Microarray printing. Plain pre-cleaned substrates were washed with piranha solution to eliminate any organic matter in their surface, activated with NaOH and functionalized with GPTMS. Coating antigens were spotted using a BioOdyssey Calligrapher MiniArrayer (Bio-Rad Laboratories, Inc. USA), controlling both temperature and humidity. The slides were maintained for 1 hour inside the spotter chamber and finally stored in a desiccator until its use. For the individual assay, 5 spots per well were printed. For the multiplexed assays, a 5 x 7 spot matrix was printed on each well with five spots replicated for each coating antigen (and 5 spots of an anti-IgG-TRITC as a printing control) (See Figure 1a).

Non-competitive indirect microarray. The screening of the avidity of all the antisera and monoclonal antibodies with the corresponding antigens was evaluated. The slides were placed on a microarray ArrayIt system which incorporated a silicon gasket that created an 8x3 wells-format on each slide. Before starting the assay, the slides were washed three times with PBST. Two-dimensional titration assays (2D-assay) were carried out based on the measurement of the binding of serial dilutions of the antisera (1/1000 to 1/64000, and zero, 100 $\mu\text{L well}^{-1}$) against different concentration of the antigens (200 $\mu\text{g mL}^{-1}$ to 25 ng mL^{-1} , and zero). From these experiments, optimum concentrations for coating antigens and antisera dilutions were chosen to generate around 10.000 – 20.000 units of fluorescence.

Microarray competitive assay. As in the non-competitive format, the slides were placed on a microarray ArrayIt system and washed three times with PBST. After that step, each analyte was added (in seawater, 50 $\mu\text{L well}^{-1}$) followed by the specific antibody for the individual assays, or the cocktail of antisera for the multiplexed analysis (in PBT2x, 50 $\mu\text{L well}^{-1}$). Each slide was washed with PBST after 30 min of incubation at RT, and the anti-IgGs-TRITC solution (1/250 in PBST, both antimouse and antirabbit IgGs, 100 $\mu\text{L well}^{-1}$) was added. After another incubation of 30 min at RT in the dark, the slides were washed three times with PBST and one with miliQ water, dried with N_2 and read with the scanner.

Scanner. Measurements were recorded on a ScanArray Gx PLUS (Perkin Elmer, USA) with a Cy3 optical filter with 10- μm resolution. The laser power and PMT

were set to 95% and 80%, respectively. The spots were measured by deducting the mean Cy3 background intensity to the mean of Cy3 foreground intensity. The competitive curves were analyzed with a four-parameter logistic equation using software [SoftmaxPro v4.7 (Molecular Devices) and GraphPad Prism v 5 (GraphPad Software Inc., San Diego, CA, USA)]. The standard curves were fitted to a four-parameter equation according to the following formula: $Y = [(A-B)/1 + (x/C)^D] + B$, where A is the maximal fluorescence, B the minimum fluorescence, C the concentration producing 50% of the difference between A and B (or IC_{50}), and D the slope at the inflection point of the sigmoid curve. The limit of detection (LOD) was defined as the concentration producing 90% of the maximal fluorescence (IC_{90}).

Matrix studies in single analyte measurement. Non-specific interferences produced by the parameters associated with the matrix of interest were studied by preparing a standard curve directly in seawater and measuring each seawater sample directly in the microarray platform.

Cross-reactivity assay. The possible interference between all the immunoreagents involved in the development of the final multiplexed platform was assessed incubating each specific antibody against the matrix of all the immobilized antigens.

Multiplexed assays and reproducibility studies. Each analyte assay was analyzed using a cocktail of antibodies versus all the coating antigens. The different assays were carried out three times within three different days, with five replicates for each point. The main features all the final assays were described as the mean of all the replicates.

Accuracy studies in the final multiplexed microarray format. The accuracy of the multiplexed fluorescent microarray for all analyte concentrations was assessed by spiking blank aSW at 5 different concentrations within the working range of each curve's analyte, a sample with a mix of all analytes and some blank samples with no analyte (being 14 sample analyzed per analyte). The sample concentrations were calculated interpolating the results by external calibration.

6 CONCLUSIONS OF THIS THESIS

6.1 Conclusions

- The production of antibodies able of detecting deltamethrin and cypermethrin, using immunogens that conserve all the characteristic epitopes of the target molecules has been carried out. The selection of the best immunoreagents as well as the optimization of the assay parameters has allowed the development of an immunoassay for the direct detection of deltamethrin in seawater with an LOD of $1.2 \mu\text{g L}^{-1}$, without any pretreatment of the sample.
- The use of aminodextran conjugates has proved useful in favouring the recognitions of the antibodies produced to the specific epitopes of the coating antigen needed for the establishment of the deltamethrin assay.
- 7 single-ELISAs of target analytes selected from different families of environmental pollutants have been developed for its direct detection in seawater samples, a matrix characterized by its high concentration in salts.
- All the assays have demonstrated to be robust and reproducible even in the presence of organic solvents such as methanol and DMSO. The feasibility of developing a multianalyte ELISA platform as a screening platform for environmental monitoring has been evidenced by the quantification of real samples and its validation by a reference chromatographic technique.
- The development of a fluorescent and multiplexed microarray platform has allowed the detection of six different families of potential pollutants of the ocean.
- It has been demonstrated the possibility of analyzing simultaneously environmental pollutants of different chemical structures and properties from the same sample and without any pretreatment. Furthermore, due to the wide selectivity of some of the immunoreagents used in this work is very much likely that the present microarray chip would be able to

detect a significant number of chemical congeners of the families selected.

- Although the EQS (environmental quality standard) values set by the Water Framework Directive 2000/60/EC are not reached by the platform proposed, the detectability achieved without any sample treatment or preconcentration step is very close to the concentrations found in the environment for most of the pollutants selected.

7 ANNEX I: LASER RELEASE OF BIOMOLECULES FROM GOLD NANOPARTICLES

7.1 Introduction

The new methods of nanomaterials synthesis and preparation, as well as the development of novel measuring and characterization techniques, have staged the great expansion nanoscience is living nowadays [196]. As previously explained during the general introduction of this thesis, the singular size-dependent properties of nano scale materials makes them promising candidates for many applications, including the ones related to the biomedical field [45, 46].

Nanotechnology offers many advantages for drug delivery and diagnostics applications. It is known that most biological functions are highly dependent on nanoscale dimension units like viruses or ribosomes, therefore, by having nanoparticles that are small enough for direct interaction with subcellular compartments, it opens up the possibility of activating intracellular events. On the other side, the larger surface-to-volume ratio of the nanocarriers could allow a larger contact area of the drug with the body, increasing the efficiency of a particular dose of the therapeutic agent and reducing potential undesired side effects or toxicity issues. Also, the high available active surface increases the cargo capability.

The increasing demand for more efficient, selective and low cost therapeutic strategies have driven research towards new designs of nanotherapeutic delivery systems, aiming to improve pharmacokinetic and pharmacodynamic properties and to increase selectivity of the active drug on the target tissues. Following this trail, different nanocarriers have been designed for a wide range of applications (see Figure 7.1), from the first generation of nanocarriers which includes dendrimers[197], polymers[198], vesicles or micelles[199, 200], to more advanced nanocomposites appeared during the 80s, which combined two ideas: the long-term formulation concept and the appearance of the first nanotechnology-based platforms; allowing the incorporation of bio-recognition elements, such as antibodies or oligonucleotides [201-203] for tissue targeted therapy.

Knowledge acquired in nanotechnology is contributing to the appearance of new generations of improved nanocarriers involving both, top-down fabrication [204] and bottom-up manufacturing techniques [205, 206]. Multistage silicon

nanocarriers, nanoparticles (including nanoshells, nanorods, nanohollows or

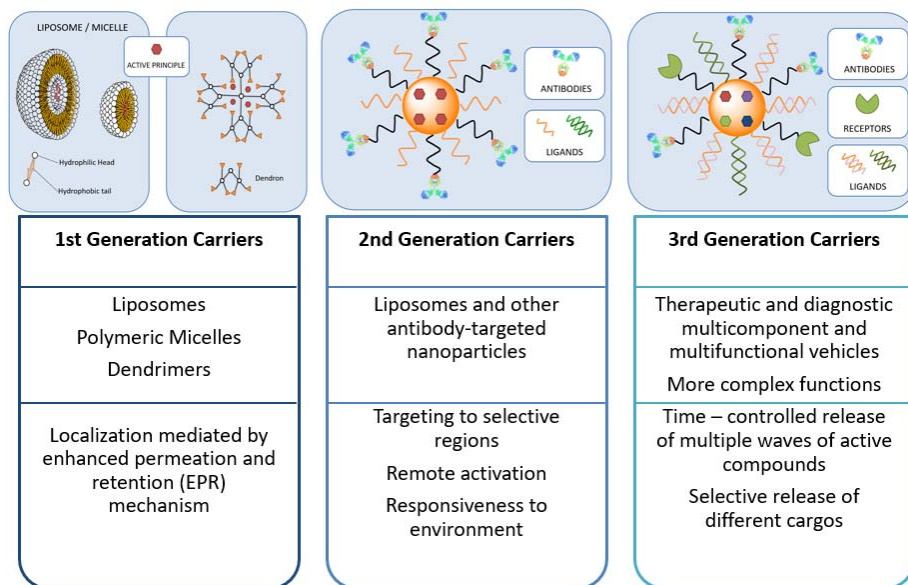


Figure 7.1. Evolution of nanocarriers' generations. Simplicity characterizes the first generation, relying in the EPR effect as the localization mechanism. On the other hand, second generation incorporates targeted-moieties increasing its action's specificity, while third generation offers multicomponent and multidosage strategies for drug delivery and other applications.

solid gold nanoparticles), nanocells but also carbon nanotubes (CNT)[207] or inorganic particles such as gold, magnetic or semiconductor nanoparticles[208-210] are some of the main representatives of this new category, broadening their applications [211-214]. Each of these types shows distinct physico-chemical properties. They can be chemically modified to reduce toxicity or immunogenicity or to accomplish efficient drug loading and release. However, their composition and biofunctionalization could influence the release mechanism in which the different nanosystems will rely for its final function.

7.1.1 BIOFUNCTIONALIZATION CHOICES

Several protocols of nanoparticles functionalization exist in the literature, however, depending on the final application of the nanoparticle system chosen, as well as the material composition of the surface of the particles themselves,

the biofunctionalization protocol selected along with the active biomolecule chosen will be different. Several derivatization strategies based on gold-thiol interactions, modification of surface functional group such as carboxylic, amino and azide residues, or exploiting electrostatic interactions have been described [215].

When discussing the biomolecule attached to the nanocarriers, its role could be linked to increase the stability of the carrier (as in the case of PEG-covered nanoparticles [216]), the targeting capabilities of the carrier, or, its final function. For that reason, depending on the final role, the biomolecules selected will be released or will be considered as structural elements of the nanocarriers. It is well known that one of the molecules for converting nanocomposites in targeted ones once administered in therapeutics applications are antibodies [217-219], being anchored by passive adsorption or by covalent binding. Oligonucleotides and peptides have been also though as targeting molecules [217, 219, 220], as in the case of aptamers, however they may also be considered the target molecule to be delivered as it will be explained in following sections. On the other hand, some elements coupled to nanocarriers can be exclusively linked to the final function of the nanocomposite. From fluorescent dyes, to enzymes, or drugs, several biomolecules have been delivered in therapeutic applications studies for the treatment of cancer, gene silencing or the control of anticoagulant factors among others [221-223].

In spite of this first differentiation with respect to the purpose of the biomolecules anchored in the nanocarriers, usually these designed nanosystems can be considered multimodal, as they could be used for both therapeutic and diagnostic applications. Antibody or oligonucleotide coupled nanoparticles have been used for the delivery of drug as explained previously, however, few examples of novel diagnostics tools based on the same conjugates can be found in the literature, some of them related to standard lateral flow configurations using gold nanoparticles [224], to more innovative methods such as biobarcode assays [225].

7.1.2 GOLD NANOPARTICLES

Noble metal nanostructures have been a subject of increasing interest recently. Within this category it can be found several morphologies including nanospheres, nanorods, nanoshells or nanocages, all of them related to several applications based on their optical features [226-229]. One of the features to be highlighted is plasmonics, an effect that can be described as an oscillation of the surface electrons and can be considered a mode of excitation localized at the interface between a metal film and the surrounding dielectric (Figure 7.2).

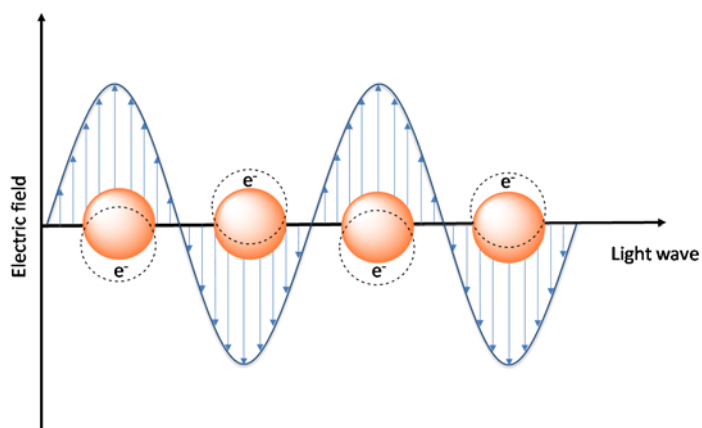


Figure 7.2. Scheme of the basics of plasmon resonance of gold nanoparticles due to collective oscillation of surface electrons with incident light at a specific wavelength.

The generation of surface plasmon waves; which are resonances states produced by the interaction with light such as surface plasmon resonance (SPR) or localized surface plasmon resonance (LSPR) is the basis of most of the applications of gold nanoparticles [228].

Within metallic nanostructures, gold nanoparticles are considered great candidates for biomedical applications (see Figure 7.3) as nanocarriers for drug and gene delivery due to their unique chemical and physical properties for transporting and unloading their payloads (small drug molecules or large biomolecules, like proteins, DNA or RNA) [230].

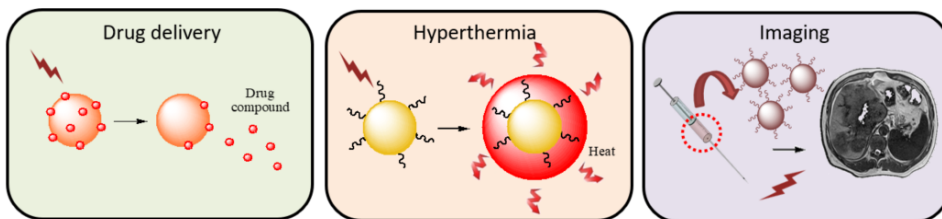


Figure 7.3. Scheme of the main application of gold nanoparticles: drug delivery, hyperthermia and imaging.

Their gold core is essentially inert and non-toxic [231], an essential requisite in biological applications; and they can be produced as monodisperse nanoparticles with cores sizes ranging from few nanometers to more than 150 nm [232-234]. Further benefits are their ready functionalization (mainly through thiol linkages). Their strong and tunable optical absorption properties could trigger drug release at remote place, turning them in excellent platforms for controlled drug delivery.

7.1.3 LASER RELEASE MECHANISMS

One of the features of the new generation of nanomaterials, is that they are (or can be designed to be particularly sensitive to environmental factors [235]. From light to pH, including temperature, ionic strength or ultrasonic waves, nanocarriers offer the advantage of a time-controlled or modulated release in comparison to traditional formulations. However, not all the parameters exploit the nanocarriers intrinsic properties to induce the release of their cargo. As an example, release based on pH changes usually take advantage of the natural environment the biological vesicle system offer to nanocarriers during its migration to the specific target[236]. Different strategies based on how pH affect the conformation of polymers composing the nanovehicles have been described [237], both for therapeutics purposes [238-240] or as theragnostic platforms [239].

Light is the main source of energy which can act as an external triggering-stimulus; offering at the same time great advantages such as the easy control of its wavelength and intensity [241]. Additionally, the area of action of the stimulus can be spatially manipulated varying the direction of the source power. For those reasons, when designing a laser-based release system the nature of the light

source is a key element. Several parameters including the wavelength, the power of the laser and the mode of irradiation are relevant features that could determine the mechanisms activated for the biomolecule's release, and for that reason they are the first step in studying and developing a nanocarrier system of release based on the light use.

Several applications based on different types of light have been described in the literature. As explained previously, ultraviolet (UV) light can be used to induce release mechanisms based on the photoexcitation of photosensitive moieties triggering phenomena of photo-induced transformation, bond cleavage, photoisomerization, or photocrosslinking [242-245]. However, other wavelengths can be considered in order to take advantage of the inner properties of the nanocarriers selected and not of the elements presents during its derivatization and functionalization. An example is near-infrared (NIR) light, with wavelengths ranging from 650nm to 900 nm, which has been used clinically for *in vivo* imaging and hyperthermic tumor treatment due to its many advantages [221]. The main reason for that preference in the selection of NIR light in *in vivo* applications is that tissues are mostly transparent to this kind of light, making NIR light safer than other wavelengths [246, 247]. Nevertheless, NIR light can be considered an attractive option as it can influence over the resonant behavior of nanostructures, allowing the establishment of nanoparticles-based strategies [248-251].

7.1.3.1 Irradiation modes

Although important, wavelength is not the only critical parameter in inducing cargo's release; the mode of irradiation upon the drug delivery system selected is also determinant (see Figure 7.4). Intensity, frequency, or potency are some of the features to be set to properly control the release mechanism induced. Moreover, choosing between continuous-wave (CW) mode of irradiation or pulsed light (PL) might condition the release mechanism involved.

One of the reasons because the irradiation mode could affect the release mechanism is the change in the shape of the nanoparticle upon irradiation.

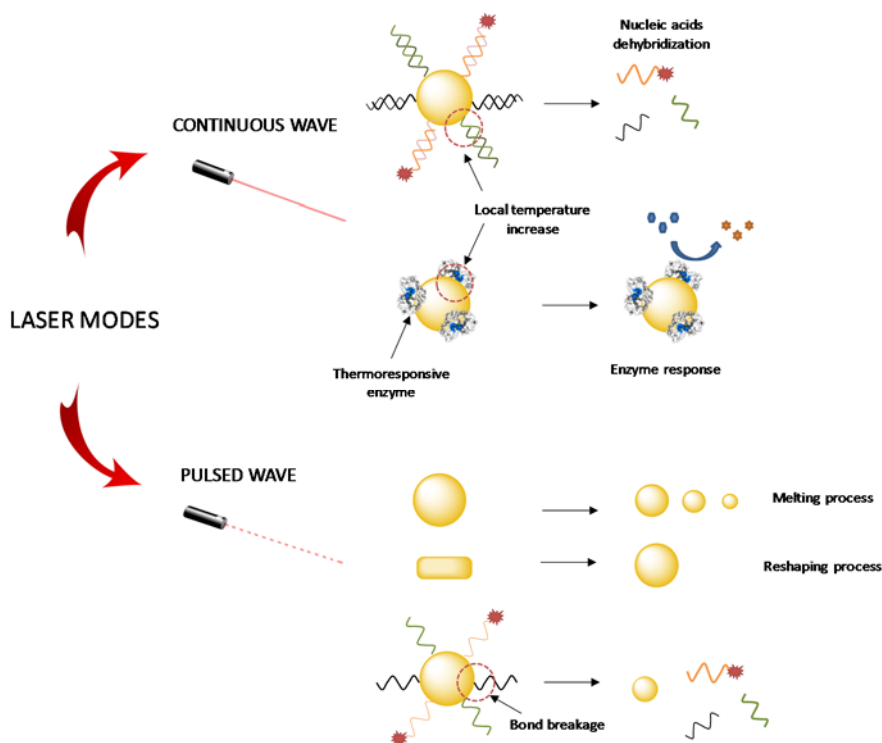


Figure 7.4. Scheme of the different laser modes and the release mechanisms involved in each mode. While using a continuous wave laser the solution temperature doesn't change, it produces a high and local increase in the nanoparticle's surface. Whereas using a pulsed wave laser the nanoparticles suffer from reshaping and melting processes, inducing the gold-thiol bond breakage, and directly releasing the attached molecules.

The use of CW laser upon gold nanoparticle solution is often associated to a rapid temperature increases of a limited area of the gold surface without increasing the ambient temperature of the solution and without affecting the gold shape [252]. Taking profit of that phenomenon, one of the usual application of the use of CW laser are related to the release of ssDNA or functional oligonucleotides [253, 254]. However, the activation of thermophilic enzymes immobilized over the gold nanocomposites are also an explorable field both in clinical and industrial applications [255].

On the other hand, the use of PL excitation upon gold nanoparticle solution, in resonance with their surface plasmon resonance, can heat NPs locally to high temperatures, inducing both melting and reshaping processes [256] Hence, through melting, and the induction of the direct break of the interaction between

the nanoparticles and the immobilized targets, the release of certain molecules can be achieved [257]. In this case the dehybridization strategy previously explained for the CW irradiation cannot be contemplated as an option, due to the melting and reshaping process of the nanoparticles and the bond breakage process, but, the direct release of nucleic acids conjugated through thiol linkage becomes a possibility [258-260]. Moreover, PL light have been demonstrated to be useful in helping nanocarriers escape the vesicle system that usually encapsulate those vehicles during drug delivery applications [258].

Despite the reasons stated during the introduction, and although several therapeutic applications of selective-release nanosystems based on the intrinsic properties of the nanocarriers have been presented in the literature, the field of diagnostics applications regarding these singular nanocarriers seems to be in the first stages.

7.2 Chapter objective

The goal of this chapter (see Figure 7.5) is to create the basis for the development of a diagnostic system based on plasmonic nanoparticles, aiming to multidetect two small-molecules related to the biomedical field. The study is currently focused in the functionalization of gold nanoparticles with fluorescent molecules and the characterization of its release by light-related mechanisms, taking profit of the inner ability of nanoplasmonics gold nanoparticles possess.

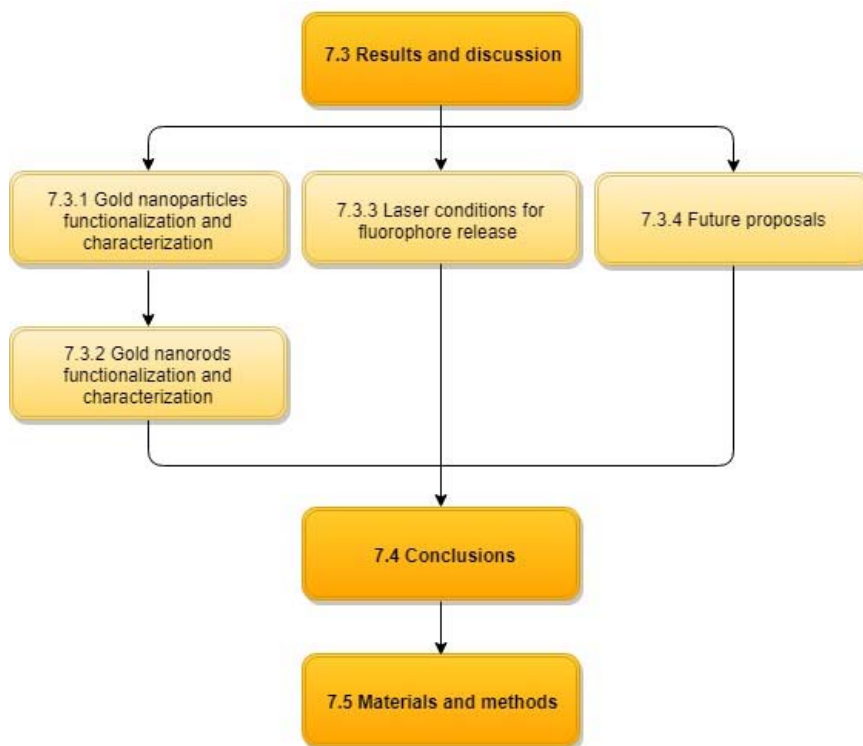


Figure 7.5. Structure of this chapter related to the different sections

During this part of the thesis, a system based on gold nanoparticles was designed aiming to take advantage of an external light stimulus for inducing the release of fluorescent biomolecules. Our assay strategy will be formed by three different steps (Figure 7.6):

1. **Functionalized gold nanoparticles**, both with specific antibodies against the small molecule target selected and fluorescent molecules that will provide an amplification of the signal through its final release.
2. **Laser irradiation** at different wavelengths, that will allow the selective release of the fluorescent molecules anchored to each gold nanoparticle.
3. **Fluorescent final readout** in solution of the fluorescent labels released during the laser treatment.

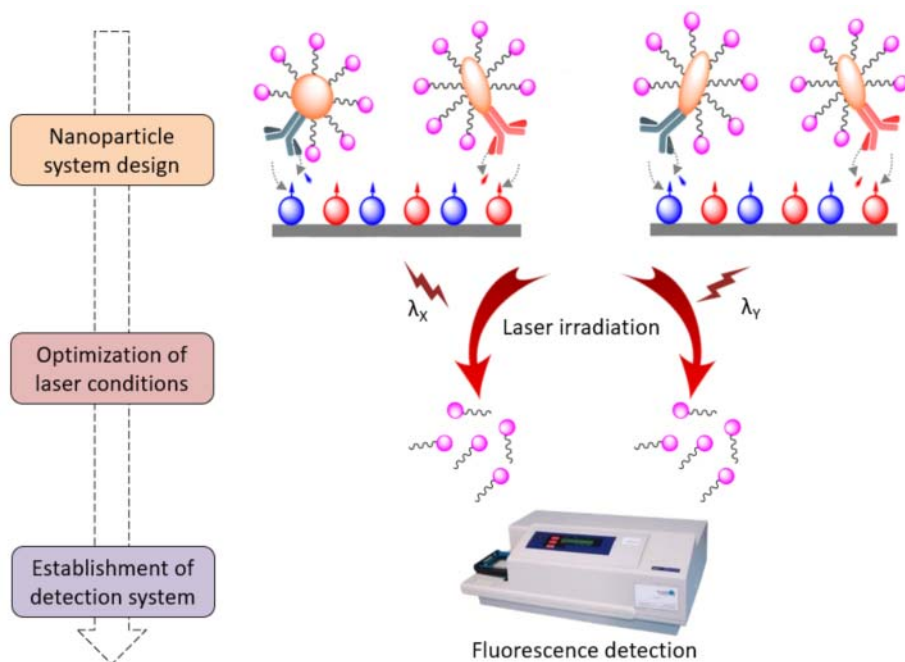


Figure 7.6. Schematic diagram of the multiplexed plasmonic strategy proposed. The nanoparticle system is based on two nanoparticles with different plasmon peaks, being of different shapes (left) or the same (right).

The final goal of this chapter was the establishment of a multiplexed platform based on a competitive format for the detection of two small molecules related to clinical diagnostics.

7.3 Results and discussion

During the development of this chapter thesis the nanoparticle system design was changed to being able to adapt to the different problems that will be discussed through the chapter. For making easier the comprehension of the evolution of the experimental process, the chapter will be divided in two sections.

7.3.1 SECTION A: SPHERICAL GOLD NANOPARTICLES FUNCTIONALIZATION AND CHARACTERIZATION

The first strategy explored during the development of the multiplexed platform proposed in [section 6.2](#) was the use of two spherical gold nanoparticles with different properties. The first ones were solid gold nanoparticles (AuNPs) while the second were hollow gold nanoparticles (HGNs) (see Figure 7.7). The goal was to demonstrate that HGNs can offer a higher cargo capacity due to its intern cavities that increase significantly the usable surface for immobilizing the biomolecules of interest.

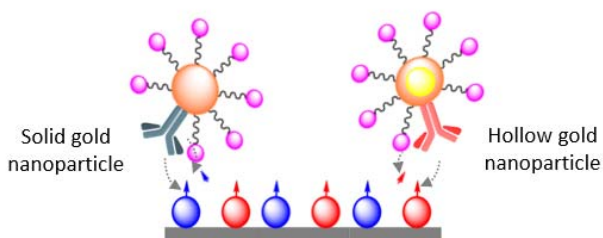


Figure 7.7. First strategy design for the multiplexed release system based on laser-light stimulation

7.3.1.1 Gold nanoparticles synthesis

AuNPs synthesis was performed by Marta Broto during her thesis and followed the Turkevich method, based on citrate reduction of gold salt [261]. Sodium citrate not only reduces gold but solvates the particles. Particles were characterized by transmission electron microscope (TEM) and UV-Vis, both methods reported 16-nm diameter with a polydispersity lower than 9 % and demonstrated high stability along time (see Figure 7.8).

On the other hand, hollow gold nanoparticles (HGNs) were provided by the group of Professor Santamaria from the Instituto de Nanociencia de Aragón (INA). HGNs were synthesized following the sacrificial galvanic replacement of cobalt nanoparticles procediment [262]. A size of 45 nm of HGNs were obtained, with a thick wall of approximately 6nm.

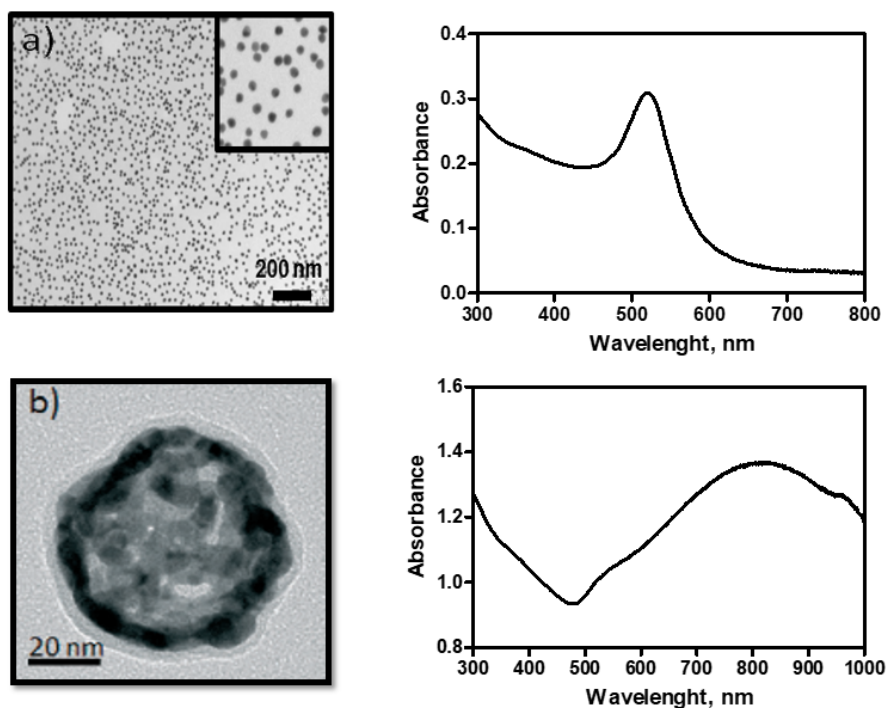


Figure 7.8. TEM images of AuNPs 16nm (a), HGNS 40nm and their respective UV-Vis spectra of the particle solution. Maximum absorbance of AuNPs corresponds to 520 nm, whereas for HGNS corresponds to 816nm.

In order to have a comparable system in terms of yield of conjugation and cargo capacity the need of two nanoparticles of the same diameter is required. For that reason, the solid AuNPs of 16nm were used as a template for the regrowth of AuNPs of 40nm.

The method followed for enlargement of colloidal Au nanoparticles is called “seeding”, based on the colloidal Au surface-catalyzed reduction of Au^{3+} by hydroxylamine (Figure 7.9) [263]. While NH_2OH is thermodynamically capable of reducing Au^{3+} to bulk metal, the reaction is accelerated in the context of Au surfaces [264]. As a result, no new particle nucleation occurs in solution, and all added Au^{3+} goes into production of larger particles.

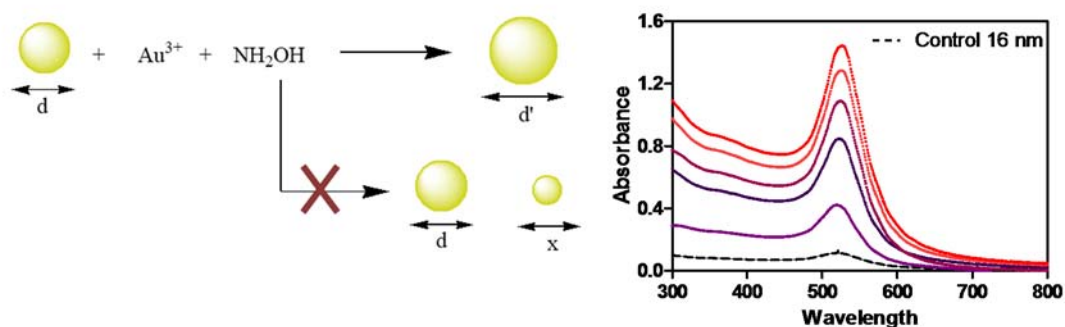


Figure 7.9. Left: Scheme of the hydroxylamine seeding procedure. Right: Growth of colloidal AuNPs by UV-vis spectrophotometry. From the control of 16nm (bottom) the different curves correspond to different additions of HAuCl₄. The growth was stopped when the maximum peak of absorbance was 525nm, the specific one related to 40nm AuNPs.

Once both systems were obtained and characterized, the functionalization and the studies of cargo capacities of both nanoparticles started.

7.3.1.2 Gold nanoparticles bioconjugation

Originally, gold nanoparticle functionalization was started by Nuria Tort and Gloria Colom in their PhD thesis and was followed by Marta Broto in her thesis. Although the final design was thought to obtain nanoparticles functionalized with both a bioreceptor and a fluorescent molecule, the first studies were focused in determining the loading capacity of nanohollows particles (HGNs) in comparison to solid gold nanoparticles (AuNPs). As a model of fluorescent molecules, oligonucleotides marked with different fluorophores including Carboxytetramethylrhodamine (TAMRA) and fluorescein (Flc) were selected.

For the conjugation of both solid and hollow nanoparticles, a pH-assisted methodology characterized for rapid protocols were selected [265]. This approach was based on the addition of a low pH buffer that reduces the repulsion between chains allowing a maximal loading. Furthermore, sodium dodecyl sulfate (SDS) present in the buffer keeps particles from aggregation, provides better stability and adds washing efficiency. Then, oligonucleotide release from the particles was done with a ligand exchange treatment, with the reagent dithiothreitol (DTT) (see Figure 7.10).

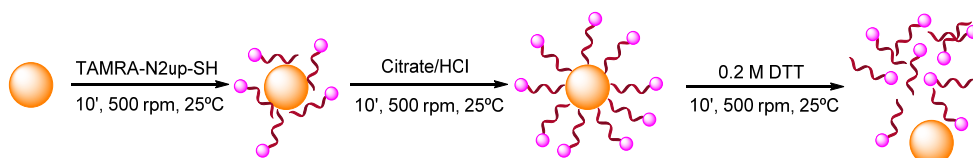


Figure 7.10. Scheme of fluorescent oligonucleotide conjugation and release for the AuNPs.

Different initial concentrations of fluorescent oligonucleotide were conjugated to the two kinds of particles and the non-conjugated oligonucleotide was characterized from the supernatants.

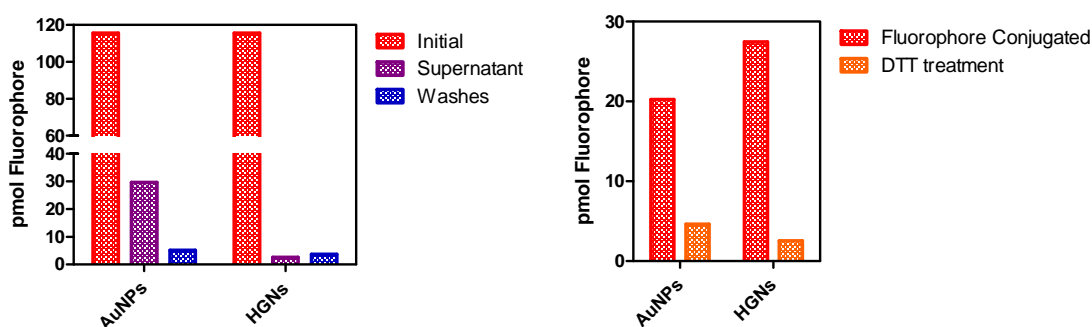


Figure 7.11. Left: Comparison of fluorophore presence in the different supernatants obtained during the conjugation process. 5 different washes were done, until no fluorophore was detected. **Right:** Comparison of fluorophore release obtained from DTT treatment for both kind of particles.

As a result, from this study we can state that HGNs has a 95% of loading capacity from the fluorophore added (Figure 7.11), in comparison with solid nanoparticles that was found a 70% using the same amount. This fact demonstrates the superior loading capacity of the gold nanohollows. However, unexpected results were obtained when studying the release of the fluorophore attached to the NPs. The first approach was to treat the conjugated nanoparticles with dithiothreitol (DTT), a reducing agent capable of breaking the thiol-gold bond (between the fluorophore and the nanoparticle). Although low in both cases, unexpectedly, the release from the nanohollows seemed to be lower than from solid particles, and these results did not change when the duration of the DTT treatment was longer or when the concentration of the reducing agent was up to 5 times higher.

As DTT treatment was not the option selected for the final assay platforms, it was decided to not invest more time in their optimization and test the laser-based release mechanism. The laser, property of the group of Manuel Arruebo

from INA, was a continuous-wave laser, with a power of 3W, a fiber to manipulate the light source, and a peak at 808nm. Nanoparticles with twice the concentration of fluorophore were proposed as a model, and fluorophore release was studied irradiating both colloidal dispersions with a diode laser (808nm from Acai Ibérica) at different times.

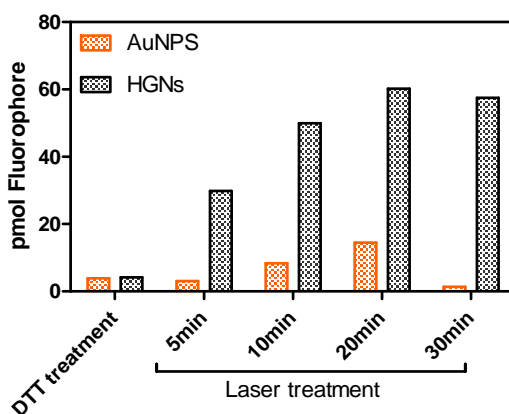


Figure 7.12. Comparison of fluorophore release obtained from DTT treatment and laser treatment at 808nm and different times, for both kind of particles, solid gold nanoparticles (AuNPs) with a plasmon peak of 532nm, and nanohollows (HGNS) with a plasmon peak of 800nm.

Although a great improve in release capabilities from HGNS were observed at different times, an unspecific release from the solid nanoparticles were observed (Figure 7.12). Initially as its peak of resonance was 532nm after the functionalization, an irradiation with an 808nm diode laser should not have resulted in a release of the attached fluorophores. A hypothesis was that the power of the laser was too high, and the nanoparticles had been destroyed releasing nonspecifically their cargo. AuNPs after irradiation didn't show the specific absorbance profile with a peak of 532nm, pointing out the possibility of nanoparticles destruction (Figure 7.13).

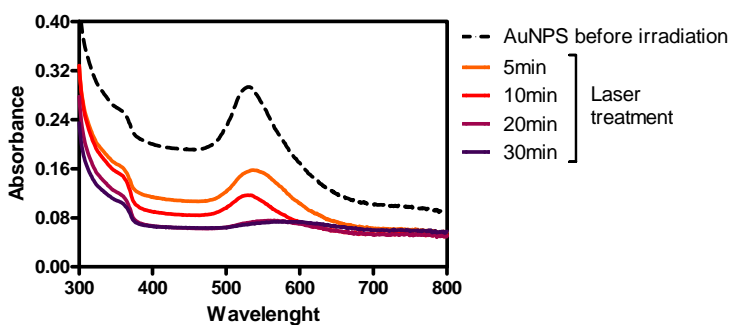


Figure 7.13. Comparison of UV-vis profile of AuNPs before and after different irradiation times. The loss of the specific 532nm peak-profile could be indicative of the nanoparticle's loss.

However, that behavior was maintained at different laser powers, and even was repeated when irradiating functionalized 16nm solid nanoparticles as controls. Another issue was that with the equipment used no control of the frequency used during the irradiation could be achieved, affecting the final energy of the pulses generated. At that point two concerns arose:

- The equipment used was not appropriate for two reasons. The wavelengths couldn't be modified for the selective release of two different systems of nanoparticles. Furthermore, the impossibility to control all the parameters of the laser as the frequency of pulses, or the energy per pulse, determined the need of search for other laser sources.
- Difficulties in the obtention of regular batches of HGNs with a reproducibility in its synthesis characterization were presented. Important differences in absorbances profiles and the lack of physicochemical characterization of late batches led to the discard of hollow nanoparticles, although the promising results regarding the superior cargo and great levels of laser-induced release obtained. Other options regarding plasmonic nanoparticles were explored.

7.3.2 SECTION B: NON-SHPERICAL GOLD NANOPARTICLES FUNCTIONALIZATION AND CHARACTERIZATION

The second strategy explored during the development of the multiplexed platform proposed in [section 7.2](#) was the use of two non-spherical gold

nanoparticles or a combination of nanoparticles with different morphologies (see Figure 7.14).

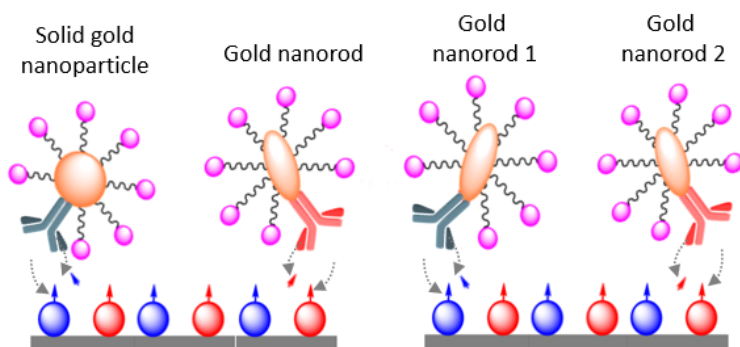


Figure 7.14. Second strategy design for the multiplexed release system based on laser-light stimulation.

Gold nanorods were considered as potential candidates for being implemented in the dual system proposed during this work. Because of their anisotropic shape, nanorods are characterized by two LSPR peaks: the transverse, fixed at approximately 530 nm, and the longitudinal, which is in the visible–near infrared region of the spectrum and varies with nanorod aspect ratio. The optical properties of noble metal nanorods have been widely characterized and exploited in analytical and biomedical applications [266].

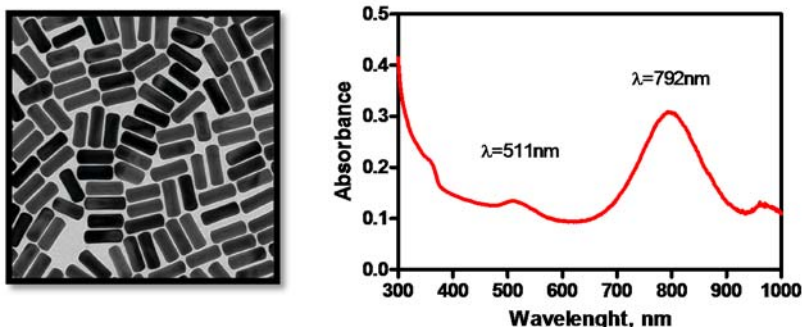


Figure 7.15. TEM images of NRs 41nm and its respective UV-Vis spectra of the particle solution. Maximum absorbance of the transversal corresponds to 511nm whereas for the longitudinal axis corresponds to 792 nm.

The hypothesis presented was that a paired system formed by a spherical nanoparticle and a nanorod could fulfil the needs of the platform presented, as long as the excitation peak of each one can be significantly differentiated (see Figure 7.15)

7.3.2.1 Gold nanoparticles and nanorods bioconjugation

As the final redout of fluorescence in the platform designed was the measure of fluorescence of the liberated molecules in solution, the model oligonucleotides used during the first stages of this chapter were replaced by fluorescent labels conjugated to polyethylene glycol (PEG) moieties (Figure 7.16).

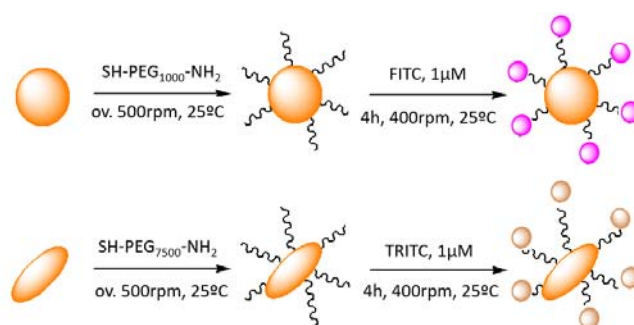


Figure 7.16. Scheme of PEG moieties and fluorescent biomolecules conjugation both for AuNPs and NRs.

PEG molecules are used not only as a way to anchor a functional group for the final incorporation of the fluorophore, but also as an approach to prevent the interaction between nanoparticles and add stability due its hydrophilic properties. It has been demonstrated that the length of the PEG chains is a critical parameter for the stabilization of nanorods [267] and for that reason the length of the PEG chain was optimized. A full coverage of a heterobifunctional PEG with a thiol and amino group was chosen in order to maximize the number of fluorophores that could be immobilized.

Once PEG conjugation procedure was established, we proceed to functionalize the particles with the fluorophores selected: fluorescein isothiocyanate (FITC) and rodamine isothiocyanate (TRITC). Several parameters like conjugation time, agitation conditions, fluorophore concentration and solubility were optimized,

until obtain yields of 93% for the conjugation of FITC to AuNPs and 64% for the conjugation of TRITC to NRs (see Figure 7.17).

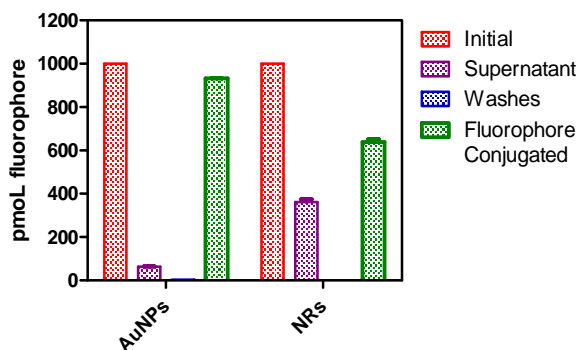


Figure 7.17. Comparison of fluorophore presence and conjugation yield in the different supernatants obtained during the conjugation process for AuNPs and NRs. 2 different washes were done, with no fluorophore detected.

The final protocol of conjugation consisted in incubating the nanoparticles and the fluorophore during 4h with an agitation of 400rpm. The Uv-vis profile was monitored during each step to ensure that any aggregation procedure took place during the functionalization of the nanoparticles. The final protocol is described in [Section 7.5](#).

7.3.3 LASER CONDITIONS FOR FLUOROPHORE RELEASE

During the development of this thesis, an exhaustive literature research was done in order to understand the underlying mechanism involved in the liberation of the biomolecules anchored on the surface of the gold nanoparticles selected for this study. Not only the wavelengths are key factors in inducing specific release but also a high number of variables including the pulsation of the beam of light used, the power of the equipment used or even the energy of each pulse generated can determine the success or the failure of the selective liberation of marker molecules.

One of the common features of the different research papers published for the liberation of molecules anchored over plasmonic nanoparticles such as nanorods, were the use of laser equipments which were able to generate

femtopulsed light. Although the energy pulses were in the range of mJ, that criteria along with the frequency used for irradiation experiments, varied between publications. Therefore, the first step was decided to be the exploration of using a femtopulsed laser for release characterization.

To carry out such experiments a collaboration with The Institute of Photonic Sciences (ICFO) were established. The proof of concept experiment was designed as follows: At a fixed time, different powers of an 808nm-femtopulsed laser were selected for irradiate both AuNPs and NRs in order to know if that parameter was decisive. After the irradiation of each sample, and after a centrifugation step in order to precipitate the nanoparticles in solution, the presence of fluorophore in the supernatant was quantified by fluorescence. As it can be observed in Figure 7.18 a considerable improvement in NRs release was obtained, while in no case a significant release was observed in the case of the spherical particles (less than a 4%).

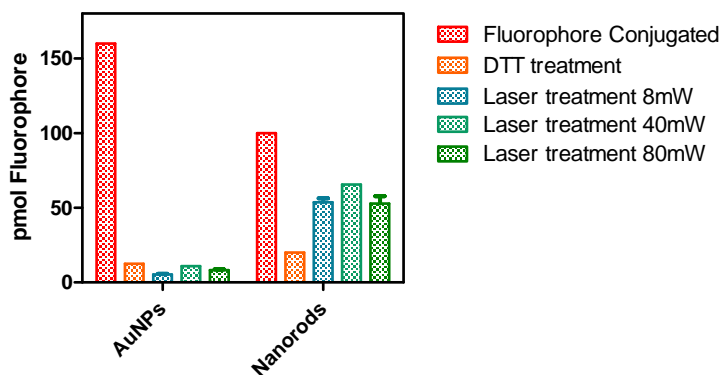


Figure 7.18. Comparison of the fluorophore release obtained from different 10 minute-laser treatments, in terms of laser power used, for both nanoparticle systems. A release of approximately 65% of the fluorophore anchored on NRs was liberated.

Finally, in order to demonstrate the right choice of using a femtopulsed laser source for the selective release needed for the diagnostic platform proposed, the use of a Neodymium:YAG laser which can work at the same wavelength and with similar energy pulses as the one previously used to be explored. The main difference was that this equipment only can generate pulsed light in the nanoseconds range, therefore, the variable of the femtopulsed light could be

studied. As we expected, no release was observed at any irradiation time, in any nanoparticle system, demonstrating that femtopulses are a key feature in inducing biomolecules release form plasmonic nanosystems.

7.3.4 FUTURE PROPOSALS

Once demonstrated that the new laser source seems to be promising to the selective liberation of fluorophores immobilized on the nanorod chosen with a minimal unspecific from spherical particles a new path for studies were opened. Sadly, the laser couldn't be tuned to wavelengths lower than 650nm, making imposible to continue of experiments with the system spherical-rod particle proposed.

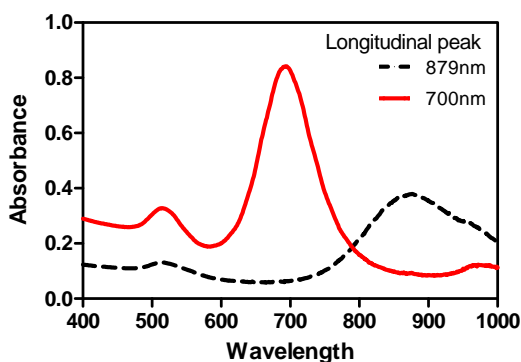


Figure 7.19. UV-Vis spectra of the two NRs particle solution proposed for the development of th dual-system of selective release. Maximum absorbance of the longitudinal peak corresponds to 879nm and 700nm for each NR.

New commercial sources for nanorods were found, and a new system based on two nanorods with longitudinal peaks between 750 and 900nm was suggested for future work (see Figure 7.19).

7.4 Conclusions

- A simple and reproducible method for the functionalization of nanorods with heterobifunctional polyethylenglicol molecules has been

developed, allowing the direct immobilization of biomolecules such as fluorophores.

- The needed conditions for the specific release of attached molecules to gold nanocomposites has been listed. The importance of the light nature in the release mechanism of the anchored molecules has become evident. The effort in searching light sources able to be stably modulated in a wide range of wavelength still stands.

7.5 Materials and methods

Reagents, materials and equipment. The chemical reagents used were obtained from Aldrich Chemical Co. (Milwaukee, WI, USA) and from Sigma Chemical Co. (St. Louis, MO, USA).

TAMRA-N2up-SH, [TAMRA]TCAAGTCGAATGTACCTCCG5[ThiC3], and FLC-N2up-SH, [FLC]TCAAGTCGAATGTACCTCCG5[ThiC6], were purchased from Sigma Chemical Co. (St. Louis, MO, USA). HS-PEG₁₀₀₀-NH₂ was also purchased from Sigma Chemical Co. HS-PEG₇₅₀₀-NH₂ was purchased from Laysan Bio, Inc (Arab, AL, USA). Nanorods with a surface peak of 808nm were purchased from Sigma Chemical Co. TS-100C (Biosan, Riga, Latvia) was used to shake nanoparticle's solutions. Eppendrofs were centrifuged with a Legend Micro (Thermo Fisher Scientific Inc.).

AuNPs synthesis. 500 μ L of gold (III) chloride trihydrate 0.1 M in milliQ were added to 150 mL of milliQ water. It was brought to boiling with the highest stirring velocity, subsequently, 4.5 mL of sodium citrate 1 % was injected to the solution. After 30' at boiling temperature it was cooled and stored in the fridge. Finally, particles were characterized by TEM and UV-Vis spectroscopy from 300 to 800 nm. Particle size of 16 nm and polydispersion < 9 % was reported.

AuNPs growth. 10 mL of seed 16nm AuNPs were added to 90 mL of milliQ water. 1mL of NH₂OH:HCl 0.2M in ultrapure water was added with the highest stirring velocity, subsequently, and maintaining the agitation, different volumes of HAuCl₄ 25.4mM were injected to the solution. After 5' after each addition, the growth of nanoparticles was followed by UV-vis spectrophotometry.

Buffers. Citrate/HCl buffer is 500 nM pH 3. PB/SDS is 10 mM, pH 7, 0.01 % SDS.

AuNPs and HGNs oligonucleotide biofunctionalization. A solution of 25,9 pmol of oligonucleotide in 20 μL of milliQ was prepared and added to 100 μL of AuNPs/HGNs stock during 10', 25°C, 500 rpm. Then, 2 μL of Citrate/HCl buffer and 2 μL of SDS 0.1% buffer were added and allowed to react 10' more. Subsequently, reaction mixture was centrifuged during 10' at 14500 G for AuNPs and 12000 G for HGNs, and the resulting pellets were resuspended and washed twice with PB/SDS.

Oligonucleotide release. 50 μL of functionalized particles were mixed with 250 μL of dithiothreitol 0.2 M in ultrapure water and let 10', 25°C, 500 rpm. Then, particles were centrifuged (10', 14500 G) and supernatant fluorescence was measured (Fluorescein: excitation 543 nm, emission 575 nm).

AuNPs and NRs fluorophore biofunctionalization. 200 μL of a solution of SH-PEG-NH₂ 1mM in ultrapure water (MW:1000KDa for AuNPs, MW:7500KDa for NRs) was added to 800 μL of AuNPs/NRs stock and let at 25°C and 500 rpm overnight. Suspensions were centrifuged during 10' (14500 G for AuNPs, 18800 G for NRs) and resuspended in 800 μL of ultrapure water. Afterwards, 180 mL of ultrapure water and 20 μL of fluorophore stock (50 μM in pure ethanol) were added and let react during 4h at 25°C and 400 rpm. Subsequently, reaction mixtures were centrifuged during 10' at the respective G conditions for each nanoparticle, and the resulting pellets were resuspended and washed at least 3 times with ultrapure water. The supernatants collected were and their fluorescence were read on a Spectramax Gemini XPS (Molecular Devices, Sunnyvale, CA, USA). During each step the absorbance profiles were followed on a Spectramax Plus (Molecular Devices, Sunnyvale, CA, USA) in order to control the possible loss or aggregation of the nanoparticles.

Laser treatment. A) Irradiation of oligonucleotide-bioconjugated AuNPs and HGNs. The irradiation was performed using an 808-nm diode laser (MDL-III-808, 0–2.5W continuous wave output; Optoengine) and a 400- μm fiberoptic cable. Different times (5,10,20 and 30') and different powers (600mW, 700mW and 820mW) were tested over 200 μL of AuNPs/HGNs. After the irradiation, nanoparticle's suspensions were centrifuged for 10 minutes (14500 G for AuNPs and 12000 G for HGNs) and fluorescence was measured by a fluorimeter (SpectraMax Gemini XPS, Molecular Devices). B) Irradiation of fluorophore-

bioconjugated AuNPs and NRs. The irradiation was performed using a confocal microscope (Nikon, D-Eclipse C1si) coupled to a Kerr lens mode-locked Ti:sapphire laser (Mira900, Coherent with 200 fs pulse duration at a frequency of 80 MHz) tuned at the NRs resonance, and 50 mJ or 10mJ of average energy. 200 μ L of nanoparticles or nanorods in solution were placed over a plastic substrate and irradiated for 10 minutes. After the irradiation, nanoparticle's suspensions were centrifuged for 10 minutes (14500 G for AuNPs and 18800 G for NRs) and fluorescence was measured by a fluorimeter (SpectraMax Gemini XPS, Molecular Devices). C) Irradiation of fluorophore-bioconjugated AuNPs and NRs (part II). The irradiation was performed using a Neodymium:YAG (neodymium-doped yttrium aluminium garnet with a 5ns pulse duration at a 10 Hz repetition rate) laser tuned at the AuNPs/NRs resonance, with 30 mJ or 40mJ of average energy. 200 μ L of nanoparticles or nanorods in solution were placed over a plastic substrate and irradiated for 10 minutes. After the irradiation, nanoparticle's suspensions were centrifuged for 10 minutes (14500 G for AuNPs and 18800 G for NRs) and fluorescence was measured by a fluorimeter (SpectraMax Gemini XPS, Molecular Devices).

8 OPTOFLUIDIC SYSTEM FOR THE DETECTION OF C- REACTIVE PROTEIN IN BIOLOGICAL SAMPLES

8.1 Introduction

Nowadays, one of the branches of innovation in the field of sensor development is focused on the topics of miniaturization and integration. Following this idea, Lab-on-a-Chip (LoC) technologies have gained significant weight in the last two decades, enabling the miniaturization of an analytical assay, with the resulting decrease of the required analysis time, sample volume and reagent consumption. As a result, nowadays it is possible to find in the literature LoC designs for applications such as drug development [268], genomics [269], clinical diagnosis [270] or cellomics [271].

However, one of the most important drawbacks of today's LoC platforms is that they still require external instrumentation for analyte detection and quantification. As a result, their entrance to the market is still limited. Steps towards addressing this issue have already been taken with the integration of transduction mechanisms in the LoC concept, such as electrochemical [272], magnetic [273] or photonics[274].

8.1.1 PDMS MATERIAL AND ITS IMPLEMENTATION IN MODULAR OPTOFLUIDIC SYSTEMS

Polymers have been associated recently with a reduction of fabrication costs and are often used in simple fabrication techniques, therefore they are considered as potential materials for the manufacture of detection systems such as sensors. Two examples can be highlighted among the two categories previously mentioned; poly(dimethylsiloxane) (PDMS) as a flexible material, and soft lithography (see Figure 8.1) as a non-photolithographic strategy based on selfassembly and replica molding for carrying out micro- and nanofabrication [275].

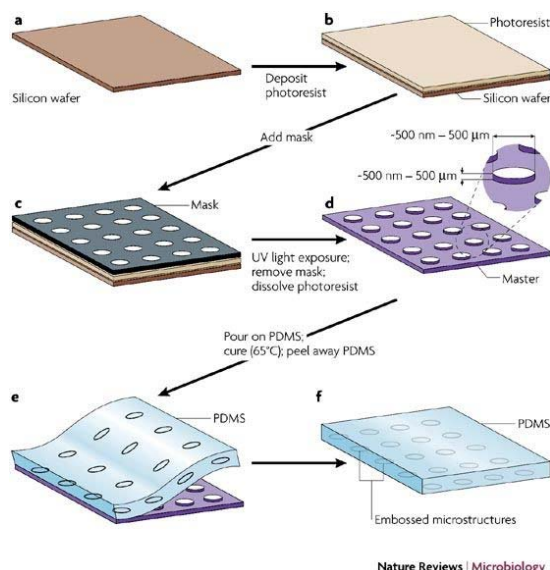


Figure 8.1 Scheme of a production process of soft lithography using PDMS as the final material. Briefly b) A photoresistant material is spin-coated on a silicon wafer. c) A mask is placed in contact with the layer of photoresist. d) The photoresist is illuminated with ultraviolet (UV) light through the mask. An organic solvent dissolves and removes photoresist that is not crosslinked. The master consists of a silicon wafer with features of photoresist in bas-relief. An expanded view of one of the microfabricated structures with its characteristic critical dimensions is shown. e) PDMS is poured on the master, cured thermally and peeled away. f) The resulting layer of PDMS has microstructures embossed in its surface [276].

Nevertheless, some drawbacks associated to those polymers must be discussed. PDMS surfaces are considered to be highly hydrophobic, favoring the non-specific adsorption of organic molecules and biomolecules related to biochemical assays. Several surface modification processes aiming to introduce hydrophilic groups on the surface of the polymer have been reported, such as oxygen plasma or UV/ozone treatments which produce silanol groups (Si-OH) on the material surface and allow the tuning of the hydrophilic/hydrophobic balance [277]. However, with time, the surfaces are prone to recover its initial hydrophobicity, making necessary the rapid introduction of subsequent chemical processes to form other functional groups to which different (bio)chemical compounds could be attached [277].

One of the approaches currently studied regarding lab-on-a-chip configurations is its synergistic combination with integrated photonic elements rising the Photonic Lab-on-a-Chip (PhLoC) concept [278, 279]. Here, the main function of microfluidics is the manipulation and transport of the analytes, while the

photonic elements transduce the (bio)chemical signal arising from the analytes in-situ to a quantifiable signal. Usually these systems are often described in the literature as monolithic configurations, in which all the required elements of the LoC are integrated in a system. However, even though monolithic PhLoCs can be considered as the configuration with the highest robustness, its main disadvantage is that a single defect on its production can cause a complete malfunction of the overall system. Additionally, it must be considered that for each application, PhLoCs could require an optimized geometry usually achieved by new fabrication cycles, which goes against the low-cost concept of the PhLoC.

Once stated that, one could think in ways to try to improve the situation. All the LoC configurations share common basic elements such as inlet/outlets, channels or flow dividers and, in the case of PhLoCs, microoptics, photonics or fiber optics for the alignment of channels. Having this idea in mind, an alternative approach could be the definition of a set of elementary and fully compatible building blocks that include the different required elements commented previously, and that could be optimized separately before its final integration into a larger system. Following that modular-way of producing LoC configurations, not only whole fabrication cycles are avoided thus lowering the price of the PhLoC, but also flexible designs and the addition of new modules in well-established designs become a possibility. As a proof of concept, the development of a LoC device based on a Modular Optofluidic System (MOPS) with colorimetric detection was carried out for the detection of C-reactive protein (CRP).

8.1.2 PROOF OF CONCEPT: CARDIOVASCULAR DISEASES

Cardiovascular diseases (CVDs) have accounted for most of the global deaths during several years. In 2012 31% of all the global deaths [280] were related to CVDs, and this numbers have not change in 2015 (see Figure 8.2). In fact, ischaemic heart disease and stroke are the world's biggest killers, accounting for a combined 15 million deaths in 2015. These diseases have remained the leading causes of death globally for more than 15 years.

CVDs are a group of disorders of the heart and blood vessels that include some diseases like coronary heart disease and cerebrovascular disease. Most of them are caused by an accumulation of fatty deposits on the inner walls of the blood

vessels, called atherosclerosis, but not all. Rheumatic heart disease can be produced produced by streptococcal infection, whereas congenital heart disease is presented at birth.

Due to the high CVDs incidence, combined with antibody availability in our group, a target analyte related to those CVDs was selected for the development of a bioassay onto modular optofluidics systems, as an early cardiovascular diseasae diagnostics platform tool. The analyte selected was a protein, C-reactive protein (CRP); which will be described below.

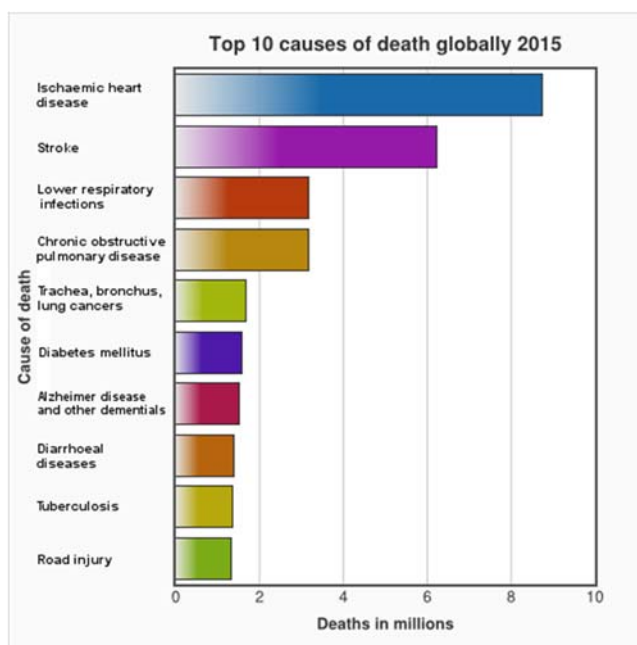


Figure 8.2. Top 10 causes of death globally in 2015, registered by the World Health Organization (WHO).

8.1.2.1 C-Reactive Protein

Nowadays several risk factors are associated with CVDs, being biomolecules that promote atherosclerosis one of them. However, due to the complex diagnosis and treatment of those diseases, and the high incidence of CVDs into modern world, the number of biomarkers proposed as risk factors for disease stage evaluation is increasing. C-reactive protein (see Figure 8.3) is one of the most studied markers when talking about inflammatory diseases, and being an acute-

phase inflammation protein, has been classified as a target for its early diagnosis [281].

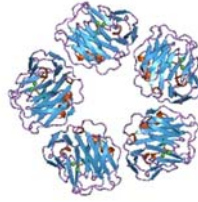


Figure 8.3. CRP conformational pentameric structure.

CRP has been stated as a risk factor for CVDs and, depending on the risk category, their levels can range from less than $1 \mu\text{g mL}^{-1}$ to more than $10 \mu\text{g mL}^{-1}$ in blood [282]. Several analytical platforms have been used for CRP quantification [283], most of them based on immunoassays, but also in surface plasmon resonance, molecularly imprinted polymers or sensors; existing some of them currently commercialized [284]. Nevertheless, future research will focus on integrated, miniaturized and multiplexed sensing platforms with co-existing biomarkers [285].

8.2 Chapter objective

The goal of this chapter (Figure 8.4) is focused on the development of an integration proof of concept, based on flexible and modular chips. Those chips will be implemented as a new and promising diagnostic tool for the detection of a biomarker related to cardiovascular diseases initial stages, C-reactive protein.

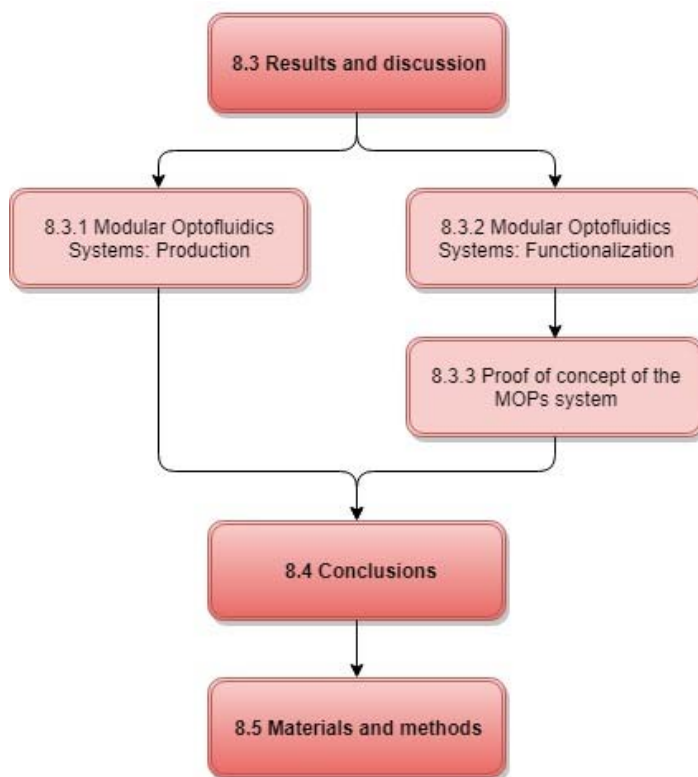


Figure 8.4. Structure of this chapter related to the different sections

8.3 Results and discussion

The section of results of this chapter describes the production of the Modular Optofluidics Systems, as well as its functionalization for the proper development of the target analyte's immunoassay selected: CRP protein. This work has been developed in collaboration with the group of Andreu Llobera of the Centro Nacional de Microelectronica (CNM), which provided the MOPs required for the establishment of the selected assay. The development of a CRP sandwich immunoassay is described both in buffer and plasma conditions, finally being applied to the quantification of clinical samples.

8.3.1 MODULAR OPTOFLUIDICS SYSTEMS: PRODUCTION

The fabrication of MOPS systems is based on soft lithography and replica molding using masters molds and requires the use of white room facilities (in this case, the MOPs were fabricated in CNM facilities). Two levels of fabrication are required: the first one which defines the optofluidics structures, and the second one which includes the frame and allowed the definition of plugs and sockets. In the case of the MOPS designed for this work, two masters were produced. The first one was designed to have all the channels, pumps and lashes of the different modular pieces, while the second master was designed to have only the frame, which will define the bottom part of the modules.

Once the masters were fabricated, the PDMS pre-polymer was obtained mixing the curing agent with the elastomer base in a 1:10 ratio (v:v). The degassed solution was poured over the masters, avoiding the bubble formation, and cured at 80°C in order to form the different parts described in Figure 8.5.

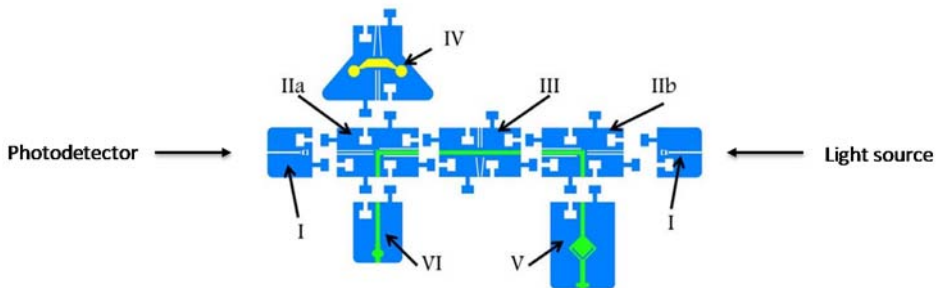


Figure 8.5. MOPS design: module I clamps a fiber optics. Light is coupled to IIa, which is transferred to a microchannel. Module II is a microchannel with a length of 1 cm. IIb brings the light which has interacted with the liquid at the microchannel to an output fiber optics, again located in a module type I. An xerogel absorbance filter (IV) [24] filter excitation wavelengths when measuring fluorescence. The fluidic inlet module (V) has an air-bubble based internal pressure regulator, which allows to obtain leak-free MOPS, fluid is finally collected with the outlet module (VI).

The different MOPS obtained were deposited over glass slides in which the functionalization process and immunochemical assay would be carried on, avoiding the unspecific interactions with other surfaces.

8.3.2 MODULAR OPTOFLUIDICS SYSTEMS: FUNCTIONALIZATION

Aiming to immobilize the capture antibody needed for the development of the sandwich assay for the detection of the model analyte, the functionalization of the PDMS surface was required. For that reason, it was decided to include functional groups which could allow the immobilization of the proper immunoreagents.

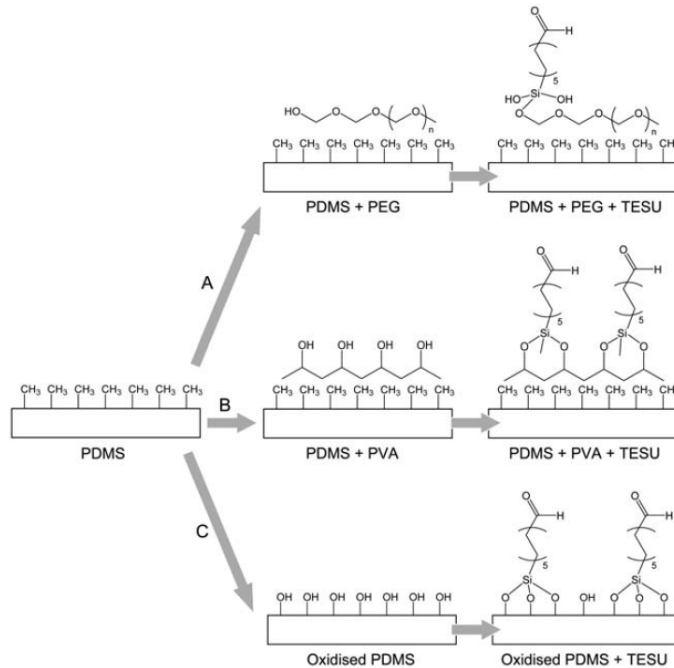


Figure 8.6. Scheme of the different modification approaches tested for the biofunctionalization of PDMS (In this case, TESU corresponds to 11-triethoxysilyl undecanal.) [286]

Different methods of functionalization were tested in previous studies [286] (see Figure 8.6) and the method of conjugation which resulted the be the most suitable was the introduction of hydroxyl (-OH) groups on the PDMS surface by physisorption of polyvinyl alcohol (PVA) polymer. This hydrophilic layer helped the biocompatibility between the PDMS surface and the further silanization of the resulting surface which allow the immobilization of the capture antibody (see Figure 8.7). Following this strategy, the LoC achieve the desired selectivity for specific analyte while minimizing interference due to non-specific adsorption of other analytes.

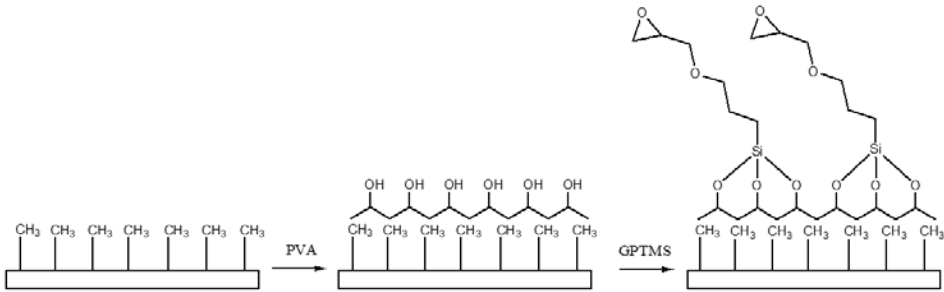


Figure 8.7. Scheme of the final modification approach followed for the biofunctionalization of the PDMS surface of the MOPS.

8.3.3 PROOF OF CONCEPT OF THE MOPS SYSTEM

As a proof of concept, the development of a LoC device based on a Modular Optofluidic System (MOPS) with colorimetric detection was carried out for the detection of CRP. The protocol of the sandwich assay is described in Figure 8.8.

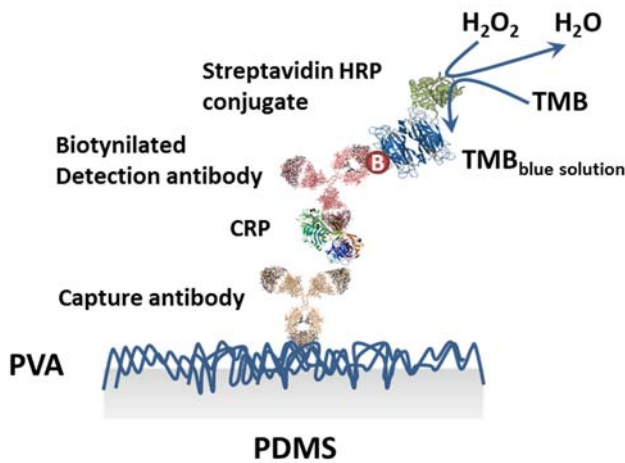


Figure 8.8. Scheme of the functionalization strategy and the sandwich assay necessary for the quantification of CRP.

8.3.3.1 Enzymatically functionalized MOPs: Validation

Having the initial goal to demonstrate the correct biofunctionalization of the MOPs system, and its feasibility to be implemented for the detection of the analyte of interest, an enzymatic study of the immobilized horseradish peroxidase enzyme was performed. This enzyme conjugated to streptavidin molecules is the responsible of the generation of a colorimetric signal by the addition of the substrate solution. As it can be observed in Figure 8.9, a buffer solution was initially injected at a constant flow of 100 $\mu\text{L}/\text{min}$ and when a stable signal was achieved, the substrate solution was injected at a constant flow of 50 $\mu\text{L}/\text{min}$. This provided with a stable colored response, which did not reach saturation. This is observed when the flow was stopped, the intensity dropped a significant value at all wavelengths. Finally, when the buffer solution was again injected, the signal was fully recovered.

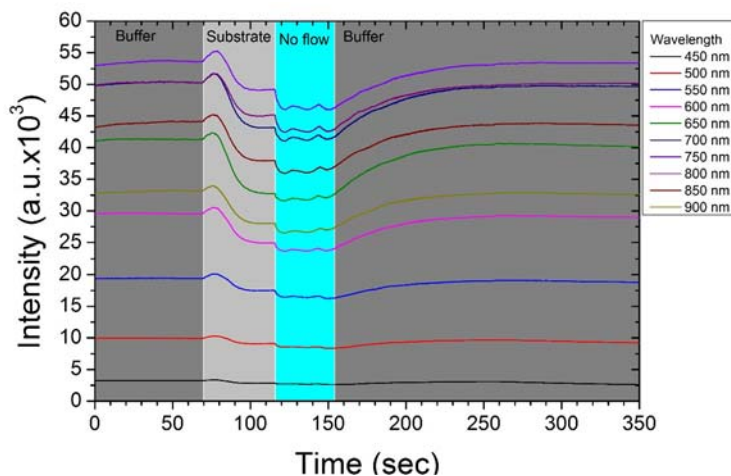


Figure 8.9 Recorded intensity as a function of time for a CRP-functionalized MOPs with a concentration of 10 ng mL^{-1} when the substrate solution was injected.

The enzymatic function of HRP was tested against different proportions of substrate solution in which 100% corresponds to a standard substrate solution of 0.01% TMB and 0.004% H_2O_2 . The variations of % are related to the relative concentration of TMB/ H_2O_2 regarding the substrate solution prepared in citrate buffer. In Figure 8.10 a saturation in the signal at higher concentrations of TMB were obtained, observing a linear range between 5 and 50% of standard substrate solution.

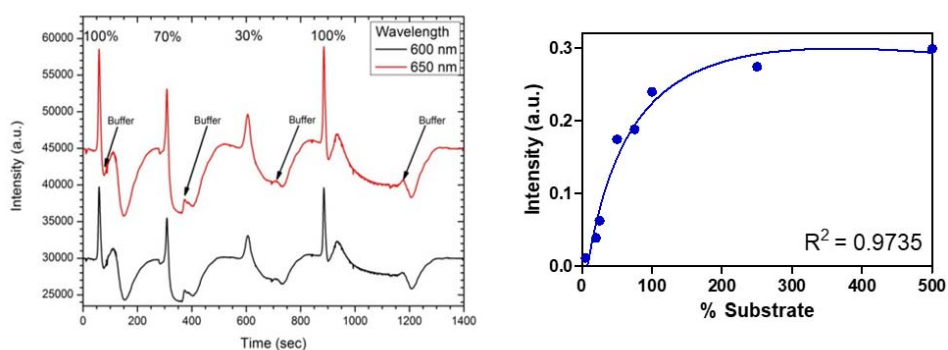


Figure 8.10 Left: Recorded intensity as a function of time for a CRP-functionalized MOPS with a concentration of 10 ng mL^{-1} when the substrate solution with some variants in % were injected. **Right:** Saturation curve of the signal obtained during all the conditions tested.

8.3.3.2 MOPs as tool for early cardiovascular diagnosis: Detection of CRP

CRP assay was selected as a demonstrator of the possible application of the designed MOPs as a clinical platform for the detection of cardiac biomarkers in biological samples. First, the establishment of a linear working range was needed for the correct quantification of real samples. For that reason, a linear calibration of CRP was performed in the MOP platform with the procedure explained in [section 8.5](#). As it can be observed in Figure 8.11 a standard linear regression was established for the CRP assay in buffer conditions with a LOD of $0.55 \pm 0.19 \text{ ng mL}^{-1}$ and a LOQ of $1.31 \pm 0.47 \text{ ng mL}^{-1}$. Therefore, a good reproducibility was achieved considering that each sample was measured twice at different concentrations in different chips.

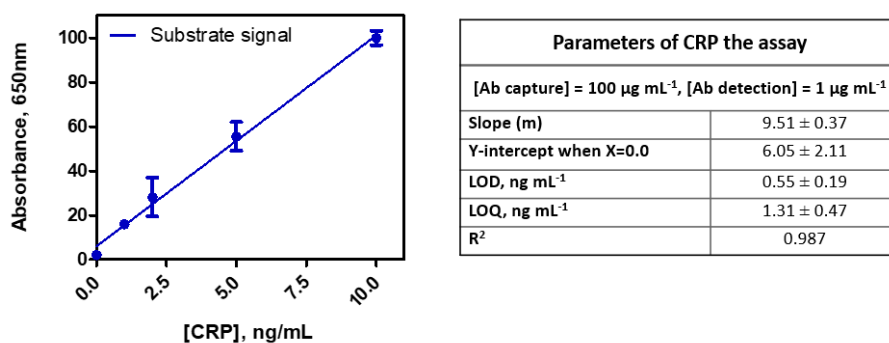


Figure 8.11. Calibration curve, conditions, and features of the CRP immunoassay on the MOPs system. The data showed correspond to the average of two assays performed on two different days. LOD corresponds to limit of detection, calculated as the mean of the zeros plus 3 times the SD. LOQ corresponds to limit of quantification, calculated as the mean of the zeros plus 10 times the SD.

8.3.3.3 Benchmark of MOPs against standardized protocols

To investigate the analytical reliability and application potential of the MOPs setup for clinical analysis, this method was compared to the quantification of a reference technique (Siemens Dimension Analyzer) and a routinely technique (ELISA). CRP is a protein present in plasma and serum in a range of 1 to 10 µg mL⁻¹ so the quantity of CRP in the plasma used for the matrix studies had to be characterized. The CRP concentration for the commercial control plasma was determined by ELISA being 2 µg mL⁻¹. According to the high detectability achieved, a high dilution factor can be performed to avoid potential matrix effect associated with biological samples such as plasma or serum. Therefore, a dilution factor of 2500 was chosen for sample's analysis to avoid the matrix interferences and to measure in the linear range of the MOPs device. 2 clinical samples were tested by diluting 2500 times in buffer together with a commercial control plasma, as a control of quantification, and an additional control plasma spiked at 25 µg mL⁻¹, both diluted 2500 times in PBST, in order to normalize the signals obtained and use an external calibration in buffer for the quantification of the samples.

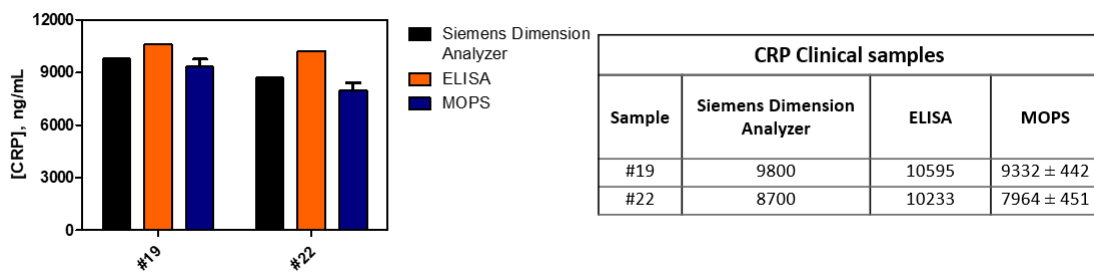


Figure 8.12 Comparison of quantification results of the CRP real samples selected for the study. Information regarding the quantification with a Siemens Dimension Analyzer (a reference technique), with ELISA (a routine technique) and MOPS is presented.

Good correlation has been observed using MOPS compared with the standardized protocols (See Figure 8.12). According to these results the MOP setup is a new and promising alternative to analyze and quantify CRP in biological samples without any pretreatment of the matrix, just by diluting it in an appropriate buffer.

8.4 Conclusions

- As a proof of concept of the possible immunoassay implementation on new surfaces, the development of a CRP immunoassay has been developed over a polymer surface of PDMS. The CRP immunoassay has achieved a great LOD of $0.55 \pm 0.19 \text{ ng mL}^{-1}$.
- The platform proposed is an optofluidic modular system which provides the miniaturization and flexibility properties so demanded by the development of POC systems. The application to real sample quantification and the validation by a reference technique demonstrates that the new platform proposed could be successfully used for clinical applications.

8.5 Materials and methodes

Reagents. The chemical reagents used were obtained from Aldrich Chemical Co. (Milwaukee, WI, USA) and from Sigma Chemical Co. (St. Louis, MO, USA). Both capture (AbCRP2) and detection (AbCRP1) antibodies were polyclonal and supplied by Audit Diagnostics (Cork, Ireland). Detection antibody was biotinylated (AbCRP1-B) using standard procedures well established in the laboratory. Streptavidin HRP conjugate were supplied from Sigma Chemical Co. (St. Louis, MO, USA). CRP standard was purchased from Fitzgerald Industries International (Acton, MA, USA). Plasma was obtained from 3H Biomedical AB (Uppsala, Sweden). Clinical plasma samples were kindly provided by Institut d'Investigació Germans Trias i Pujol (IGTP), and were previously analyzed by a Siemens Dimension analyzer, a LOCI® chemiluminescent technology.

Buffers. The buffers used are the same than [section 3.6](#).

MOPs fabrication. The mixture of pre-PDMS was poured over the master mold carefully, to avoid overflow, and subsequently cured for 20 minutes at 80°C. The PDMS modules were exposed to a source of oxygen plasma, a barrel etcher (Surface Technology Systems, Newport, UK). Both sections were brought in contact using deionized water as lubricant, previously to its alignment with the help of a microscope. Finally, once aligned, the MOP systems were heated at 80°C causing its irreversible sealing.

MOPs biofunctionalization and immunochemical assay. MOPs were functionalized following an immobilization protocol previously tested, resulting into the use of a PVA coating layer for the optimum incorporation of biomolecules onto the PDMS surfaces. The method was finally used with slightly modifications. The further biofunctionalization of the MOPS allowed the development of an immunochemical assay for CRP quantification. Briefly, CRP detection was carried out in a sandwich immunoassay, using two anti-CRP antibodies as a capture and biotinylated detection antibody; being the final signal acquired by the addition of and Streptavidin-HRP conjugated and a solution of H₂O₂/TMB as the colored substrate. All the solutions and liquids were pumped using a perfusion pump at the corresponding flow rate (model Fusion 200, Chemyx Inc., Stafford, TX). *A) Derivatization.* PDMS surfaces were cleaned with ethanol (1 mL) and ultrapure water (1 mL) at 100 µL/min. The modification

of the PDMS was performed pumping a solution of PVA at 1 mg mL^{-1} (1 mL) at $50 \text{ } \mu\text{L min}^{-1}$. Afterwards, the surfaces were cleaned with ultrapure water (1 mL) and ethanol (1 mL) at $100 \text{ } \mu\text{L min}^{-1}$. The functionalization of the surface was performed pumping a solution of 2.5% of GPTMS in freshly distilled ethanol (1 mL) at $50 \text{ } \mu\text{L min}^{-1}$. The surfaces were cleaned with ethanol and dried with nitrogen. *B) CRP Immunochemical assay.* A solution of $100 \text{ } \mu\text{g mL}^{-1}$ of the AbCRP2 capture antibody in PBS (1 mL) were pumped into the MOPS at $20 \text{ } \mu\text{L min}^{-1}$. Then, the chips were rinsed with PBST (1 mL) at $100 \text{ } \mu\text{L min}^{-1}$. The CRP standard at different concentrations, or the samples to be analyzed, were prepared in PBST and then introduced into the MOPs chips (1 mL) at $50 \text{ } \mu\text{L min}^{-1}$. Then, the chips were rinsed with PBST at $100 \text{ } \mu\text{L min}^{-1}$. A solution of the biotinylated detection antibody AbCRP1-B at $1 \text{ } \mu\text{g mL}^{-1}$ in PBST (1 mL) was pumped at $50 \text{ } \mu\text{L min}^{-1}$. Then, the chips were rinsed again with PBST at $100 \text{ } \mu\text{L min}^{-1}$. A solution of streptavidin-HRP conjugate at $1 \text{ } \mu\text{g mL}^{-1}$ in PBST (1 mL) at $50 \text{ } \mu\text{L min}^{-1}$ was introduced into MOPs chips. Then, a citrate solution (1 mL, 0.05 M, pH=5.5) was pumped through the chip at $100 \text{ } \mu\text{L min}^{-1}$ and finally, a substrate solution was added to the MOPs. The final signal was acquired by a High-Resolution Spectrometer (Model HR4000) using a halogen light source (Model HL-2000-FHSA) (Ocean Optics Inc., FL, USA). The absorbance data was recorded using the spectroscopy software OceanView (Ocean Optics Inc., FL, USA). The analysis of the data was based on the use of GraphPad Prism 5.03 (GraphPad Software Inc., San Diego, CA, USA).

9 BIBLIOGRAPHY

1. Rodriguez-Mozaz, S., M.J. Lopez de Alda, and D. Barcelo, *Biosensors as useful tools for environmental analysis and monitoring*. Anal Bioanal Chem, 2006. **386**(4): p. 1025-41.
2. Kolpin, D.W.F., E.T.; Meyer, M.T.; Thurman, E.M.; Zaugg, S.D.; Barber, L.B.; Buxton, H.T., *Pharmaceuticals, Hormones and Other Organic Wastewaters Contaminants in U.S. Streams, 1999-2000: A National Reconnaissance*. Environ. Sci. Technol, 2002. **36**: p. 1202-1211.
3. Ebele, A.J., M. Abou-Elwafa Abdallah, and S. Harrad, *Pharmaceuticals and personal care products (PPCPs) in the freshwater aquatic environment*. Emerging Contaminants, 2017. **3**(1): p. 1-16.
4. Shephard, S., et al., *Surveillance indicators and their use in implementation of the Marine Strategy Framework Directive*. ICES Journal of Marine Science: Journal du Conseil, 2015. **72**(8): p. 2269-2277.
5. *Directive 2008/105/EC of the European Parliament and of the Council of 16 December 2008 on environmental quality standards in the field of water policy, amending and subsequently repealing Council Directives 82/176/EEC, 83/513/EEC, 84/156/EEC, 84/491/EEC, 86/280/EEC and amending Directive 2000/60/EC of the European Parliament and of the Council*. 2008: <http://data.europa.eu/eli/dir/2008/105/oj>.
6. Bizkarguenaga, E., et al., *Solid-phase extraction combined with large volume injection-programmable temperature vaporization-gas chromatography-mass spectrometry for the multiresidue determination of priority and emerging organic pollutants in wastewater*. J Chromatogr A, 2012. **1247**: p. 104-17.
7. Al-Qaim, F.F., et al., *Multi-residue analytical methodology-based liquid chromatography-time-of-flight-mass spectrometry for the analysis of pharmaceutical residues in surface water and effluents from sewage treatment plants and hospitals*. J Chromatogr A, 2014. **1345**: p. 139-53.
8. Cavaliere, C., et al., *Multiresidue analysis of endocrine-disrupting compounds and perfluorinated sulfates and carboxylic acids in sediments by ultra-high-performance liquid chromatography-tandem mass spectrometry*. J Chromatogr A, 2016. **1438**: p. 133-42.
9. Petrie, B., et al., *Multi-residue analysis of 90 emerging contaminants in liquid and solid environmental matrices by ultra-high-performance liquid chromatography tandem mass spectrometry*. J Chromatogr A, 2016. **1431**: p. 64-78.
10. Andrade-Eiroa, A., et al., *Solid-phase extraction of organic compounds: A critical review (Part I)*. TrAC Trends in Analytical Chemistry, 2016. **80**: p. 641-654.
11. Farré, M., L. Kantiani, and D. Barceló, *Advances in immunochemical technologies for analysis of organic pollutants in the environment*. TrAC Trends in Analytical Chemistry, 2007. **26**(11): p. 1100-1112.
12. Rusling, J.F., *Multiplexed electrochemical protein detection and translation to personalized cancer diagnostics*. Anal Chem, 2013. **85**(11): p. 5304-10.
13. Herbath, M., et al., *Exploiting fluorescence for multiplex immunoassays on protein microarrays*. Methods Appl Fluoresc, 2014. **2**(3): p. 032001.
14. Yamanishi, C.D., C.J. H-C, and S. Takayama, *Systems for multiplexing homogeneous immunoassays*. Bioanalysis, 2015. **7**(12): p. 1545-1556.
15. Ateya, D.A., et al., *The good, the bad, and the tiny: a review of microflow cytometry*. Anal Bioanal Chem, 2008. **391**(5): p. 1485-98.
16. Lin, G., D. Makarov, and O.G. Schmidt, *Magnetic sensing platform technologies for biomedical applications*. Lab Chip, 2017. **17**(11): p. 1884-1912.
17. Seidel, M. and R. Niessner, *Chemiluminescence microarrays in analytical chemistry: a critical review*. Anal Bioanal Chem, 2014. **406**(23): p. 5589-612.

18. Desmet, C., L.J. Blum, and C.A. Marquette, *Multiplex microarray ELISA versus classical ELISA, a comparison study of pollutant sensing for environmental analysis*. Environ Sci Process Impacts, 2013. **15**(10): p. 1876-82.
19. Nagl, S., M. Schaeferling, and O.S. Wolfbeis, *Fluorescence Analysis in Microarray Technology*. Microchimica Acta, 2005. **151**(1-2): p. 1-21.
20. Pollard, H.B., et al., *Protein microarray platforms for clinical proteomics*. Proteomics – Clinical Applications, 2007. **1**(9): p. 934-952.
21. González-Martínez, M.A.P., R.; Maquieira, A., *Comparison of Multianalyte Immunosensor Formats for On-Line Determination of Organic Compounds*. Anal. Chem. , 2001. **73**: p. 4326-4332.
22. Mitchell, J., *Small molecule immunosensing using surface plasmon resonance*. Sensors (Basel), 2010. **10**(8): p. 7323-46.
23. Mauriz, E., et al., *Multi-analyte SPR immunoassays for environmental biosensing of pesticides*. Anal Bioanal Chem, 2007. **387**(4): p. 1449-58.
24. McNamee, S.E., et al., *Multiplex biotoxin surface plasmon resonance method for marine biotoxins in algal and seawater samples*. Environ Sci Pollut Res Int, 2013. **20**(10): p. 6794-807.
25. Guo, Y.R., et al., *Gold immunochromatographic assay for simultaneous detection of carbofuran and triazophos in water samples*. Anal Biochem, 2009. **389**(1): p. 32-9.
26. Xing, C., et al., *Ultrasensitive immunochromatographic assay for the simultaneous detection of five chemicals in drinking water*. Biosens Bioelectron, 2015. **66**: p. 445-53.
27. Peng, T., et al., *Performance of fluorescence microspheres-based immunochromatography in simultaneous monitoring of five quinoxalines*. Food and Agricultural Immunology, 2017: p. 1-11.
28. Jain, K.K., *Nanotechnology in clinical laboratory diagnostics*. Clin Chim Acta, 2005. **358**(1-2): p. 37-54.
29. Dunbar, S.A., *Applications of Luminex xMAP technology for rapid, high-throughput multiplexed nucleic acid detection*. Clin Chim Acta, 2006. **363**(1-2): p. 71-82.
30. Feng, L.N., et al., *Ultrasensitive multianalyte electrochemical immunoassay based on metal ion functionalized titanium phosphate nanospheres*. Anal Chem, 2012. **84**(18): p. 7810-5.
31. Kong, F.Y., et al., *Simultaneous electrochemical immunoassay using CdS/DNA and PbS/DNA nanochains as labels*. Biosens Bioelectron, 2013. **39**(1): p. 177-82.
32. Tang, J., et al., *Magneto-controlled graphene immunosensing platform for simultaneous multiplexed electrochemical immunoassay using distinguishable signal tags*. Anal Chem, 2011. **83**(13): p. 5407-14.
33. Nishi, K., et al., *Fluorescence-Based Bioassays for the Detection and Evaluation of Food Materials*. Sensors, 2015. **15**(10): p. 25831-25867.
34. Yamanishi, C.D., J.H.-C. Chiu, and S. Takayama, *Systems for multiplexing homogeneous immunoassays*. Bioanalysis, 2015. **7**(12): p. 1545-1556.
35. Godin, J., et al., *Microfluidics and photonics for Bio-System-on-a-Chip: a review of advancements in technology towards a microfluidic flow cytometry chip*. J Biophotonics, 2008. **1**(5): p. 355-76.
36. Fraga, M., et al., *Multi-detection method for five common microalgal toxins based on the use of microspheres coupled to a flow-cytometry system*. Analytica Chimica Acta, 2014. **850**: p. 57-64.
37. Meimaridou, A., et al., *Color encoded microbeads-based flow cytometric immunoassay for polycyclic aromatic hydrocarbons in food*. Analytica Chimica Acta, 2010. **672**(1-2): p. 9-14.
38. Yu, H.W., et al., *Multiplex competitive microbead-based flow cytometric immunoassay using quantum dot fluorescent labels*. Anal Chim Acta, 2012. **750**: p. 191-8.

39. He, J., et al., *Patterned Plasmonic Nanoparticle Arrays for Microfluidic and Multiplexed Biological Assays*. Analytical Chemistry, 2015. **87**(22): p. 11407-11414.
40. Valera, E., A. Hernandez-Albors, and M.P. Marco, *Electrochemical coding strategies using metallic nanopores for biosensing applications*. Trac-Trends in Analytical Chemistry, 2016. **79**: p. 9-22.
41. Wang, L., F. Feng, and Z. Ma, *Novel electrochemical redox-active species: one-step synthesis of polyaniline derivative-Au/Pd and its application for multiplexed immunoassay*. Sci Rep, 2015. **5**: p. 16855.
42. Zhang, S., et al., *Metal ions-based immunosensor for simultaneous determination of estradiol and diethylstilbestrol*. Biosens Bioelectron, 2014. **52**: p. 225-31.
43. Parra, L., et al., *Physical Sensors for Precision Aquaculture: A Review*. IEEE Sensors Journal, 2018. **18**(10): p. 3915-3923.
44. Namour, P., M. Lepot, and N. Jaffrezic-Renault, *Recent trends in monitoring of European water framework directive priority substances using micro-sensors: a 2007-2009 review*. Sensors (Basel), 2010. **10**(9): p. 7947-78.
45. Li, L., et al., *Synthesis, Properties, and Environmental Applications of Nanoscale Iron-Based Materials: A Review*. Critical Reviews in Environmental Science and Technology, 2006. **36**(5): p. 405-431.
46. Webber, M.J., et al., *Supramolecular biomaterials*. Nat Mater, 2016. **15**(1): p. 13-26.
47. Araci, I.E. and P. Brisk, *Recent developments in microfluidic large scale integration*. Curr Opin Biotechnol, 2014. **25**: p. 60-8.
48. Duncan, P.N., S. Ahrar, and E.E. Hui, *Scaling of pneumatic digital logic circuits*. Lab Chip, 2015. **15**(5): p. 1360-5.
49. Barbosa, A.I. and N.M. Reis, *A critical insight into the development pipeline of microfluidic immunoassay devices for the sensitive quantitation of protein biomarkers at the point of care*. Analyst, 2017. **142**(6): p. 858-882.
50. WHO, *Environmental Health Criteria 97 - Deltamethrin.pdf*. International Programme on Chemical Safety, World Health Organization; Geneva, Switzerland,, 1990: p. 1-133.
51. Lee, H.-J., et al., *Enzyme-linked immunosorbent assay for the pyrethroid deltamethrin*. J. Agric. Food Chem., 2002. **50**: p. 5526-5532.
52. Mak, S.K., et al., *Development of a class selective immunoassay for the type II pyrethroid insecticides*. Analytica Chimica Acta, 2005. **534**(1): p. 109-120.
53. Antwi, F.B. and G.V. Reddy, *Toxicological effects of pyrethroids on non-target aquatic insects*. Environ Toxicol Pharmacol, 2015. **40**(3): p. 915-23.
54. Brander, S.M., et al., *Pyrethroid Pesticides as Endocrine Disruptors: Molecular Mechanisms in Vertebrates with a Focus on Fishes*. Environ Sci Technol, 2016. **50**(17): p. 8977-92.
55. Katagi, T. and H. Tanaka, *Metabolism, bioaccumulation, and toxicity of pesticides in aquatic insect larvae*. Journal of Pesticide Science, 2016. **41**(2): p. 25-37.
56. Bradberry, S.M., et al., *Poisoning due to Pyrethroids*. Toxicological Reviews, 2005. **24**(2): p. 93-106.
57. Ray, D.E. and J.R. Fry, *A reassessment of the neurotoxicity of pyrethroid insecticides*. Pharmacol Ther, 2006. **111**(1): p. 174-93.
58. Muir, D.C.G., G.P. Rawn, and N.P. Grift, *Fate of the pyrethroid insecticide deltamethrin in small ponds: a mass balance study.pdf*. J. Agric. Food Chem., 1985. **33**: p. 603-609.
59. Elliott, M., et al., *Synthetic insecticide with a new order of activity*. Nature, 1974. **248**: p. 710-711.
60. Hao, X.L., et al., *Development of an Enzyme-Linked Immunosorbent Assay for the alpha-Cyano Pyrethroids Multiresidue in Tai Lake Water*. J. Agric. Food Chem., 2009. **57**: p. 3033-3039.

61. Hernandez, T., et al., *Simple Method to Determine Residual Cypermethrin and Deltamethrin in Bovine Milk*. Journal of the Brazilian Chemical Society, 2014. **25**(9): p. 1656-1661.
62. Martínez-Larrañaga, M.R., et al., *In vitro relative potency of Type II pyrethroids and mixture dose-effects on oxidative stress cytotoxicity in SH-SY5Y, HepG2 and Caco-2 human cell lines*. Toxicology Letters, 2014. **229**: p. S45.
63. Palma, D.C.A., et al., *Simultaneous Determination of Different Classes of Pesticides in Breast Milk by Solid-Phase Dispersion and GC/ECD*. Journal of the Brazilian Chemical Society, 2014. **25**(8): p. 1419-1430.
64. Taheri, N., et al., *Chemiluminescent Enzyme Immunoassay for Rapid Detection of Three α -Cyano Pyrethroid Residues in Agricultural Products*. Food Analytical Methods, 2016. **9**(10): p. 2896-2905.
65. Wolansky, M.J. and J.A. Harrill, *Neurobehavioral toxicology of pyrethroid insecticides in adult animals: a critical review*. Neurotoxicol Teratol, 2008. **30**(2): p. 55-78.
66. Ullah, S., et al., *Cypermethrin induced toxicities in fish and adverse health outcomes: Its prevention and control measure adaptation*. J Environ Manage, 2018. **206**: p. 863-871.
67. Sharma, D. and B. Ansari, *Effect of the synthetic pyrethroid Deltamethrin and the neem-based pesticide Achook on the reproductive ability of zebrafish, Danio rerio (Cyprinidae)*. Archives of Polish Fisheries, 2010. **18**(3).
68. Montanha, F.P., et al., *Clinical, biochemical and haemathological effects in Rhamdia quelen exposed to cypermethrin*. Arq. Bras. Med. Vet. Zootec, 2014. **66**(3): p. 697-704.
69. Shi, X., et al., *Developmental toxicity of cypermethrin in embryo-larval stages of zebrafish*. Chemosphere, 2011. **85**(6): p. 1010-6.
70. Moschet, C., et al., *Picogram per liter detections of pyrethroids and organophosphates in surface waters using passive sampling*. Water Res, 2014. **66**: p. 411-22.
71. Ensminger, M.P., et al., *Pesticide occurrence and aquatic benchmark exceedances in urban surface waters and sediments in three urban areas of California, USA, 2008-2011*. Environ Monit Assess, 2013. **185**: p. 3697-3710.
72. Weston, D.P. and M.J. Lydy, *Urban and Agricultural Sources of Pyrethroid Insecticides to the Sacramento-San Joaquin Delta of California*. Environ. Sci. Technol., 2010. **44**: p. 1833-1840.
73. Hladik, M.L. and K.M. Kuivila, *Assessing the occurrence and distribution of pyrethroids in water and suspended sediments*. J Agric Food Chem, 2009. **57**(19): p. 9079-85.
74. Feo, M.L., et al., *Presence of pyrethroid pesticides in water and sediments of Ebro River Delta*. Journal of Hydrology, 2010. **393**(3-4): p. 156-162.
75. Xing, Z., et al., *Pesticide application and detection in variable agricultural intensity watersheds and their river systems in the maritime region of Canada*. Arch Environ Contam Toxicol, 2012. **63**(4): p. 471-83.
76. Vryzas, Z., et al., *Determination and aquatic risk assessment of pesticide residues in riparian drainage canals in northeastern Greece*. Ecotoxicol Environ Saf, 2011. **74**(2): p. 174-81.
77. Bille, L., et al., *First report of a fish kill episode caused by pyrethroids in Italian freshwater*. Forensic Sci Int, 2017. **281**: p. 176-182.
78. Kuivila, K.M., et al., *Occurrence and potential sources of pyrethroid insecticides in stream sediments from seven U.S. metropolitan areas*. Environ Sci Technol, 2012. **46**(8): p. 4297-303.
79. Palmquist, K., et al., *Environmental fate of pyrethroids in urban and suburban stream sediments and the appropriateness of Hyalella azteca model in determining ecological risk*. Integr Environ Assess Manag, 2011. **7**(3): p. 325-35.
80. Laskowski, D.A., *Physical and chemical properties of Pyrethroids.pdf*. Rev Environ Contam Toxicol, 2002. **174**: p. 49-170.

81. Loos, R., *Analytical methods relevant to the European Commission's 2012 proposal on Priority Substances under the Water Framework Directive*. 2012, JRC Scientific and Policy Reports.
82. Pavan, F.A., et al., *Determination of deltamethrin in cattle dipping baths by high-performance liquid chromatography*. *J. Agric. Food Chem.*, 1999. **47**: p. 174-176.
83. Boonchiangma, S., W. Ngeontae, and S. Srijaranai, *Determination of six pyrethroid insecticides in fruit juice samples using dispersive liquid-liquid microextraction combined with high performance liquid chromatography*. *Talanta*, 2012. **88**: p. 209-15.
84. Hu, L., et al., *In-syringe low-density ionic liquid dispersive liquid-liquid microextraction for the fast determination of pyrethroid insecticides in environmental water samples by HPLC-DAD*. *RSC Adv.*, 2016. **6**(73): p. 69218-69225.
85. Mukdasai, S., C. Thomas, and S. Srijaranai, *Two-step microextraction combined with high performance liquid chromatographic analysis of pyrethroids in water and vegetable samples*. *Talanta*, 2014. **120**: p. 289-96.
86. López-López, T., et al., *Determination of pyrethroids in vegetables by HPLC using continuous on-line post-elution photoirradiation with fluorescence detection*. *Anal Chim Acta*, 2001. **447**: p. 101-111.
87. Vazquez, P.P., A.R. Mughari, and M.M. Galera, *Solid-phase microextraction (SPME) for the determination of pyrethroids in cucumber and watermelon using liquid chromatography combined with post-column photochemically induced fluorimetry derivatization and fluorescence detection*. *Anal Chim Acta*, 2008. **607**(1): p. 74-82.
88. Shirani, M., et al., *Solid-Phase Extraction Combined with Dispersive Liquid-Liquid Microextraction for the Simultaneous Determination of Deltamethrin and Permethrin in Honey by Gas Chromatography-Mass Spectrometry*. *Food Analytical Methods*, 2016. **9**(9): p. 2613-2620.
89. Kim, E., M.D. Baaske, and F. Vollmer, *Towards next-generation label-free biosensors: recent advances in whispering gallery mode sensors*. *Lab on a Chip*, 2017. **17**(7): p. 1190-1205.
90. Zanchetta, G., et al., *Emerging applications of label-free optical biosensors*. *Nanophotonics*, 2017. **6**(4).
91. Ionescu, R.E., et al., *Impedimetric immunosensor for the specific label free detection of ciprofloxacin antibiotic*. *Biosens Bioelectron*, 2007. **23**(4): p. 549-55.
92. Lee, H.-J., et al., *Development of an Enzyme-Linked Immunosorbent Assay for the Pyrethroid Cypermethrin*. *J. Agric. Food Chem.*, 2004. **52**: p. 1039-1043.
93. Zhang, Q., et al., *Immunoassay development for the class-specific assay for types I and II pyrethroid insecticides in water samples*. *Molecules*, 2010. **15**(1): p. 164-77.
94. Kong, Y., et al., *Development of a monoclonal antibody-based enzyme immunoassay for the pyrethroid insecticide deltamethrin*. *J Agric Food Chem*, 2010. **58**(14): p. 8189-95.
95. Lee, N., D.P. McAdam, and J.H. Skerit, *Development of Immunoassays for Type II Synthetic Pyrethroids. 1. Hapten Design and Application to Heterologous and Homologous Assays*. *J. Agric. Food Chem.*, 1998. **46**: p. 520-534.
96. Queffelec, A.-L., et al., *Hapten Synthesis for a Monoclonal Antibody Based ELISA for Deltamethrin*. *J. Agric. Food Chem.*, 1998. **46**: p. 1670-1676.
97. Oubiña, A., et al., *Chapter 7 Immunoassays for environmental analysis*, in *Techniques and Instrumentation in Analytical Chemistry*, D. Barceló, Editor. 2000, Elsevier. p. 287-339.
98. Oubiña, A., et al., *Immunoassays for environmental analysis.*, in *Sample Handling and Trace Analysis of Pollutants: Techniques, Applications and Quality Assurance*, D. Barceló, Editor. 2000, Elsevier Science B.V.: Techniques and Instrumentation in Analytical Chemistry. p. 287-339.

99. Galve, R., et al., *Development and Evaluation of an Immunoassay for Biological Monitoring Chlorophenols in Urine as Potential Indicators of Occupational Exposure*. Anal. Chem., 2002. **74**: p. 468-478.
100. Nichkova, M., M. Gemani, and M.P. Marco, *Immunochemical Analysis of 2,4,6-Tribromophenol for Assessment of Wood Contamination*. J. Agric. Food Chem., 2008. **56**: p. 29-34.
101. Ali, H.R., et al., *Occurrence and distribution of antifouling biocide Irgarol-1051 in coastal waters of Peninsular Malaysia*. Mar Pollut Bull, 2013. **70**(1-2): p. 253-7.
102. Zhou, J.L., *Occurrence and persistence of antifouling biocide Irgarol 1051 and its main metabolite in the coastal waters of Southern England*. Sci Total Environ, 2008. **406**(1-2): p. 239-46.
103. Garcia-Galan, M.J., M.S. Diaz-Cruz, and D. Barcelo, *Occurrence of sulfonamide residues along the Ebro River basin: removal in wastewater treatment plants and environmental impact assessment*. Environ Int, 2011. **37**(2): p. 462-73.
104. Wu, M.H., et al., *Occurrence, fate and interrelation of selected antibiotics in sewage treatment plants and their receiving surface water*. Ecotoxicol Environ Saf, 2016. **132**: p. 132-9.
105. Guan, J., et al., *Simultaneous determination of 12 pharmaceuticals in water samples by ultrasound-assisted dispersive liquid-liquid microextraction coupled with ultra-high performance liquid chromatography with tandem mass spectrometry*. Anal Bioanal Chem, 2016. **408**(28): p. 8099-8109.
106. Na, G., et al., *Occurrence, distribution, and bioaccumulation of antibiotics in coastal environment of Dalian, China*. Mar Pollut Bull, 2013. **69**(1-2): p. 233-7.
107. Ge, J., et al., *Occurrence, distribution and seasonal variations of polychlorinated biphenyls and polybrominated diphenyl ethers in surface waters of the East Lake, China*. Chemosphere, 2014. **103**: p. 256-62.
108. Shelver, W.L., et al., *Development of a magnetic particle immunoassay for polybrominated diphenyl ethers and application to environmental and food matrices*. Chemosphere, 2008. **73**(1 Suppl): p. S18-23.
109. Hinteman, T., et al., *Field study using two immunoassays for the determination of estradiol and ethinylestradiol in the aquatic environment*. Water Res, 2006. **40**(12): p. 2287-94.
110. Routledge, E.J., et al., *Identification of estrogenic chemicals in STW Effluent. 2. In vivo responses in trout and roach*. Environ. Sci. Technol, 1998. **32**: p. 1559-1565.
111. Barbaro, E., et al., *Domoic acid at trace levels in lagoon waters: assessment of a method using internal standard quantification*. Anal Bioanal Chem, 2013. **405**(28): p. 9113-23.
112. Bargu, S., et al., *Influence of the Mississippi River on Pseudo-nitzschia spp. Abundance and Toxicity in Louisiana Coastal Waters*. Estuaries and Coasts, 2016. **39**(5): p. 1345-1356.
113. Hall, L.W., et al., *An ecological risk assessment for the use of Irgarol 1051 as an algacide for antifoulant paints*. Crit Rev Toxicol, 1999. **29**(4): p. 367-437.
114. Cassi, R., I. Tolosa, and S. de Mora, *A survey of antifoulants in sediments from Ports and Marinas along the French Mediterranean coast*. Mar Pollut Bull, 2008. **56**(11): p. 1943-8.
115. Gough, M.A., J. Fothergill, and J.D. Hendrie, *A Survey of Southern England Coastal Waters for the s-Triazine Antifouling Compound Irgarol 1051*. Mar Pollut Bull, 1994. **28**(10): p. 613-620.
116. Hall, L.W., Jr., et al., *Monitoring of Irgarol 1051 concentrations with concurrent phytoplankton evaluations in East Coast areas of the United States*. Mar Pollut Bull, 2005. **50**(6): p. 668-81.
117. Park, Y.H., et al., *Use of antimicrobial agents in aquaculture*. Rev. sci. tech. Off. int. Epiz., 2012. **31**(1): p. 189-197.

118. Adrian, J., et al., *Generation of Broad Specificity Antibodies for Sulfonamide Antibiotics and Development of an Enzyme-Linked Immunosorbent Assay (ELISA) for the Analysis of Milk Samples*. J. Agric. Food Chem., 2009. **57**: p. 385-394.
119. Forti, A.F. and G. Scortichini, *Determination of ten sulphonamides in egg by liquid chromatography-tandem mass spectrometry*. Anal Chim Acta, 2009. **637**(1-2): p. 214-9.
120. Tschmelak, J., et al., *Biosensor for Seven Sulphonamides in Drinking, Ground, and Surface Water with Difficult Matrices*. Analytical Letters, 2004. **37**(8): p. 1701-1718.
121. Hirsch, R., et al., *Occurrence of antibiotics in the aquatic environment*. Sci. Total Environ., 1999. **225**: p. 109-118.
122. Oliveri Conti, G., et al., *Determination of illegal antimicrobials in aquaculture feed and fish: An ELISA study*. Food Control, 2015. **50**: p. 937-941.
123. Ambekar, C.S., et al., *Metabolism of chloramphenicol succinate in human bone marrow*. Eur. J. Clin. Pharmacol., 2000. **56**: p. 405-409.
124. Schulster, M., A.M. Bernie, and R. Ramasamy, *The role of estradiol in male reproductive function*. Asian J Androl, 2016. **18**(3): p. 435-40.
125. McCarthy, M.M., *Estradiol and the developing brain*. Physiol Rev, 2008. **88**(1): p. 91-124.
126. Derouiche, L., et al., *Developmental exposure to Ethinylestradiol affects transgenerationally sexual behavior and neuroendocrine networks in male mice*. Sci Rep, 2015. **5**: p. 17457.
127. Huang, B., et al., *Effects and bioaccumulation of 17beta-estradiol and 17alpha-ethynylestradiol following long-term exposure in crucian carp*. Ecotoxicol Environ Saf, 2015. **112**: p. 169-76.
128. Le Curieux-Belfond, O., et al., *Short-term bioaccumulation, circulation and metabolism of estradiol-17β in the oyster Crassostrea gigas*. Journal of Experimental Marine Biology and Ecology, 2005. **325**(2): p. 125-133.
129. Loos, R., *Analytical methods for possible WFD 1st watch list substances*. 2015, JRC Science and Policy Report.
130. Linares, V., M. Belles, and J.L. Domingo, *Human exposure to PBDE and critical evaluation of health hazards*. Arch Toxicol, 2015. **89**(3): p. 335-56.
131. Stubbings, W.A. and S. Harrad, *Extent and mechanisms of brominated flame retardant emissions from waste soft furnishings and fabrics: A critical review*. Environ Int, 2014. **71**: p. 164-75.
132. Marchitti, S.A., et al., *Polybrominated Diphenyl Ethers in Human Milk and Serum from the U.S. EPA MAMA Study: Modeled Predictions of Infant Exposure and Considerations for Risk Assessment*. Environ Health Perspect, 2017. **125**(4): p. 706-713.
133. Zhang, H., et al., *Prenatal PBDE and PCB Exposures and Reading, Cognition, and Externalizing Behavior in Children*. Environ Health Perspect, 2017. **125**(4): p. 746-752.
134. Akortia, E., et al., *A review of sources, levels and toxicity of polybrominated diphenyl ethers (PBDEs) and their transformation and transport in various environmental compartments*. Environ Rev, 2016. **24**(3): p. 253-273.
135. Costa, L.G. and G. Giordano, *Developmental neurotoxicity of polybrominated diphenyl ether (PBDE) flame retardants*. Neurotoxicology, 2007. **28**(6): p. 1047-1067.
136. Viberg, H., et al., *Neonatal exposure to higher brominated diphenyl ethers, hepta-, octa-, or nonabromodiphenyl ether, impairs spontaneous behavior and learning and memory functions of adult mice*. Toxicol Sci, 2006. **92**(1): p. 211-8.
137. Bates, S.S., D.L. Garrison, and R.A. Horner, *Bloom dynamics and physiology of domoic-acid-producing Pseudo-nitzschia Species*. Springer-Verlag: Heidelberg. 2008. 267-292.
138. Clayden, J., B. Read, and K.R. Hebditch, *Chemistry of domoic acid, isodomoic acids, and their analogues*. Tetrahedron, 2005. **61**(24): p. 5713-5724.
139. Slevin, J.T., J.F. Collins, and T. Coyle, *Analogue interactions with the brain receptor labeled by [3H]kainic acid*. Brain Res, 1983. **265**: p. 169-172.

140. Rodriguez, I., et al., *Monitoring of freshwater toxins in European environmental waters by using novel multi-detection methods*. Environ Toxicol Chem, 2017. **36**(3): p. 645-654.
141. Gulland, F.M.D., et al., *Domoic acid toxicity in Californian sea lions (*Zalophus californianus*) clinical signs, treatment and survival*. Vet. Rec., 2002. **150**: p. 475-480.
142. Lefebvre, K.A., et al., *From sanddabs to blue whales the pervasiveness of domoic acid*. Toxicon, 2002. **40**: p. 971-977.
143. Amzil, Z., et al., *Domoic acid accumulation in French shellfish in relation to toxic species of *Pseudo-nitzschia multiseriata* and *P. pseudodelicatissima**. Toxicon, 2001. **39**: p. 1245-1251.
144. Takahashi, E., et al., *Occurrence and seasonal variations of algal toxins in water, phytoplankton and shellfish from North Stradbroke Island, Queensland, Australia*. Mar Environ Res, 2007. **64**(4): p. 429-42.
145. Vale, P. and M.A.M. Sampayo, *Domoic acid in Portuguese shellfish and fish*. Toxicon, 2001. **39**: p. 893-904.
146. Ballesteros, B., et al., *Influence of the hapten design on the development of a competitive ELISA for the determination of the antifouling agent Irgarol 1051 at trace levels*. Analytical Chemistry, 1998. **70**(19): p. 4004-4014.
147. Ballesteros, B., et al., *Preparation of antisera and development of a direct enzyme-linked immunosorbent assay for the determination of the antifouling agent Irgarol 1051*. Anal. Chim. Acta, 1997. **347**: p. 139-147.
148. Adrian, J., et al., *Generation of broad specificity antibodies for sulfonamide antibiotics and development of an enzyme-linked immunosorbent assay (ELISA) for the analysis of milk samples*. J. Agric. Food Chem., 2009. **57**: p. 385-394.
149. Font, H., et al., *Immunochemical Assays for Direct Sulfonamide Antibiotic Detection in Milk and Hair Samples Using Antibody Derivatized Magnetic Nanoparticles*. J. Agric. Food Chem., 2008. **56**: p. 736-743.
150. Font, H., et al., *Immunochemical Assays for Direct Sulfonamide Antibiotic Detection In Milk and Hair Samples Using Antibody Derivatized Magnetic Nanoparticles*. J. Agric. Food Chem., 2008. **56**: p. 736-743.
151. Shelver, W.L., et al., *Hapten syntheses and antibody generation for the development of a polybrominated flame retardant ELISA*. J. Agric. Food Chem., 2005. **53**: p. 3840-3847.
152. Traynor, I.M., et al., *Immunobiosensor Detection of Domoic Acid as a Screening Test in Bivalve Molluscs: Comparison with Liquid Chromatography-Base Analysis*. J. AOAC Int 2006. **89**(3): p. 868-872.
153. Pico, Y., et al., *Current trends in solid-phase-based extraction techniques for the determination of pesticides in food and environment*. J Biochem Biophys Methods, 2007. **70**(2): p. 117-31.
154. Pedrouzo, M., et al., *Pharmaceutical determination in surface and wastewaters using high-performance liquid chromatography-(electrospray)-mass spectrometry*. Journal of Separation Science, 2007. **30**(3): p. 297-303.
155. Telepchak, M.J., T.F. August, and G. Chaney, *Forensic and Clinical applications of Solid Phase Extraction*. 2004: Humana Press.
156. Baggiani, C., L. Anfossi, and C. Giovannoli, *Solid phase extraction of food contaminants using molecular imprinted polymers*. Anal Chim Acta, 2007. **591**(1): p. 29-39.
157. Liska, I., *Fifty years of solid-phase extraction in water analysis - historical development and overview*. J. Chromatogr. A, 2000. **885**: p. 3-16.
158. EPA, U., *Pharmaceuticals and Personal Care Products in Water, Soil, Sediment, and Biosolids by HPLC/MS/MS*. 2007.
159. Nichkova, M. and M.P. Marco, *Development and evaluation of C18 and immunosorbent solid-phase extraction methods prior immunochemical analysis of chlorophenols in human urine*. Analytica Chimica Acta, 2005. **533**(1): p. 67-82.

160. Zhang, Y., et al., *Rapid determination of ractopamine residues in edible animal products by enzyme-linked immunosorbent assay: development and investigation of matrix effects*. J Biomed Biotechnol, 2009. **2009**: p. 579175.
161. Sanvicens, N., B. Varela, and M.-P. Marco, *Immunochemical Determination of 2,4,6-Trichloroanisole as the Responsible Agent for the Musty Odor in Foods. 2. Immunoassay Evaluation*. J. Agric. Food Chem., 2003. **51**: p. 3932-3939.
162. Estévez, M.-C., et al., *Analysis of Nonylphenol: Advances and Improvements in the Immunochemical Determination Using Antibodies Raised against the Technical Mixture and Hydrophilic Immunoagents*. Environ. Sci. Technol., 2006. **40**: p. 559-568.
163. Galve, R., et al., *Development and Evaluation of an Immunoassay for Biological Monitoring Chlorophenols in Urine as Potential Indicators of Occupational Exposure*. Anal Chem, 2002. **74**: p. 468-478.
164. Belleville, E., et al., *Quantitative microarray pesticide analysis*. Journal of Immunological Methods, 2004. **286**(1-2): p. 219-229.
165. McNamee, S.E., et al., *Development of a planar waveguide microarray for the monitoring and early detection of five harmful algal toxins in water and cultures*. Environ Sci Technol, 2014. **48**(22): p. 13340-9.
166. Tamarit-Lopez, J., et al., *Direct hapten-linked multiplexed immunoassays on polycarbonate surface*. Biosens Bioelectron, 2011. **26**(5): p. 2694-8.
167. Broto, M., et al., *Immunochemical detection of penicillins by using biohybrid magnetic particles*. Food Control, 2015. **51**: p. 381-389.
168. Kantiani, L., et al., *Development and validation of a pressurised liquid extraction liquid chromatography–electrospray–tandem mass spectrometry method for β -lactams and sulfonamides in animal feed*. Journal of Chromatography A, 2010. **1217**(26): p. 4247-4254.
169. Martínez, K., I. Ferrer, and D. Barceló, *Part-per-trillion level determination of antifouling pesticides and their byproducts in seawater samples by off-line solid-phase extraction followed by high-performance liquid chromatography–atmospheric pressure chemical ionization mass spectrometry*. Journal of Chromatography A, 2000. **879**(1): p. 27-37.
170. Jelić, A., M. Petrović, and D. Barceló, *Multi-residue method for trace level determination of pharmaceuticals in solid samples using pressurized liquid extraction followed by liquid chromatography/quadrupole-linear ion trap mass spectrometry*. Talanta, 2009. **80**(1): p. 363-371.
171. Tor, E.R., B. Puschner, and W.E. Whitehead, *Rapid Determination of Domoic Acid in Serum and Urine by Liquid Chromatography–Electrospray Tandem Mass Spectrometry*. Journal of Agricultural and Food Chemistry, 2003. **51**(7): p. 1791-1796.
172. López de Alda, M.J. and D. Barceló, *Use of solid-phase extraction in various of its modalities for sample preparation in the determination of estrogens and progestogens in sediment and water*. Journal of Chromatography A, 2001. **938**(1): p. 145-153.
173. Desmet, C., L.J. Blum, and C.A. Marquette, *High-throughput multiplexed competitive immunoassay for pollutants sensing in water*. Anal Chem, 2012. **84**(23): p. 10267-76.
174. Dobosz, P., et al., *Massive immuno multiresidue screening of water pollutants*. Anal Chem, 2015. **87**(19): p. 9817-24.
175. Fan, Z., et al., *Sensitive immunoassay detection of multiple environmental chemicals on protein microarrays using DNA/dye conjugate as a fluorescent label*. J Environ Monit, 2012. **14**(5): p. 1345-52.
176. Stoevesandt, O.T., M.J.; He, M., *Protein microarrays: high-throughput tools for proteomics*. Expert. Rev. Proteomics, 2009. **6**(2): p. 145-157.
177. Barbulovic-Nad, I., et al., *Bio-microarray fabrication techniques--a review*. Crit Rev Biotechnol, 2006. **26**(4): p. 237-59.

178. Morais, S., et al., *Analytical prospect of compact disk technology in immunosensing*. Anal Bioanal Chem, 2008. **391**(8): p. 2837-44.
179. Pease, A.C., et al., *Light-generated oligonucleotide arrays for rapid DNA sequence analysis*. Proc. Natl. Acad. Sci., 1994. **91**(5022-5026).
180. Li, L., et al., *Single-cell multiple gene expression analysis based on single-molecule-detection microarray assay for multi-DNA determination*. Anal Chim Acta, 2015. **854**: p. 122-8.
181. Julian, M.T., et al., *CD26/DPPIV inhibition alters the expression of immune response-related genes in the thymi of NOD mice*. Mol Cell Endocrinol, 2016. **426**: p. 101-12.
182. Strauss, L., et al., *Detecting Staphylococcus aureus Virulence and Resistance Genes: a Comparison of Whole-Genome Sequencing and DNA Microarray Technology*. J Clin Microbiol, 2016. **54**(4): p. 1008-16.
183. Shelver, W.L.S., N.W.; Franek, M.; Rubio, F.R., *ELISA for Sulfonamides and Its Application for Screening in Water Contamination*. J Agric Food Chem, 2008. **56**: p. 6609-6615.
184. Wang, J., et al., *Development of an enzyme-linked immunosorbent assay based a monoclonal antibody for the detection of pyrethroids with phenoxybenzene multiresidue in river water*. J Agric Food Chem, 2011. **59**(7): p. 2997-3003.
185. Rivasseau, C.R., P.; Deguin, A.; Hennion, M.-C., *Evaluation of an ELISA Kit for the Monitoring of Microcystins (Cyanobacterial Toxins) in Water and Algae Environmental Samples*. Environ Sci Technol, 1999. **33**: p. 1520-1527.
186. Morais, S.T.-G., L.A.; Arnandis-Chover, T.; Puchades, R.; Maquieira, A., *Multiplexed Microimmunoassays on a Digital Versatile Disk*. Anal Chem, 2009. **81**: p. 5646-5654.
187. Mastichiadis, C.K., S. E.; Christofidis, I.; Koupparis, M. A.; Wilets, C.; Misiakos, K., *Simultaneous Determination of Pesticides Using a Four-Band Disposable Optical Capillary Immunosensor*. Anal. Chem., 2002. **74**: p. 6064-6072.
188. Tschmelak, J., et al., *Automated Water Analyser Computer Supported System (AWACSS) Part II: Intelligent, remote-controlled, cost-effective, on-line, water-monitoring measurement system*. Biosens Bioelectron, 2005. **20**(8): p. 1509-19.
189. Rodriguez-Mozaz, S., et al., *Simultaneous multi-analyte determination of estrone, isoproturon and atrazine in natural waters by the RIver ANALyser (RIANA), an optical immunosensor*. Biosensors and Bioelectronics, 2004. **19**(7): p. 633-640.
190. North, S.H., et al., *Effect of Physicochemical Anomalies of Soda-Lime Silicate Slides on Biomolecule Immobilization*. Anal. Chem., 2010. **82**: p. 406-412.
191. Carion, O., et al., *Polysaccharide microarrays for polysaccharide-platelet-derived-growth-factor interaction studies*. Chembiochem, 2006. **7**(5): p. 817-26.
192. Herranz, S., et al., *Dextran-Lipase Conjugates as Tools for Low Molecular Weight Ligand Immobilization in Microarray Development*. Analytical Chemistry, 2013. **85**(15): p. 7060-7068.
193. Massia, S.P., J. Stark, and D.S. Letbetter, *Surface-immobilized dextran limits cell adhesion and spreading*. Biomaterials, 2000. **21**: p. 2253-2261.
194. Wang, D., et al., *Carbohydrate microarrays for the recognition of cross-reactive molecular markers of microbes and host cells*. Nat. Biotechnol 2002. **20**: p. 275-281.
195. Pla-Roca, M., et al., *Antibody colocalization microarray: a scalable technology for multiplex protein analysis in complex samples*. Mol Cell Proteomics, 2012. **11**(4): p. M111 011460.
196. Bürgi, B.R. and T. Pradeep, *Societal implications of nanoscience and nanotechnology in developing countries*. Curr. Sci, 2006. **90**(5): p. 645-658.
197. Kesharwani, P., K. Jain, and N.K. Jain, *Dendrimer as nanocarrier for drug delivery*. Progress in Polymer Science, 2014. **39**(2): p. 268-307.
198. Li, Y.L., et al., *Biodegradable Polymer Nanogels for Drug/Nucleic Acid Delivery*. Chemical Reviews, 2015. **115**(16): p. 8564-8608.

199. Biswas, S., et al., *Recent advances in polymeric micelles for anti-cancer drug delivery*. European Journal of Pharmaceutical Sciences, 2016. **83**: p. 184-202.
200. Vader, P., et al., *Extracellular vesicles for drug delivery*. Advanced Drug Delivery Reviews, 2016. **106**: p. 148-156.
201. Wang, A.Z., et al., *Biofunctionalized targeted nanoparticles for therapeutic applications*. Expert Opin. Biol. Ther., 2008. **8**(8): p. 1063-1070.
202. Shahbazi, R., B. Ozpolat, and K. Ulubayram, *Oligonucleotide-based theranostic nanoparticles in cancer therapy*. Nanomedicine, 2016. **11**(10): p. 1287-1308.
203. Heravi-Shargh, V., H. Hondermarck, and M. Liang, *Antibody-targeted biodegradable nanoparticles for cancer therapy*. Nanomedicine, 2016. **11**(1): p. 63-79.
204. Yu, H.D., et al., *Chemical routes to top-down nanofabrication*. Chem Soc Rev, 2013. **42**(14): p. 6006-18.
205. Thiruvengadathan, R., et al., *Nanomaterial processing using self-assembly-bottom-up chemical and biological approaches*. Rep Prog Phys, 2013. **76**(6): p. 066501.
206. Hsu, H.H., P.R. Selvaganapathy, and L. Soleymani, *Bottom-Up Top-Down Fabrication of Structurally and Functionally Tunable Hierarchical Palladium Materials*. Journal of the Electrochemical Society, 2014. **161**(7): p. D3078-D3086.
207. Wong, B.S., et al., *Carbon nanotubes for delivery of small molecule drugs*. Advanced Drug Delivery Reviews, 2013. **65**(15): p. 1964-2015.
208. Baeza, A., D. Ruiz-Molina, and M. Vallet-Regi, *Recent advances in porous nanoparticles for drug delivery in antitumoral applications: inorganic nanoparticles and nanoscale metal-organic frameworks*. Expert Opinion on Drug Delivery, 2017. **14**(6): p. 783-796.
209. Elzoghby, A.O., A.L. Hemasa, and M.S. Freag, *Hybrid protein-inorganic nanoparticles: From tumor-targeted drug delivery to cancer imaging*. Journal of Controlled Release, 2016. **243**: p. 303-322.
210. Liong, M., et al., *Multifunctional inorganic nanoparticles for imaging, targeting, and drug delivery*. ACS Nano, 2008. **2**(5): p. 889-896.
211. Richtering, W., et al., *Could multiresponsive hollow shell-shell nanocontainers offer an improved strategy for drug delivery*. Nanomedicine, 2016. **11**(22): p. 2879-2883.
212. Taylor, K., et al., *Nanocell targeting using engineered bispecific antibodies*. MAbs, 2015. **7**(1): p. 53-65.
213. Ahmadi, A. and S. Arami, *Potential applications of nanoshells in biomedical sciences*. J Drug Target, 2013.
214. Martinez, J.O., et al., *Multifunctional to multistage delivery systems : The evolution of nanoparticles for biomedical applications*. Chin Sci Bull., 2012. **57**(31): p. 3961-3971.
215. Yeh, Y.C., B. Creran, and V.M. Rotello, *Gold nanoparticles: preparation, properties, and applications in bionanotechnology*. Nanoscale, 2012. **4**(6): p. 1871-80.
216. Liu, Y., et al., *Synthesis, stability, and cellular internalization of gold nanoparticles containing mixed peptide-poly(ethylene glycol) monolayers*. Anal Chem, 2007. **79**: p. 2221-2229.
217. Wang, A.Z., et al., *Biofunctionalized targeted nanoparticles for therapeutic applications*. Expert Opin. Biol. Ther., 2008. **8**(8): p. 1063-1070.
218. Fay, F. and C.J. Scott, *Antibody-targeted nanoparticles for cancer therapy*. Immunotherapy, 2011. **3**(3): p. 381-394.
219. Debbage, P., *Targeted Drugs and Nanomedicine Present and Future*. Curr Pharm Des, 2009. **15**: p. 153-172.
220. Aravind, A., et al., *Aptamer-conjugated polymeric nanoparticles for targeted cancer therapy*. Drug Deliv Transl Res, 2012. **2**(6): p. 418-36.
221. Yang, G., et al., *Near-infrared-light responsive nanoscale drug delivery systems for cancer treatment*. Coordination Chemistry Reviews, 2016. **320-321**: p. 100-117.

222. Huschka, R., et al., *Gene Silencing by Gold Nanoshell-Mediated Delivery and Laser-Triggered Release of Antisense Oligonucleotide and siRNA*. *ACS Nano*, 2012. **6**(9): p. 7681-7691.
223. de Puig, H.C.-R., A.; Flemister, D. Baxamusa, S. H.; Hamad-Schifferli, K., *Selective Light-Triggered Release of DNA from Gold Nanorods Switches Blood Clotting On and Off*. *PLoS ONE*, 2013. **8**(7): p. e68511.
224. Ngom, B., et al., *Development and application of lateral flow test strip technology for detection of infectious agents and chemical contaminants: a review*. *Anal Bioanal Chem*, 2010. **397**(3): p. 1113-35.
225. Kurkina, T. and K. Balasubramanian, *Towards in vitro molecular diagnostics using nanostructures*. *Cell Mol Life Sci*, 2012. **69**(3): p. 373-88.
226. Adams, S. and J.Z. Zhang, *Unique optical properties and applications of hollow gold nanospheres (HGNs)*. *Coordination Chemistry Reviews*, 2016. **320-321**: p. 18-37.
227. Boote, B.W., H. Byun, and J.-H. Kim, *Silver–Gold Bimetallic Nanoparticles and Their Applications as Optical Materials*. *Journal of Nanoscience and Nanotechnology*, 2014. **14**(2): p. 1563-1577.
228. Huang, X. and M.A. El-Sayed, *Gold nanoparticles: Optical properties and implementations in cancer diagnosis and photothermal therapy*. *Journal of Advanced Research*, 2010. **1**(1): p. 13-28.
229. Xia, Y., *Optical sensing and biosensing based on non-spherical noble metal nanoparticles*. *Anal Bioanal Chem*, 2016. **408**(11): p. 2813-25.
230. Ghosh, P., et al., *Gold nanoparticles in delivery applications*. *Adv Drug Deliv Rev*, 2008. **60**(11): p. 1307-15.
231. Connor, E.E., et al., *Gold nanoparticles are taken up by human cells but do not cause acute cytotoxicity*. *Small*, 2005. **1**(3): p. 325-7.
232. Turkevich, J., P.C. Stevenson, and J. Hillier, *A study of the nucleation and growth processes in the synthesis of colloidal gold, discuss*. *Discuss. Faraday Soc.*, 1951. **11**: p. 55-75.
233. Schmid, G., *Large clusters and colloids — metals in the embryonic state*. *Chem. Rev.*, 1992. **92**: p. 1709-1727.
234. Grabar, K.C., et al., *Preparation and characterization of Au colloid monolayers*. *Anal Chem*, 1995. **67**: p. 735-743.
235. Mura, S., J. Nicolas, and P. Couvreur, *Stimuli-responsive nanocarriers for drug delivery*. *Nat Mater*, 2013. **12**(11): p. 991-1003.
236. Gao, W., J.M. Chan, and O.C. Farokhzad, *pH-Responsive Nanoparticles for Drug Delivery*. *Mol Pharm*, 2010. **7**(6): p. 1913-1920.
237. Colombo, P., et al., *Novel platforms for oral drug delivery*. *Pharm Res*, 2009. **26**(3): p. 601-11.
238. Zeng, J., et al., *Superparamagnetic Reduction/pH/Temperature Multistimuli-Responsive Nanoparticles for Targeted and Controlled Antitumor Drug Delivery*. *Mol Pharm*, 2015. **12**(12): p. 4188-99.
239. Yilmaz, G., et al., *Poly(methacrylic acid)-Coated Gold Nanoparticles: Functional Platforms for Theranostic Applications*. *Biomacromolecules*, 2016. **17**(9): p. 2901-11.
240. Jia, X., et al., *Novel fluorescent pH/reduction dual stimuli-responsive polymeric nanoparticles for intracellular triggered anticancer drug release*. *Chemical Engineering Journal*, 2016. **295**: p. 468-476.
241. Alvarez-Lorenzo, C., L. Bromberg, and A. Concheiro, *Light-sensitive intelligent drug delivery systems*. *Photochem. Photobiol* 2009. **85**: p. 848-860.
242. Barhoumi, A., Q. Liu, and D.S. Kohane, *Ultraviolet light-mediated drug delivery: Principles, applications, and challenges*. *J Control Release*, 2015. **219**: p. 31-42.

243. Jiang, J., et al., *Polymer Micelles Stabilization on Demand through Reversible Photo-Cross-Linking*. *Macromolecules*, 2007. **40**: p. 790-792.
244. Jiang, Z., et al., *Controlled protein delivery from photosensitive nanoparticles*. *Journal of Biomedical Materials Research Part A*, 2015. **103**(1): p. 65-70.
245. Tong, R., et al., *Photoswitchable nanoparticles for triggered tissue penetration and drug delivery*. *J Am Chem Soc*, 2012. **134**(21): p. 8848-55.
246. Simpson, C.R., et al., *Near-infrared optical properties of ex vivo human skin and subcutaneous tissues measured using the Monte Carlo inversion technique*. *Phys. Med. Biol.*, 1998. **43**(9): p. 2465-2478.
247. Weissleder, R., *A clearer vision for in vivo imaging*. *Nat. Biotechnol.*, 2001. **19**(4): p. 316-317.
248. Feng, Q., et al., *Tumor-targeted and multi-stimuli responsive drug delivery system for near-infrared light induced chemo-phototherapy and photoacoustic tomography*. *Acta Biomater*, 2016. **38**: p. 129-42.
249. Huang, X., S. Neretina, and M.A. El-Sayed, *Gold nanorods: from synthesis and properties to biological and biomedical applications*. *Adv Mater*, 2009. **21**(48): p. 4880-910.
250. Liu, J., et al., *NIR-triggered anticancer drug delivery by upconverting nanoparticles with integrated azobenzene-modified mesoporous silica*. *Angew Chem Int Ed Engl*, 2013. **52**(16): p. 4375-9.
251. You, J., G. Zhang, and C. Li, *Exceptionally High Payload of Doxorubicin in Hollow Gold Nanospheres for Near-Infrared Light-Triggered Drug Release*. *ACS Nano*, 2010. **4**(2): p. 1033-1041.
252. Haine, A.T.N., T., *Drug delivery systems controlled by irradiation of near infrared light*. *Journal of Photopolymer Science and Technology*, 2015. **28**(5): p. 705-710.
253. Huschka, R., et al., *Light-Induced Release of DNA from Gold Nanoparticles: Nanoshells and Nanorods*. *Journal of the American Chemical Society*, 2011. **133**(31): p. 12247-12255.
254. Yamashita, S., et al., *Controlled-release system of single-stranded DNA triggered by the photothermal effect of gold nanorods and its in vivo application*. *Bioorg Med Chem*, 2011. **19**(7): p. 2130-5.
255. Blankschien, M.D., et al., *Light-Triggered Biocatalysis Using Thermophilic Enzyme-Gold Nanoparticle Complexes*. *ACS Nano*, 2013. **7**(1): p. 654-663.
256. Link, S., et al., *Laser-Induced Shape Changes of Colloidal Gold Nanorods Using Femtosecond and Nanosecond Laser Pulses*. *J. Phys. Chem. B*, 2000. **104**: p. 6152-6163.
257. Jain, P.K., W. Qian, and M.A. El-Sayed, *Ultrafast Cooling of Photoexcited Electrons in Gold Nanoparticle-Thiolated DNA Conjugates Involves the Dissociation of the Gold-Thiol Bond*. *J. Am. Chem. Soc.*, 2006. **128**: p. 2426-2433.
258. Braun, G.B., et al., *Laser-Activated Gene Silencing via Gold Nanoshell-siRNA Conjugates*. *ACS Nano*, 2009. **3**(7): p. 2007-2015.
259. Lu, W., et al., *Tumor site-specific silencing of NF-kappaB p65 by targeted hollow gold nanosphere-mediated photothermal transfection*. *Cancer Res*, 2010. **70**(8): p. 3177-88.
260. Wijaya, A.S., S. B.; Pallares, I. G.; Hamad-Schifferli, K., *Selective Release of Multiple DNA Oligonucleotides from Gold Nanorods*. *ACS Nano*, 2009. **3**(1): p. 80-86.
261. Kimling, J., et al., *Turkevich Method for Gold Nanoparticle Synthesis Revisited*. *J. Phys. Chem. B*, 2006. **110**: p. 15700-15707.
262. Scheartzberg, A.M., et al., *Synthesis, Characterization, and Tunable Optical Properties of Hollow Gold Nanospheres*. *J. Phys. Chem. B*, 2006. **110**: p. 19935-19944.
263. Bron, K.R. and M.J. Natan, *Hydroxylamine Seeding of Colloidal Au Nanoparticles in Solution and on Surfaces*. *Langmuir*, 1998. **14**: p. 726-728.
264. Stremmsdoerfer, G., et al., *Autocatalytic Deposition of Gold and Palladium onto n - GaAs in Acidic Media*. *J. Electrochem. Soc.*, 1988. **135**: p. 2881-2885.

265. Zhang, X., M.R. Servos, and J. Liu, *Instantaneous and quantitative functionalization of gold nanoparticles with thiolated DNA using a pH-assisted and surfactant-free route*. J Am Chem Soc, 2012. **134**(17): p. 7266-9.
266. Mannelli, I. and M.P. Marco, *Recent advances in analytical and bioanalysis applications of noble metal nanorods*. Anal Bioanal Chem, 2010. **398**(6): p. 2451-69.
267. Niidome, T., et al., *Poly(ethylene glycol)-modified gold nanorods as a photothermal nanodevice for hyperthermia*. J Biomater Sci Polym Ed, 2009. **20**(9): p. 1203-15.
268. Wu, M.H., S.B. Huang, and G.B. Lee, *Microfluidic cell culture systems for drug research*. Lab Chip, 2010. **10**(8): p. 939-56.
269. Marcus, J.S., W.F. Anderson, and S.R. Quake, *Parallel picoliter RT-PCR assays using microfluidics*. Anal Chem, 2006. **78**: p. 956-958.
270. Menegatti, E., et al., *Lab-on-a-chip: emerging analytical platforms for immune-mediated diseases*. Autoimmun Rev, 2013. **12**(8): p. 814-20.
271. Shevkopyas, S.S., et al., *Biomimetic autoseparation of leukocytes from whole blood in a microfluidic device*. Anal Chem, 2005. **77**: p. 933-937.
272. Kimmel, D.W., et al., *Electrochemical sensors and biosensors*. Anal Chem, 2012. **84**(2): p. 685-707.
273. Hoshino, K., et al., *Microchip-based immunomagnetic detection of circulating tumor cells*. Lab Chip, 2011. **11**(20): p. 3449-57.
274. Balslev, S., et al., *Lab-on-a-chip with integrated optical transducers*. Lab Chip, 2006. **6**(2): p. 213-7.
275. Xia, Y. and G.M. Whitesides, *Soft Litography*. Angew. Chem. Int. Ed., 1998. **37**: p. 550-575.
276. Weibel, D.B., W.R. Diluzio, and G.M. Whitesides, *Microfabrication meets microbiology*. Nat Rev Microbiol, 2007. **5**(3): p. 209-18.
277. Bodas, D. and C. Khan-Malek, *Hydrophilization and hydrophobic recovery of PDMS by oxygen plasma and chemical treatment—An SEM investigation*. Sensors and Actuators B: Chemical, 2007. **123**(1): p. 368-373.
278. Llobera, A., et al., *Biofunctionalized all-polymer photonic lab on a chip with integrated solid-state light emitter*. Light: Science & Applications, 2015. **4**(4): p. e271.
279. Vila-Planas, J., et al., *Cell analysis using a multiple internal reflection photonic lab-on-a-chip*. Nat Protoc, 2011. **6**(10): p. 1642-55.
280. Organization, W.H. *The top 10 causes of death*. 2016; Available from: <http://www.who.int/mediacentre/factsheets/fs310/en/>.
281. Black, S., I. Kushner, and D. Samols, *C-reactive Protein*. J Biol Chem, 2004. **279**(47): p. 48487-90.
282. Ridker, P.M., *Clinical Application of C-Reactive Protein for Cardiovascular Disease Detection and Prevention*. Circulation, 2003. **107**(3): p. 363-369.
283. Algarra, M., D. Gomes, and J.C. Esteves da Silva, *Current analytical strategies for C-reactive protein quantification in blood*. Clin Chim Acta, 2013. **415**: p. 1-9.
284. Brouwer, N. and J. van Pelt, *Validation and evaluation of eight commercially available point of care CRP methods*. Clinica Chimica Acta, 2015. **439**: p. 195-201.
285. Vashist, S.K., et al., *Bioanalytical advances in assays for C-reactive protein*. Biotechnology Advances, 2016. **34**(3): p. 272-290.
286. Ibarlucea, B., et al., *Selective functionalisation of PDMS-based photonic lab on a chip for biosensing*. Analyst, 2011. **136**(17): p. 3496-502.

10 ACRONYMS AND ABBREVIATIONS

10.1 Acronyms and abbreviations

2D	Two Dimensional
Ab	Antibody
Abs	Absorbance
AD	Aminodextran
Ag	Antigen
APS	Ammonium PerSulfate
As	Antiserum
ASP	Amnesic Shellfish Poison
aSW	Artificial seawater
AuNP	Gold nanoparticle
BDE	Brominated diphenylether
BSA	Bovine Serum Albumin
CAP	Chloramphenicol
CIBER-BBN	Centro de Investigación Biomédica en red – Bioingeniería, Biomateriales y Nanomedicina
CNM	Centro Nacional de Microelectrónica
CRP	C-Reactive Protein
CSIC	Spanish Council for Scientific Research
CVD	CardioVascular Diseases
CW	Continuous wave
Da	Dalton
DA	Domoic acid
DCC	N-dicyclohexylcarbodiimide
DDS	Dimethyldichlorosilane
DEA	Diethylaminoethanol
DMF	N-dimethylformamide
DNA	DeoxyriboNucleic Acid
DPHA	Dihydropteroic Acid
DTT	Dithiothreitol
DVD	Drinking Water Directive
E2	17 β estradiol
EC	European Commission
EDC	1-Ethyl-3-(3-dimethylaminopropyl)carbodiimide
EIA	Enzyme ImmunoAssay
ELFA	Enzyme-Linked Fluorescent ImmunoAssay

ELISA	Enzyme-Linked ImmunoSorbent Assay
EPA	Environmental Protection Agency
EQS	Environmental Quality Standard
EU	European Union
FITC	Fluorescein isothiocyanate
Fic	Fluorescein
Fv	Fragment variable
GC-MS/MS	Gas chromatography coupled to mass spectrometry
GPTMS	3-(Glycidyoxypropyl)trimethoxysilane
HCH	Horseshoe Crab Hemocyanin
HGNs	Hollow Gold Nanoparticles
HPLC	High Performance Liquid Chromatography
HPLC-FD	High Performance Liquid Chromatography – fluorescence detection
HRGC	High Resolution Gas Chromatography
HRMS	High Resolution Mass Spectrometry
HRP	HorseRadish Peroxidase
IA	ImmunoAssay
IC ₅₀	Concentration in which the signal is 50 % inhibited
IC ₉₀	Concentration in which the signal is 10 % inhibited
ICFO	The Institute of Photonic Sciences
IgG	Immunoglobulin G
IGTP	Institut d'investigació Germans Trias i Pujol
INA	Institute of Nanoscience of Aragon
IQAC	Institute of Advanced Chemistry of Catalonia
KDa	KiloDalton
LC-MS/MS	Liquid Chromatography coupled to Mass Spectrometry
LDL	Low-Density Lipoprotein
LFA	Lateral Flow Assay
LOC	Lab-On-a-Chip
LOCI	Luminescent Oxygen Channeling Assay
LOD	Limit Of Detection
LSPR	Localized Surface Plasmon Resonance
MAb	Monoclonal Antibody
MALDI-TOF-MS	Matrix Assisted Laser Desorption Ionization - Time of Flight Mass Spectrometry
MOPS	Modular Optofluidic System
MW	Molecular Weight

Nb4D	Nanobiotechnology for Diagnostics Group
NHS	N-HydroxySuccinimide
NR	Nanorod
OCMO	O-CarboxyMethylOxime
PAb	Polyclonal Antibody
PBA	phenozybenzaldehyde
PBDE	Polybrominated Dyphenil Ether
PBS	Phosphate Buffered Saline solution
PBST	Phosphate Buffered Saline Tween-20 solution
PBT	Standard PBST with the absence of salts
PCB	Polychlorinated biphenyl
PCR	Polymerase Chain Reaction
PDMS	Polydimethylsiloxane
PEG	PolyEthylene Glycol
PEG-SH	thiolated PolyEthylene Glycol
PhLOC	Photonic Lab-On-a-Chip
PL	Pulsed light
POC	Point-Of-Care
POP	Persistent Organic Pollutant
P_{ow}	Partition coefficient n-octanol/water
PVA	PolyVinyl Alcohol
QDs	Quantum Dots
REACH	Registration, Evaluation, Authorisation and Restriction of Chemicals
RPM	Revolutions Per Minute
RFU	Relative Fluorescence Units
RT	Room Temperature
SA	Sulphonamide
SDS	Sodium Dodecyl Sulphate
SPE	Solid Phase Extraction
SPR	Surface Plasmon Resonance
SPY	Sulfapyridine
TAMRA	5-Carboxytetramethylrhodamine
TBP	Tribromophenol
TBT	Tributyltin
TEM	Transmission electron microscopy
TMB	3,3',5,5'-TetraMethylBenzidine
TRITC	Tetramethylrhodamine

UV	Ultraviolet
WFD	Water Framework Directive
WHO	World Health Organization